BUILDING BLOCKS OF SELF-ORGANIZED CRITICALITY

By

Ryan Woodard

RECOMMENDED:

Advisory Committee Chair

Chair, Department of Physics

APPROVED:

Dean, College of Natural Science and Mathematics

Dean of the Graduate School

August 23, 2004
Date

BUILDING BLOCKS OF SELF-ORGANIZED CRITICALITY

A

THESIS

Presented to the Faculty

of the University of Alaska Fairbanks

in Partial Fulfillment of the Requirements

for the Degree of

DOCTOR OF PHILOSOPHY

By

Ryan Woodard, B.S., M.S.

Fairbanks, Alaska

August 2004

Abstract

Why are we having difficulty developing economical nuclear fusion? How can a squirrel cause a statewide power blackout? How do correlations arise in a random complex system? How are these questions related? This thesis addresses these questions through a study of self-organized criticality (SOC). Among the systems that have been proposed as SOC are confined fusion plasmas, the Earth's magnetosphere and earthquake faults.

SOC describes how large-scale complex behavior can emerge from small-scale simple interactions. The essence of SOC is that many dynamical systems, regardless of underlying physics, share a common nonlinear mechanism: local gradients grow until exceeding some critical gradient and then relax in events called avalanches. Avalanches range in size from very small to system-wide. Interactions of many avalanches over long times result in robust statistical and dynamical signatures that are surprisingly similar in many different physical systems. Two of the more well-known signatures are power law scaling of probability distribution functions (PDFs) and power spectra. Of particular interest in the literature for approximately a century are $1/f$ spectra.

I studied the SOC running sandpile model and applied the results to confined and space plasmas. My tools were power spectra, PDFs and rescaled range (R/S) analysis. I found that SOC systems with random external forcing store memory of previous states in their local gradients and can have dynamical correlations over very long time scales regardless of how weak the external forcing is. At time scales much longer than previously thought, the values of the slope of the power spectra, β, and the Hurst exponent, H, are different from the values found for white noise. As forcing changes, β changes in the range $0.4 \lessapprox \beta \leq 1$ but the Hurst exponent remains relatively constant, $H \approx 0.8$. The same physics that produces a $1/f$ spectrum at strong forcing produces a $f^{-0.4}$ spectrum at weaker forcing. Small amounts of diffusive spreading added to the two dimensional SOC sandpile greatly decreases the frequency and maximum size of large transport events. More diffusion increases the frequency of large events to values much greater than for systems without diffusion.

Table of Contents

Signature Page i
Title Page ii
Abstract iii
Table of Contents iv
List of Figures vii
List of Tables x
List of Other Materials xi
List of Appendices xii
Acknowledgements xiii
1 Introduction **1**
1.1 Randomness, Complex Systems and Long Time Correlations 2
1.2 Probability Density Functions, Power Spectrum and Rescaled Range Analysis 4
1.3 Self-Organized Criticality 15
1.4 SOC Models 18
1.5 SOC and the Transport Problem in Fusion Plasmas 23
1.6 Motivation for Dissertation 29
1.7 Statement of Work 30
Bibliography 32
2 Building Blocks of Self-Organized Criticality, Part I: The Very Low Drive Case **37**
2.1 Introduction 37
2.2 Model 39
2.3 Methods 40
2.4 Results 41
2.4.1 Regions A and B: Pulse Shapes 42
2.4.2 Region C: Quiet Times 47
2.4.3 Region D: SOC and Correlated Events 49
2.4.4 Region E: Anticorrelated Events 53
2.5 Conclusions 55
Bibliography 57

3 Building Blocks of Self-Organized Criticality, Part II: Transition from Very Low Drive to High Drive **60**
3.1 Introduction 60
3.2 Model and Methods 62
3.3 Results 63
3.4 Distinguishing Between Low and High Drive 69
3.5 Discussion 72
3.6 Conclusions 76
Bibliography 78
4 On The Identification of SOC Dynamics in the Sun-Earth System **80**
4.1 Introduction 80
4.2 Power Laws, the Power Spectrum and R/S Analysis 82
4.3 Self-Organized Criticality and the Sun-Earth System 87
4.4 Effect of Strength of External Forcing and System Size 89
4.5 Effect of Length of Time Series 95
4.6 Conclusions 96
Bibliography 98
5 Transport Events and Correlation Lengths in a SOC Confined Plasma Model **101**
5.1 Introduction 101
5.2 Model 104
5.3 Methods 107
5.4 Results 108
5.5 Discussion 114
5.6 Conclusions 120
Bibliography 122
6 Conclusions **124**
6.1 Summary of Results 124
6.1.1 Long Time Correlations Exist in Very Weakly Driven SOC Systems . 124
6.1.2 Long Time Is Relative 124

6.1.3 The Same Physics Produces Different Spectra 125
6.1.4 There Is Only One SOC Region in the Spectrum and R/S 125
6.1.5 The Hurst Exponent Measures the Same Physics Consistently 125
6.1.6 $1/f$ Is Not Always $1/f$ 126
6.1.7 Added Diffusion Reduces 'SOCness' 126
6.2 The Worth of Sandpiles 126
Bibliography 131
A Comment on "Do Earthquakes Exhibit Self-Organized Criticality?" (Phys. Rev. Lett. 92, 228501 (2004)) **132**
Bibliography 134
B Slides from Oral Defense **135**

List of Figures

1.1 PDF of earthquake magnitudes in interior Alaska. 6
1.2 Power spectrum of seismic record of Shishaldin Volcano, Alaska, 15 November 2002. 7
1.3 Power spectrum of AE index for 1980-1981. 8
1.4 Power spectrum of floating potential of Wendelstein 7-AS stellarator. 8
1.5 Time series and R/S analysis for a sine curve. 12
1.6 R/S analysis for AE index for 1980-1981. 13
1.7 Time series, power spectra and R/S analysis of 3 samples of fractional Gaussian noise. 14
1.8 Flips time series from running sandpile model for low and high drive. . . . 20
1.9 Rules of the one dimensional running sandpile. 21
1.10 Image of simulated tokamak field lines. 25
1.11 Image of simulated plasma turbulence along toroidal field lines and in poloidal cross sections of tokamak. 29

2.1 Partial flips time series from running sandpile model for low drive and space-time diagram and flips time series of separate avalanches. 43
2.2 Power spectra and R/S analysis of flips for low drive sandpile for $P_0L^2 = 0.2$ and L = $20, (ADD50, 100)200, 1000$. 43
2.3 Cartoons of distinct regions and their breakpoints and causes of power spectra and R/S analysis of sandpile flips. 44
2.4 Power spectra and R/S analysis of low drive sandpile: original series, with quiet times removed and with pulses shuffled. 45
2.5 Cartoon definitions of trapezoidal, rectangular and triangular pulses and power spectra of 5 trapezoids with changing a and b. 46
2.6 Correlations between avalanches because of memory in local gradients. . . 51
2.7 Breakpoint of beginning of anticorrelated region versus driving rate for three different system sizes. 54

3.1 Power spectra of flips time series of L = 200 sandpile for five orders of magnitude of effective driving rate in $P_0L^2 \in (0.002, 296)$. 64
3.2 (a) Power spectra and (b) R/S analysis of flips for different driving rates. . . 65
3.3 Cartoons of distinct regions and their breakpoints and causes of power spectra and R/S analysis of sandpile flips. 66
3.4 Inverse breakpoints of the power spectra versus breakpoints of R/S analysis for flips time series of different size sandpiles and driving rate. 67
3.5 Breakpoints of power spectra and R/S analysis versus driving rate for L = 200 sandpile. 68
3.6 H, β, average quiet time and average duration versus five orders of magnitude of effective driving rate. 69
3.7 Hurst exponent versus driving rate for (a) L = 200 and (b) L = 800, 1600. . . . 70
3.8 Rescaling of power spectra of two different systems with $P_0L^2 = 2.0$, one with L = 200 and one with L = 2000. 73
3.9 (a) Power spectra and (b) R/S analysis for fractional Gaussian noise of H = 0.8 with and without quiet times added. Numbers shown are β for spectra and H for R/S. 74
3.10 Section of flips time series for high drive sandpile and definition of a superpulse. 75
3.11 Power spectra and R/S for high drive with superpulses changed. Numbers shown are β for spectra and H for R/S. 76

4.1 Time series and power spectra of AE index, sandpile and Gaussian noise. . 84
4.2 Time series and R/S analysis of sine curve. 85
4.3 Time series, power spectrum and R/S analysis of a sawtooth pulse. 87
4.4 Power spectra and R/S analysis of flips of running sandpile model for three different values of effective drive, P_0L^2. 90
4.5 Power spectrum of AE index 1980-1981 and cartoon of time scales of additional spectrum. 96

5.1 Mapping of tokamak poloidal cross section to two dimensional sandpile. . . 103

5.2 Cartoon showing how plasma flows across fixed probes in a confinement device. 105
5.3 A cartoon of triangular diffusive spreading in the two dimensional sandpile. 107
5.4 Two subsets of time series of sandpile flips with and without triangle spreading of width 3. 109
5.5 (a) Power spectra and (b) R/S of sandpile flips time series with and without triangle spreading of width 3. 110
5.6 Probability distribution functions of flux event sizes through the middle row of the sandpile for various (a) triangular and (b) random spreading widths. 111
5.7 Maximum cross correlation between center row of the sandpile and downhill neighbors versus (a) radial separation and (b) poloidal separation for various triangular spreading widths. 113
5.8 Probability distribution functions of flux event sizes through the middle row of the sandpile with and without poloidal bulk flow. 114
5.9 Cartoon of two dimensional sandpile and fixed probes with and without poloidal bulk flow. 117
5.10 Maximum cross correlation versus poloidal separation. 118
5.11 Cross correlation of flux time series versus poloidal separation and time lag. 119
5.12 Maximum cross correlation versus poloidal separation after the cross correlation function has been unwrapped. 119
5.13 Poloidal correlation length versus flow rate. 120

A.1 FRTDFs of the instantaneous avalanching activity in a $L = 2000$ sandpile for avalanches with sizes above different thresholds (pdfs shifted for clarity). Inset: FRTDFs (in lin-log scale) for same data after shuffling avalanches. . . 133

List of Tables

4.1 Time period, resolution, slopes of first two spectral regions and breakpoint of AE index data. 92

List of Other Materials

A CD-ROM of Thesis, Defense and Sandpile Code . . . . . Pocket

List of Appendices

A Comment on "Do Earthquakes Exhibit Self-Organized Criticality?" (Phys. Rev. Lett. **92**, 228501 (2004)) 132

B Slides from Oral Defense 135

Acknowledgements

10 years. 6 offices. 6 homes. 5 advisors. 4 very different research projects. 1 Ph.D. You do the math. Was it worth it? Emphatically, yes. Why did I do it? Read the conclusions for the answer. This section is to thank people. Actually, I think that only part of the purpose of this section is to thank people. The main purpose of this section, really, is to write notes to my future self to help remember who and what were going on in my life during these fun years.

First, I am forever grateful to David Newman, my fifth, final and most successful advisor. Or the only one who could not successfully think of a way to ditch me. He gave me an incredible opportunity: he paid me to sit down and learn neat stuff. How lucky am I? And for anything that I learned, he was, at worst, just as excited about it as me. More often, though, he was far more excited about it than I was. That constant positive enthusiasm contrasted so often with my frequent gloomy ways. I do believe in long time correlations: without his never failing, always supportive attitude for over four years I would not have finished. Thank you very, very much, David, for the events and for the quite times. It has been fun and I learned neat stuff. My only complaint is that you do not drink beer.

Second, and speaking of an always supportive attitude and constant positive enthusiasm contrasting with my frequent gloomy ways, I give one billion and seven thank yous to my sweet patootie, best friend and fellow Braves fan, Dr. Hilary Jane Fletcher, who once again is in another country as I write the acknowledgements to a thesis. This time, though, it is mine. And you know? Perhaps I also could have done it without you but I probably would have dawdled longer if it were not for your relocation to the southern hemisphere. So thank you for the extra motivation and for all of your patience. And for being so much darn fun. I will see you soon. You do drink beer, so no complaints there.

Third, I would like to thank me for sticking it out. You, oh Fickle Fist of Fate, did your best to derail me many times. But in the end, I am writing this and you are sulking in a corner. Eat my dust.

Now that the top three are out of the way, I would like to thank, in order of appearance:

- my committee:
  - John Olson, member of many of my previous committees, teacher of and believer in the sanctity of mathematical formalism, proper grammar and punctuation, the meaning of the word 'dynamics,' the use of a seven iron and the art of hallway discussions about the beauty of science;
  - Brenton Watkins, for many a lunch and pint at Pike's and for lessons in being a relaxed physicist;
  - Renate Wackerbauer, for listening to and commenting on my same repetitive talk during Tuesday group meetings for a couple of years;
  - Martin Truffer, for entering UAF as a grad student *after* I did, proving to the world that he can drink a lot and still graduate and be hired as a professor at UAF years before I write word one of my thesis and then serve on my committee (it is almost embarrassing);
- a mi comité español:
  - Raúl Sánchez, por jugar en la arena conmigo, por alojarme y guiarme, por insultar a David y por enseñarme palabrotas en Español;
  - Ben Carreras, por sus tests de realidad, buen vino, sus sinceras y cuidadosas repuestas a tantas preguntas y, también, por insultar a David;
  - Maria Varela, por más lecciones de palabrotas, insultar a Raúl, alojarme en Madrid y en Oak Ridge y por ofrecer siempre una bonita sonrisa;
- Mom and dad, for guitar lessons and a VIC-20;
- Cara, for visiting next week;
- Herr Doktor Professor Kurt Vogel, for inspiration in all things physics and whitewater;
- Kurt Wiesenfeld, for giving me my first sandpile;
- Charlie Stevens, I just want to put your name in my thesis;
- Bob and Ann, for dinners, gin, beer and for letting me win The Race;
- my first 4 advisors, for collectively and unconsciously arranging things to end this way;

• The Crane Courtiers: Drs. Ted, Alison, Jen, Peter, Laura, Tom, Matt, Carrie, Bevin, Matt, Dana, Martin, Katariina, Hans, Veronika, all who went before me and showed me how;
• The Third Flouriers: Drs. Rowdy, Michelle, Pete, Jackie, Josh 'I am thirsty' Stachnik;
• Willis, for the Double 'n' Tundra experience and experimental evidence that two entangled tussocks with the same quantum numbers cannot easily occupy the same orbital;
• The UAF Pubtenders: Brian, Eric, Casey, Jeri, Scott (especially Brian The Fan);
• All Disciples of The Church of the Holy Triumvirate of Guitars, Frisbees and Beer;
• Rich Collins, for telling me in 1998 that this is the only time in my life when I will be allowed to freely go deep into a subject and be paid to do it;
• Dave Covey and Chris Swingley, for educating me and sharing in the GNU/Linux way;
• Judie Triplehorn, for **always** being helpful and for the GI library;
• Twink and Geo, for supporting the OXO cause from across the puddle;
• Nick Watkins, for being the first non-TACSer to notice and speak up (thank you!);
• Brad Werner, faithful observer of the American Way and positive source of encouragement about my research;
• John Craven, for lectures, memos and rants about minutiae concerning thesis format;
• Mary Parsons and Barbara Day for so much help and for being so pleasant while oftentimes being surrounded by E.M.s and Fs.;
• Uma Bhatt, for making brownies and cookies without nuts;
• the UAF Chemistry Department, especially Sheila Chapin and Larry 'Go Braves' Duffy, for continuing to befriend me after a jump to the other hallway;
• Richard  Stallman, Linus  Torvolds, Leslie LaTeX Lamport, Guido van 

Rossum, Evgeny Grace Stambulchik and Ian  Murdock;
• and all of those other people.

"If a fractal relationship is a reasonably good approximation, even if only over a decade or so, it will prove useful in descriptions of spatial functions and should stimulate searches for the underlying bases for correlation."

—Bassingthwaighte and Raymond

"The goal of research is to be the first kid on your block to know something."

—Joe Ford, Curmudgeon of Complexity

Chapter 1
Introduction

How do correlations arise in a seemingly random complex system and what are their signatures? The study of self-organized criticality (SOC) [1, 2, 3] is one attempt to address this question. SOC is a general theory that has been applied in many physical and social fields to try to help understand why very disparate systems share remarkably similar quantitative signatures. This dissertation studies three such signatures of a SOC model, the running sandpile, and discusses what they reveal about long time dynamical correlations in a SOC system and how this can be applied to studies of confined and space plasmas. The signatures are the probability density function (PDF), the power spectrum and the rescaled range (R/S). The running sandpile has been studied and used as a guide in SOC for over twenty years, since shortly after the introduction of SOC itself in 1987. This dissertation overturns some of the conclusions and assumptions from earlier studies that have been accepted since then and also presents investigations of an extension of the model that has not been previously studied.

The main result of this work is that systems with random external forcing can have dynamical correlations over very long time scales. That is, current events will affect later events even when 'later' may seem much longer than what accepted theory says about the upper limit of such correlations. This is relevant in, for example, fusion energy research partly because such correlations are observed in turbulent transport in confined plasmas, in contradiction to traditional linear plasma diffusion theory. This anomalous diffusion is a major impediment to attaining the high value of the product of density, confinement time and temperature needed to achieve sustained economical fusion.

The rest of this introduction will elaborate on some of the terms used so far, such as random, complex system and long time correlations, and will define and discuss the three signatures mentioned above. Since signatures of PDFs and spectra (specifically, power laws in the measures) play an important role in the motivation for the development of SOC, they are explained first. Afterwards, an overview of the history and models of SOC will be presented followed by a discussion of the transport problem in fusion plasmas and how that led to study of SOC as a relevant model for these plasmas. This last part will set up the motivation that led to the research in this dissertation.

Signatures of the running sandpile are studied in Chapters 2 and 3. Applications of the model to space plasmas are presented in Chapter 4 and to confined plasmas in Chapter 5. Chapters 2–5 and Appendix A are papers that have been or will be submitted to journals [4, 5, 6, 7, 8].

1.1 Randomness, Complex Systems and Long Time Correlations

The definition of randomness can be endlessly debated. Starting with quantum mechanics, one could say that the entire universe is random and that predictability is impossible. Even though people make predictions that seem to be correct, the outcome of, for instance, a chicken thrown through the air may actually be slightly off from calculations due to the inherent randomness of the quantum world and the lack of knowledge of all initial conditions of the system (the universe).

That said, we sidestep the philosophical issues and use a practical and intuitive definition of randomness in this dissertation. We are concerned with macroscopic systems on scales far larger than anything quantum; systems such as tectonic faults and confined and space plasmas. Instead of debating whether or not any process can ever be *truly* random, we assume that some are and look at the implications. In particular, we study the response of a generic coupled system to random forcing.

To build up a working picture of these ideas, start with the accepted notion of tossing a fair coin, where the outcomes of heads and tails each has 50% probability. Again, we ignore the possibility that knowledge of all initial conditions can predict the outcome of the toss; this is Everyman's Coin Toss and the action of the toss is referred to as Rule #1. If heads is labeled as 1 and tails as 0 then flipping the coin once per minute and recording the outcome of each flip results in a random time series of numbers. There are no correlations in the time series, as the outcome at time n does not affect the outcome at $n+1$.

To construct a more complicated system, but still not a complex system, take a large number of coin flippers, arrange them in a grid of rows and columns and make all coins flip simultaneously (applying Rule #1 to each coin) and then record the separate random time series. Each series will look similar to the others and, when measured by the methods of the next section, will have the same quantitative signatures. A different time series, though, can be created by adding up the number of tails at each time step. For N coin

flippers, the value of this time series at each time step will hover around $N/2$ and the signatures of the series will be the same as for the individual cases.

We make things a bit more interesting by creating a new rule, Rule #2: after each flip, each coin flipper must look at the coins of his nearest neighbors and flip his coin over if 3 out of 4 of the neighbors' coins are different. After an initial flip, the coins would be pretty evenly distributed but most likely there will be more of one side showing than the other since an exact 50-50 split is far less likely than a non-50-50 split. Say that more tails are showing after Rule #1 at time step n. Now Rule #2 is applied and the majority of tails is made stronger at time step $n+1$ as some lone heads are surrounded by 3 tails. There are temporal correlations, where a majority of tails creates more tails at the next time step. Also, there are spatial correlations as the average size of tail clusters increases. At time step $n+2$ all coins are flipped again and the system is reset. In this most recent communal flip, the memory that was in the system has been lost and there are no correlations longer than 2 time steps.

By simplifying the system, we can increase the correlations. Allow only one coin flipper (chosen at random) to apply Rule #1 at each time step. At the next time step, all coin flippers will apply Rule #2. As before, from time step n to $n+1$, the tails correlations persist. But now at time step $n+2$ the system is not completely reset, only a single coin is. The rest of the system retains its memory from the previous step. Spatial patterns of clusters of tails persist for many time steps, creating longer correlations.

This is the essence of a randomly driven complex system with long time correlations. The system is randomly driven because only one site, chosen at random, is changed (or possibly changed, since a tail has a 50% chance of remaining a tail after Rule #1 is applied). The system is complex because many agents are coupled to one another. Even though the rules that are followed are very simple, the large number of coupled sites (coin flippers) makes intuition alone a very weak tool with which to study long time correlations in the system. The correlations in space and time persist because the majority of the memory is retained from one time step to the next.

The above model is closely analogous to the Ising model of solid state physics that describes magnetization of ferromagnets [9]. In it, instead of flipping coins, a ferromagnet is modeled by a lattice of vectors, each of which can be in one of two states, up or down. The

vectors represent the spin angular momentum and the magnetic moment of a single electron. The coupling between electrons means that a lone spin down electron surrounded completely by spin up electrons will flip its spin to reach a lower energy state. The coupling strength is inversely related to the temperature, so that there is greater probability of a vector *not* being affected by its neighbors at higher temperatures. This models the absence of magnetization at high temperatures in real ferromagnetic material. Using the simple model of a two dimensional grid of two-state vectors and the rule of nearest neighbor coupling, the Ising model predicts the macroscopic magnetization of the ferromagnet. An important point is that the *low level physics* of the system has been replaced by a simple model with which correct predictions can be made.

Analytical methods, such as the renormalization group [9], can be and have been successfully used to attack the Ising model but computers are ideal for this type of problem, especially when slight changes in the rules or parameter space are explored. The type of model of grids and rules based only on the state of the nearest neighbors are called cellular automata and they have been implemented on computers as subjects of recreation and research. Important early examples include John Conway's Game of Life [10] and Stephen Wolfram's studies of the statistical mechanics of cellular automata [11]. Both of these works used early microcomputers to show the world that very simple systems can exhibit surprisingly complex behavior. More importantly, these and more recent studies (discussed below) show that the same simple systems can successfully model macroscopic behavior. In the same way that all computer models necessarily leave out some of the physics of the system, cellular automaton models retain only the most relevant physics. In the case of the Ising model, the most relevant physics reduces to the directions of the spin vectors of an electron's nearest neighbors. Electromagnetism and quantum mechanics do not enter into this version of the model.

1.2 Probability Density Functions, Power Spectrum and Rescaled Range Analysis

Power law scaling ($f(x) = cx^{-\beta}$) of the probability density function (PDF) and power spectrum are historically important in the study of complex systems and SOC. Such signatures in one or both measures of many different systems have been seen for years and have motivated the search for underlying principles that are possibly common to many processes.

Power laws imply scale-free behavior over their range, meaning that there is no characteristic time and/or space scale within that range, in contrast to Gaussian and exponential functions, for instance.

Power laws are seen as straight lines when plotted on doubly logarithmic axes, with slope β. Because of this and because of the large range of scales studied in this dissertation, most plots will be on log-log axes. For PDFs and power spectra, the convention is that β is defined as positive for a line that has a negative slope. For R/S analysis, a measure that is defined below, the exponent is referred to as H and is positive for a positive slope.

The PDF is approximated by the normalized histogram of values for a data series. It gives the probability of finding a certain value in the series. It gives no information on the ordering of the series, though; randomly shuffling the values of the series will give the identical PDF. The PDF of a single coin flipper comprises two points: $f(0) = f(1) = 0.5$. The PDF of the series of N uncoupled coin flippers would be approximated by a Gaussian curve centered at $N/2$. Power law PDFs will be seen when we discuss SOC below but for now, in terms of the coin flippers, consider the sizes of connected clusters of tails (or heads). An analogous measure is made in SOC systems and the PDF of the cluster sizes follows a power law PDF.

A famous power law PDF is the Gutenberg-Richter law of earthquake frequency versus magnitude, with $\beta \approx 1$ over several orders of magnitude for worldwide data [12]. For different tectonic systems, β can take on other values. An example of this is earthquake magnitude data for interior Alaska, where $\beta = 1.9$ (Figure 1.1).

Similar power laws are seen in PDFs of very different systems. Examples include PDFs of the sizes of individual auroral regions in the Earth's magnetosphere [13, 14] and blackout regions in electrical power grids [15, 16, 17], to name a few. Earthquakes, the magnetosphere and power grids are very different from each other and are studied in completely separate fields of science. But the similarity of their PDFs and other features suggest a possible shared mechanism and it is from this point of view that SOC is applied to them.

The power spectrum $S(f)$ of a data series $X(t)$ is defined as the square of the Fourier transform, $S(f) = |F(f)|^2$, where $F(f)$ is the Fourier transform of $X(t)$. The spectrum shows the range of frequencies over which power contributes more or less to the signal and can be an indicator of randomness and correlations in the data. For our purposes, the study

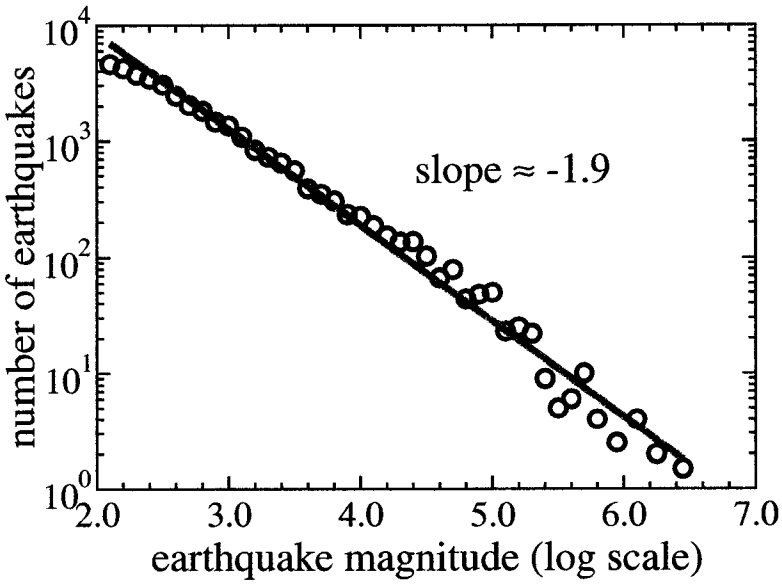

Figure 1.1. PDF of earthquake magnitudes in interior Alaska. Data courtesy of Hilary Fletcher, (formerly of) Geophysical Institute, University of Alaska Fairbanks, USA.

of the spectrum can be reduced to two simple questions: 1) Is the spectrum that of a random series? 2) If not, what process or processes in the system under study produces the nonrandom signal?

The power spectrum of a completely random and uncorrelated time series is flat, called f^0 scaling because of the dependence of the spectrum on the frequency. Three random time series with different PDFs (binary, Gaussian and uniform) will each have the same f^0 scaling of the spectrum. Any random shuffling of any of the series would not change either the PDF or the spectrum. Since one signature of three different series can be the same, multiple measures must often be used to characterize a system. Knowledge of only the spectra of the three series is not enough to distinguish them; in this case the PDF is also needed. The theme of the need for multiple measures to characterize a system is important in this dissertation. We will show that the PDF and spectrum can be supplemented by a third measure, R/S analysis, to more fully understand the dynamics of the SOC model. We will define dynamics in Section 1.3.

If the answer to question 1 above is that the series is not random, then what else is revealed by spectrum? A simple sine curve produces a sharp peak at its fundamental

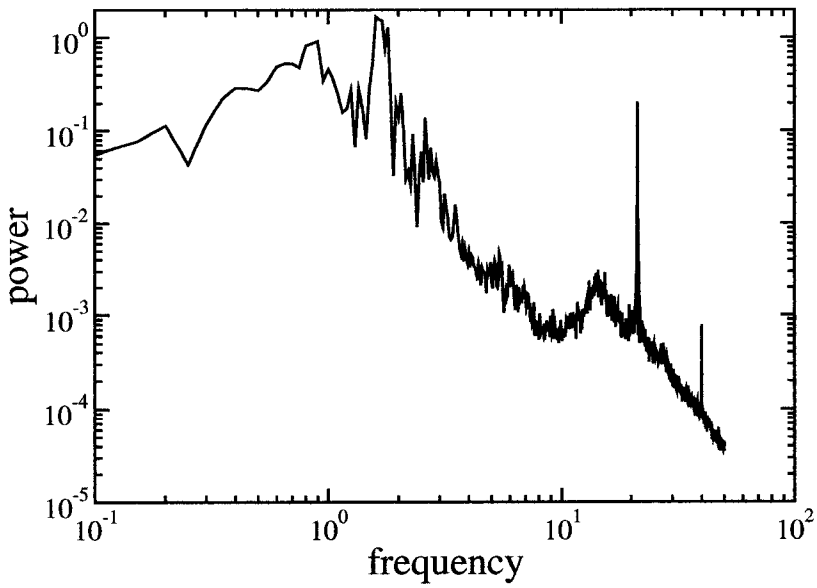

Figure 1.2. Power spectrum of seismic record of Shishaldin Volcano, Alaska, 15 November 2002. Data courtesy of Jackie Caplan-Auerbach, Alaska Volcano Observatory, Fairbanks, Alaska, USA.

frequency. More complicated is the spectrum of a seismic record from Shishaldin Volcano in Alaska, Figure 1.2, where spikes and larger features intermingle. Interpretation of such a spectrum is not trivial.

Our interest lies in between these two extremes and, as with PDFs, is with spectra that scale as power laws. First, note that f^0 is a power law with scaling exponent 0. Other power law spectra are seen in physical systems. An example is the spectrum of the auroral electrojet (AE) index, first seen by [18] in 1990 (Figure 1.3). The meaning and relevance of the AE index is debated (see, for example, [19]) but at the least can be taken as some response of the coupling between the magnetosphere and the solar wind. Another example of a power law scaling spectrum is that of the floating potential fluctuations in a confined plasma, Figure 1.4. Note that the spectra of both the AE index and the floating potential have *multiple* power law scaling regions. Besides understanding why the power laws and their specific slopes exist, to fully understand the system one must also understand why breakpoints between regions occur where they do. We explore this in later chapters.

An issue in the literature concerns a specific power law scaling in power spectra. Values

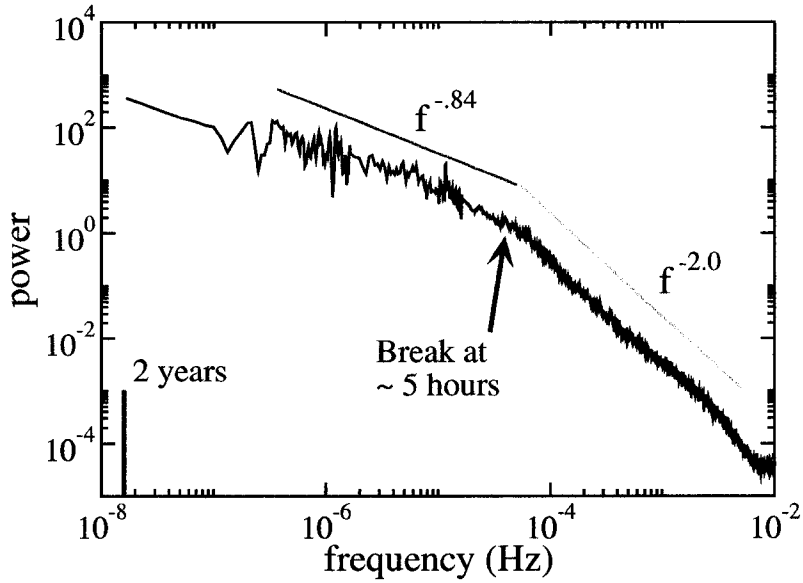

Figure 1.3. Power spectrum of AE index for 1980-1981. Data courtesy of World Data Center for Geomagnetism, Kyoto, Japan, `http://swdcdb.kugi.kyoto-u.ac.jp/`.

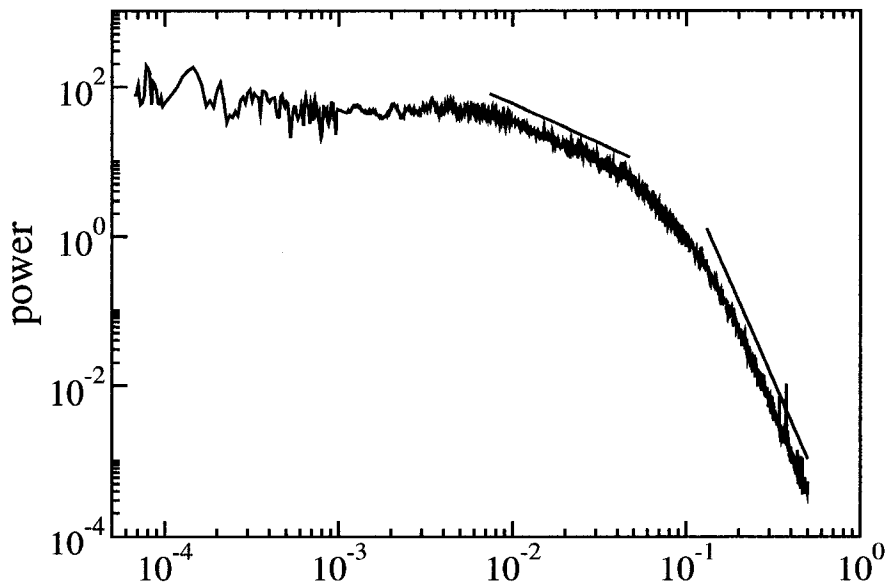

Figure 1.4. Power spectrum of floating potential of Wendelstein 7-AS stellarator. We gratefully acknowledge the group at Wendelstein 7-AS for allowing us to use this data.

of $\beta = 1$ appear in the low frequency limit of the spectra of many physical processes, where it is referred to as $1/f$ noise [20, 21, 22, 23, 24]. $1/f$ is deemed more 'interesting' than, say, f^{-2} for at least two reasons. First, some Poisson processes are known to produce spectra that scale as $1/(1+(f/f_c)^2)$, where f_c is some characteristic frequency of the system. Yet often $1/f$ noise is seen in systems that appear to be randomly driven. Second, the $1/f$ scaling persists to time scales much longer than that of the known low level physics in the systems. This implies long time correlations that are not simply explained by the known physics. This modern mystery still inspires much current work [25, 26] but no general theory that purports to explain the origin of $1/f$ is widely accepted. One aim of SOC was to be such a theory; the first paper on SOC [1] is subtitled "An Explanation of $1/f$ noise." We will elaborate on $1/f$ and SOC below.

The third measure used in this dissertation is called rescaled range (R/S) analysis and is used to measure correlations in a series. To gain a feel for correlations, consider a time series of some measured quantity, $X(t)$. A finite time series has a definite mean and there is some time t_0 when the quantity is above that mean. The series is correlated on some time scale τ if at time $t_0+\tau$ the quantity is, on average, more likely to also be above rather than below the mean. The series is anticorrelated if at time $t_0+\tau$ the quantity is, on average, more likely to be below rather than above the mean. (The same idea holds when swapping 'above' and 'below'.) Finally, the series is uncorrelated when neither case is more likely. The term persistence is often used as a synonym for correlation.

R/S analysis was first developed by Hurst in 1951 [27] while surveying for the Aswan Dam on the Nile River in Egypt. The Nile River levels have been monitored for over two thousand years and, thus, an exceptionally long time series for a geophysical system was available. His task was to calculate how large to make the dam so that the reservoir could prevent flooding in rainy years and could contain enough water for steady discharge during extended periods of drought. He thought that he could base his calculations on historical minimum and maximum flow rates. He called the difference between the maximum and minimum the range.

A finite time series always has a minimum and maximum but Hurst discovered a property of the series that implied that they could not guarantee that his dam would always be large enough. His discovery was that the farther back in time that he examined the Nile

data record the larger were the fluctuations of the range. He found the same behavior in time series of many other geophysical systems, such as tree ring growth rate and sediment layer thickness in lakes, and in non-geophysical systems like stock prices. Hurst's work was later studied in great depth by Mandelbrot and Wallis in 1969 (their collected works and other relevant follow-up papers by Mandelbrot appear in the Selecta [23, 28]). Their conclusion was that certain systems always have the possibility of 'wild fluctuations' that are greater than any before seen in the time record.

The extent of such fluctuations is quantified by the Hurst exponent, H, estimated with R/S analysis. For a time series $X(t)$, the record is divided into subsets of length τ, the time lag. The rescaled range is defined as $R'(\tau) \equiv R(\tau)/S(\tau)$, where $S(\tau)$ is the standard deviation of the subset and

$$R(\tau) = \max_{1\le k\le\tau} W(k,\tau) - \min_{1\le k\le\tau} W(k,\tau) \quad \text{(range)},$$

$$W(k,\tau) = \sum_{t=1}^{k}(X_t - \langle X\rangle_\tau) \quad \text{(cumulative deviation) and}$$

$$\langle X\rangle_\tau = \frac{1}{\tau}\sum_{t=1}^{\tau} X_t \quad \text{(mean)}.$$

If the rescaled range of the time series scales as $R'(\tau) \sim \tau^H$, the slope of the plot of $R'(\tau)$ versus the time lag τ on a doubly logarithmic plot is the Hurst exponent, H. The time lag usually starts at 2 and is increased by powers of 2 so that in a time series of $1,048,576 = 2^{20}$ points, for instance, the R/S plot has 20 points.

To gain intuition for R/S analysis, visualize a long time series. Divide the series up into sequential nonoverlapping intervals of length τ and subtract the mean of each interval from all values within that interval. Within each interval is a minimum and maximum value, the difference between which is the range, R. Also, each interval has a standard deviation, S. The rescaled range $R' = R/S$, in a sense, is a normalized range. The values of R' from all intervals of the same length are averaged. The division by S takes into account the fluctuations of the rest of the interval. Two intervals can have the same range but one may be very smooth, such as all zeroes, with the only fluctuations being the two excursions from zero to the minimum and maximum. The standard deviation of this interval is much smaller than that of the other interval that appears noisier because it has many nonzero values, not just the two excursions. R', then, is much greater for the smoother interval

because the range R represents much more 'abnormal' behavior for the series over this one time lag.

Do not get lost in absolute values of R', though. The point of this measure is not individual values but how the average value scale as the time lag is increased. After $R'(\tau)$ of all nonoverlapping intervals of the series are averaged, they are plotted versus τ on log-log axes. This is a nondecreasing function because the rescaled range for larger τ always includes that of smaller τ. The slope of the plot is an estimate of H and is in the range $[0, 1]$.

A value of $0.5 < H \leq 1$ implies correlations, $0 < H < 0.5$ anticorrelations and $H = 0.5$ lack of correlations [28]. After the work of Hurst and Mandelbrot, other methods for estimating H were found. Opinions in the literature differ over which method is best for calculating H. Other techniques for calculating H include scaled window variance [29], detrended fluctuation analysis [30] and structure functions [31]. Values of H estimated by different methods are very similar when in the correlated range ($H > 0.5$) [32, 33, 34]. The main results of this dissertation are for values of H in this range.

The simplest example of R/S analysis is for a sine curve, as shown in Figure 1.5. There is an obvious breakpoint in the plot at a time (arbitrary units) lag at approximately the period of the sine curve (the inverse of the frequency where a spike would be found in the spectrum of the same series). Below the break, $H = 1$ and above the break $H = 0$. $H = 1$ indicates the strongest positive correlations. All consecutive, nonoverlapping intervals of the sine curve of any time lag will have the same value of R'. As τ increases so does R' since a interval now includes more and more of a single period. When the time lag equals the period, the (rescaled) range is at its maximum. This is why the break occurs and why $H = 0$ above the break.

A random time series has $H = 0.5$ [28], a value that would be found for the time series of the uncoupled coin flippers. In the same way that the power spectra of three time series with different PDFs (binary, Gaussian and uniform) scale as f^0, R/S analysis finds $H = 0.5$ for all three series. Again, neither the spectrum nor the R/S analysis can differentiate the series; the PDF is needed.

An interesting application of using R/S analysis to calculate H is in evaluating various computer algorithms for pseudorandom number generators (PRNGs) [35]. In that study, the quality of various PRNGs is evaluated based on the length of a data series that can

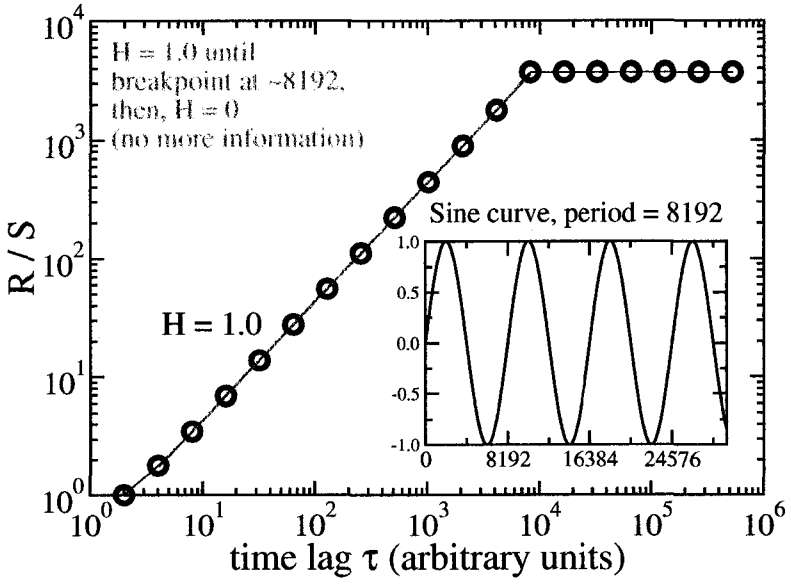

Figure 1.5. Time series and R/S analysis for a sine curve.

be produced where $H = 0.5$. The R/S plots show breakpoints at time lags approximately equal to known periodicities of the PRNG. PRNGs have been evaluated over the years in different ways; using R/S analysis does not necessarily shed new light on the quality of the generators but shows a correlation between random series of numbers and $H = 0.5$.

The R/S analysis for the AE index data from before is shown in Figure 1.6. As in the power spectrum, there is a break in the spectrum between two distinct power law regions. The causes of the high values of H in the AE index, indicating correlations in the data, have been studied by [36]. There is still no accepted theory to explain the breakpoint in the spectrum and R/S.

Algorithms exist that can generate Gaussian-distributed time series with arbitrary values of H in the range [0, 1]. These are called fractional Gaussian noise (fGn) [28]. The name comes from simple Gaussian noise which is made up of the increments of a random walk or Brownian motion. As said before, a random time series with a Gaussian PDF has $H = 0.5$ and $\beta = 0$. But this is just a special case of the more general fGn. Artificial fractional Gaussian noise can be made that has long time correlations or anticorrelations. When integrated, fGn produces fractional Brownian motion (fBm). Series of fBm with $H > 0.5$ are smoother than other series with smaller values of H (Figure 1.7).

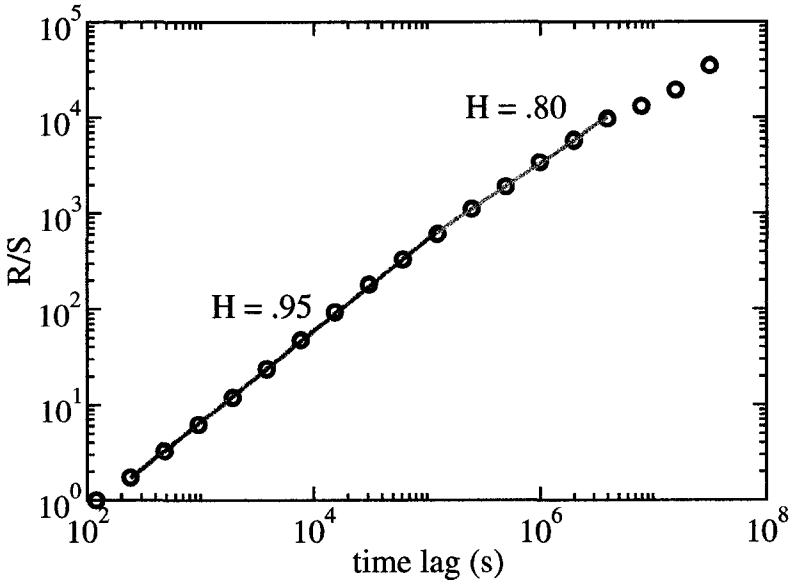

Figure 1.6. R/S analysis for AE index for 1980-1981. Data courtesy of World Data Center for Geomagnetism, Kyoto, Japan, `http://swdcdb.kugi.kyoto-u.ac.jp/`.

For a time series of values generated from a fGn algorithm, H is related to the slope of the power spectrum β by $\beta = 2H - 1$ [37]. But care must be taken when using this relation for a number of reasons. First, consider the time series X_B of a random walk (Brownian motion) whose increments are, by definition, Gaussian distributed. The increments themselves form a time series X_G, where $X_G(n) = X_B(n+1) - X_B(n)$. The power spectra of the two time series are related by $\beta_B = \beta_G + 2$, since X_B is the integration of X_G. In the relation $\beta = 2H - 1$, β stands for β_G so that $\beta_B = 2H + 1$, where H is calculated for the increments X_G, *not* the integrated X_B.

More importantly for this work, the relation $\beta = 2H - 1$ is derived for Gaussian statistics [37]. For SOC data in this study, which are not always Gaussian distributed, we find that this relation does not always hold; we demonstrate this in Chapter 3. There is no requirement imposed by R/S analysis that limits its use to only Gaussian distributed data just as there is no similar requirement for using the power spectrum. For the sandpile, we find that β and H are related differently depending on the time scale and drive regime over which they are measured.

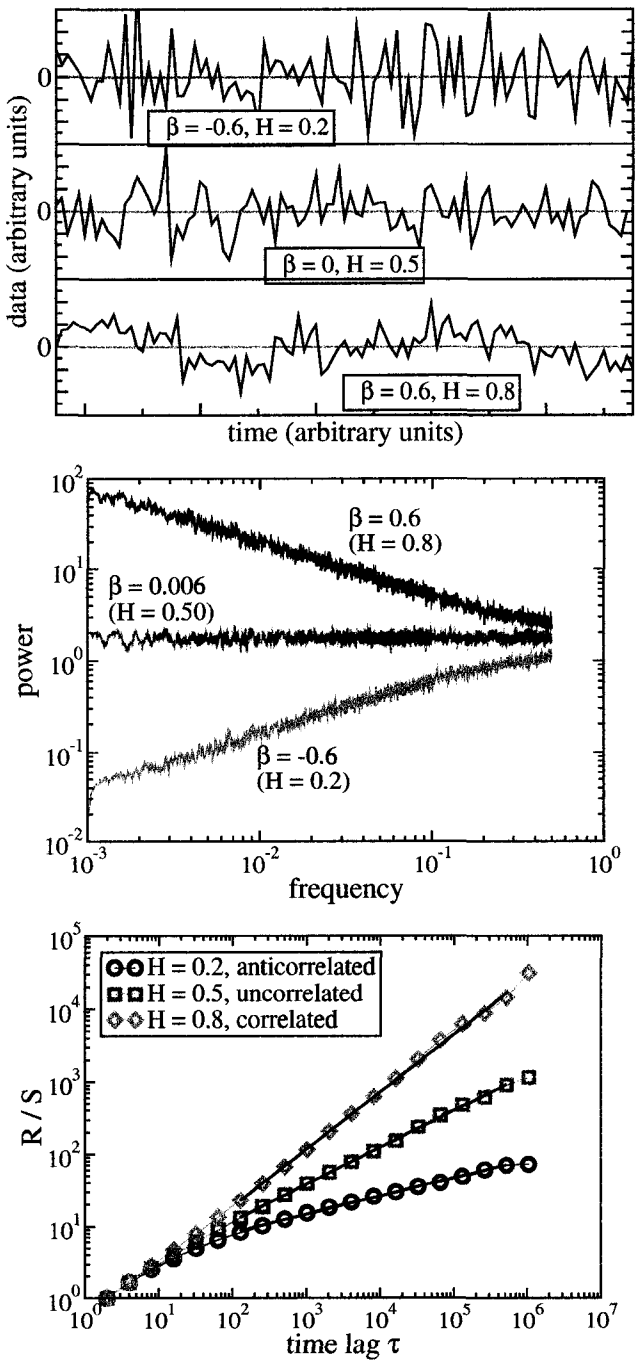

Figure 1.7. Time series, power spectra and R/S analysis of 3 samples of fractional Gaussian noise.

1.3 Self-Organized Criticality

In physics, dynamics has traditionally meant the study of systems evolving in time due to fundamental physical forces. We use a slightly more general definition here. We define a dynamical system as "a means of describing how one state develops into another state over the course of time."[38] Dynamics, then, is the study of how dynamical systems evolve in time. In a simple model, such as the one I study in this dissertation, rules are applied to the system so that it changes from one state to the next. The rules in good simple models represent underlying physical processes but there does not have to be a one-to-one mapping between the rules of the system and a fundamental physical force and there does not have to be a one-to-one mapping between a model time step and a human time step. Measures like the power spectrum and R/S analysis describe different characteristics (which we call dynamical characteristics) of a time series from a dynamical system. We want to understand what those measures say about how the system time behavior changes.

Self-organized criticality is a theory about dynamics that describes how certain large-scale complex behavior can emerge from a system of small-scale simple interactions. In terms of coin flippers, SOC systems can be modeled in the same way, as a coupled grid of agents whose behavior depends upon nearest neighbors. But we cannot push this analogy further because rather than just the state of the nearest neighbor, the knowledge of the gradients between neighbors is needed. In the processes that we study, besides information, a quantity, such as mass, density or stress, is also transported from one neighbor to another.

SOC concerns nonequilibrium systems that have, on average, a constant global gradient of some quantity that is maintained through two opposing mechanisms: an external forcing that increases the gradient and internal transport of the quantity that relatively quickly (to the forcing) reduces the gradient, an event known as an avalanche. A strong motivation for the development of and continued interest in SOC is the observation that many seemingly unrelated systems in nature display similar signatures of this complex behavior even though the underlying physics greatly differs from case to case. A substantial effort in the field, including this report, is to identify and to explain signatures from defined SOC models so that they can be compared with those of physical systems. If a system shares enough signatures with such models then the techniques and intuition about SOC can be applied to it. What is gained through this is an understanding of the system

on a conceptual level higher than that of simply knowing the rules of local interactions.

SOC is a joining of two terms, self-organized and criticality. The 'criticality' part comes from concepts in statistical mechanics. Recall the Ising model and ferromagnets. Above what is known as the Curie temperature, a ferromagnet has no magnetization. When the material is cooled, magnetization suddenly appears at the critical (Curie) temperature. At this temperature, in terms of the Ising model, the coupling strength is such that one vector flipping to spin up can cause a new cluster of spin up vectors to form. The size of the new cluster can be anywhere from a single vector to the order of the entire system. Disturbances in a system at the critical point are scale-free up to the size of the system. One feature of criticality concerns the correlation length. At temperatures above the Curie point, the correlation length is essentially zero, since disturbances do not propagate beyond the nearest neighbor. But at criticality, the correlation length is theoretically infinite; in practice, it is limited by the system size. A PDF of cluster sizes for a system at criticality scales as a power law, as does the PDF of avalanche sizes in a SOC system.

The 'self-organized' part of SOC means that, unlike the temperature of a ferromagnet, there is not a parameter that needs to be tuned in order for the system to be critical. That is, the system naturally evolves to criticality. Part of what this means is that the correlation length is on the order of the system size and the PDF of event sizes scales as a power law.

Books [3, 39] and numerous papers [40, 41] give detailed overviews of SOC. To get a flavor of the potential generality of the theory, an oft-used shortcut is to look at examples of the different systems that have been studied as possibly SOC. Such systems include ones mentioned above in the context of power laws, such as confined fusion plasmas [42, 43, 44, 45], the magnetosphere [46, 47, 6], tectonic systems [48], electrical power networks [49, 15, 16] and communication networks [17]. Note how very different these systems are from each other and that entire fields of study are devoted to separately understanding them. In short, what all of these systems seem to have in common are gradients that build up and persist and are then reduced in relatively quick bursts of activity. The signatures of some measures of this avalanching activity are remarkably similar in systems proposed as SOC.

If the mechanisms of SOC are possibly common to all of these systems, a fundamental question is raised: why would one expect there to be a common mechanism in these

systems? We discuss two answers to this: 1) different systems share analogous dynamical processes and 2) certain measures (or signatures) from a system are very similar to the same measures from other different systems. This second feature is not necessarily expected because the underlying physics of a particular system is often very different from that of others. Also, in many of these cases, the signatures themselves are not understood in terms of the fundamental physics. That is, models specific to a system that include all known low level physics do not always reproduce observed signatures.

In the same way that the Ising model reduces all physics to a grid of coupled vectors, a SOC model can reduce all physics in a system to four parameters that describe the analogous dynamical process: size, forcing, threshold and response. For a given system of finite size, an external agent randomly increases local gradients of some measure (such as heat or density, for example) at a statistically steady rate until one or more exceed a critical gradient, producing an event that transports and relaxes the local gradient(s). The relaxation event is referred to as an avalanche. The measure is conserved in that it enters the system via the external drive and exits at the boundary of the system. (Nonconservative models also exist [50] but we will not discuss them.) Such a general description can be applied to many systems in the world and this is the starting point in the SOC journey.

The notion of these discrete events is important in SOC and crucial to this dissertation. Seemingly discrete events are associated with many systems in nature: floods in rivers, earthquakes, real mud and snow avalanches, magnetic field vortices in superconductors, plasma bursts in tokamaks. These events, in the language of SOC, are all avalanches, all occur over large ranges of sizes and all have been studied as possible examples of SOC.

Given a system with a size, forcing, threshold and response, what are the *consequences* of such dynamics? That is, what are the signatures of a series of these discrete events? How do they change if the system is driven so strongly that the events overlap in time and/or space? The interaction of many avalanches over long times produces characteristic signatures of the system. These questions and these signatures are the subject of this dissertation.

Two of the more well-known examples of these signatures are regions in PDFs and in power spectra that scale as power laws. One signature of SOC is that avalanches of all sizes, from a single event up to ones that span the entire system, are possible and that the

probability distribution of these sizes is fit by a power law over a broad range. (Recall the criticality discussion above.) Power law power spectra imply long time correlation, since the power laws persist to low frequencies where the time scales are much longer than those of single avalanches.

Simply observing power law scaling in a system does not necessarily mean that it is SOC. Much in the literature discusses how power laws can occur without SOC as a mechanism (see, for example, [51] and references therein). So SOC implies more than just this type of signature. Other observed characteristics in model and possible SOC systems include: bursty time series that appear different from simple random noise, scaling of power law regions with system size, a relation between the different values of β for the PDFs and spectra [40] and structures in the transported quantity. Examples mentioned above exhibit some or all of these signatures. But no single model specific to any one system can reproduce all of these observed signatures. For instance, no known 'physics-based' plasma model, one based on classical plasma theory, reproduces all of these features that are regularly observed in confinement devices [52]. SOC is a simple general model that does qualitatively reproduce all of these signatures and this is why it has been proposed as a common mechanism.

Before turning to a discussion of SOC models, we emphasize that a key feature in a system that has SOC dynamics is that the time scales of the external drive and the internal avalanches are well-separated. The time taken by an avalanche to reduce a gradient is much shorter than that needed by the external forcing to build it up. But the nonlinear effect of a critical gradient limits the frequency of avalanches so that there is a long-term steady state where input is balanced by output.

1.4 SOC Models

Implicit in the above is that distinct events in a system can be identified but doing so is not necessarily trivial for physical or model systems. Identifying them is easier, though, in the SOC model that we use (the directed running sandpile) because this model is a cellular automaton with an output signal of nonnegative integers. When the model driving rate is very low, discrete events are easily identified as regular patterns of nonzero values in the time series separated by sequences of zeros (Figure 1.8(a)). This is one of the advantages

of using simple cellular-based models.

Here we describe the model that we use and give a brief overview of other SOC models. Jensen states the case of these models very well [39]:

> All the models are inspired by some physical system: sandpiles, earthquakes, magnetic vortex motion, forest fires, interface growth, or biological evolution. The models are defined in terms of a dynamical variable—for example, the local slope of the sand heap or the stress in the earthquake fault. The dynamical variable or field is updated in every time step according to some algorithm. The choice of the updating algorithm is, to some degree, arbitrary. The criteria for choosing the relevant definitions are, for the most part, simplicity and intuition. Statistical mechanicians have this overall belief that complexity arises from simplicity: that the intricate and complex behavior found in many systems is due to the large number of degrees of freedom. All the models described in this chapter are formulated according to this paradigm. In addition, they are all designed with an eye toward numerical ease and efficiency when simulated on computers.
>
> ...As always, when building models of Nature, one proceeds through steps of increasing refinement, and so also for models of SOC systems. Perhaps it is worth mentioning that just because a model doesn't capture *all* features of a specific system, this need not imply that the model doesn't capture *any* aspects at all.

The prototypical SOC model is known as the sandpile. The name was chosen to produce a good, simple mental picture, not because it models real sandpiles. There are many varieties of sandpile models; we will describe the one-dimensional directed one here and others below. Consider a one dimensional grid of L cells. Each cell contains an integer number of "sand grains"; this number is the height of the cell (Figure 1.9). Sand is added to each cell by a "rain" U_0 from above. That is, at each time step for each cell, there is a probability $0 < P_0 < 1$ that U_0 grains of sand will be added to it. For this study, $U_0 = 1$. The units of P_0 are grains per time step per cell. Total input current into the entire system is defined as $\overline{J_{IN}} = P_0 L$ grains per time step. The local gradient Z_n is the difference in height

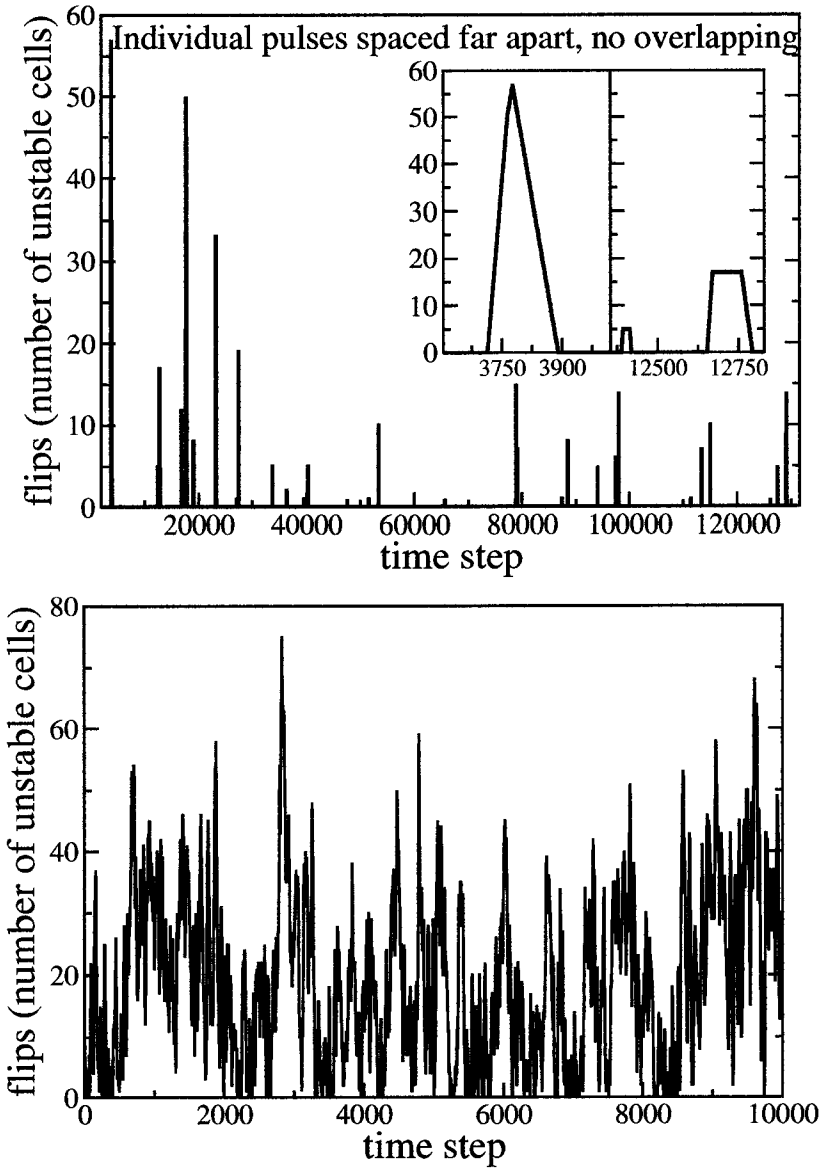

Figure 1.8. Flips time series from running sandpile model for low and high drive. Note the different scales on all axes. In the low drive case (a), there are approximately 30 distinct and separated events in $\sim 10^6$ time steps. In the high drive case (b) there is almost constant activity of many overlapping events in $\sim 10^5$ time steps.

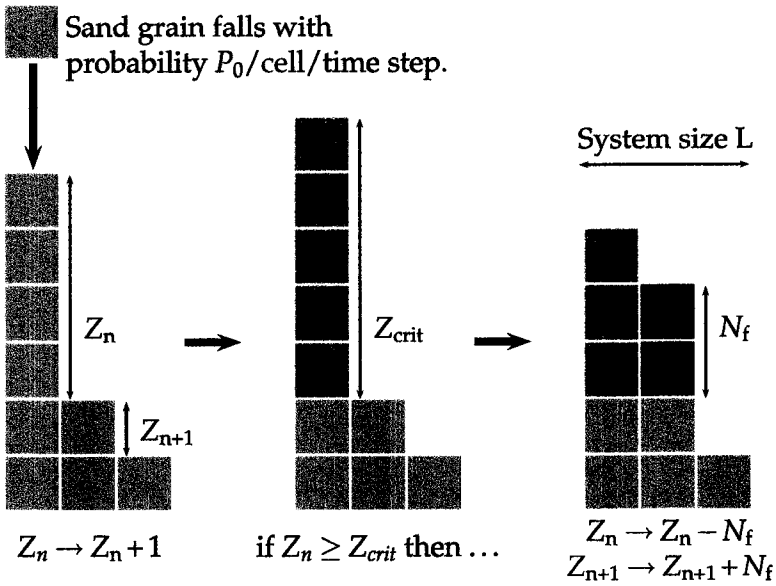

Figure 1.9. Rules of the one dimensional running sandpile.

between two neighboring cells. If this local gradient exceeds a critical gradient Z_{crit} then an avalanche occurs. An avalanche stabilizes the local gradient by transferring N_f grains of sand from the higher cell to the lower. This avalanche can make Z_{n+1} and/or Z_{n-1} unstable at the next time step so that the avalanche spreads to other cells. The size of the avalanche can be measured in three ways: the total number of cells reached, the total number of time steps with activity and the integration of the total number of active cells per time step. The PDF of each measure is fit by a power law [39]. Sand exits the sandpile only through the bottom cell when it is unstable. Because of the sandpile rules, the instantaneous output current $\overline{J_{OUT}}_I$ is either 0 or N_f. When the system is in steady state, the long time average output current equals the average input current, $\overline{J_{OUT}} = \overline{J_{IN}}$.

The picture of this model to keep in mind is of a thin (real) sandpile between two closely-spaced frictionless parallel vertical glass sheets on a table against a wall underneath a slow and steady rain of sand. The wall, table and pair of glass sheets define three orthogonal planes. The high end of the pile builds up against the wall while the low end empties off of the edge of the table. That is, mass is added equally (on average, over time) at all positions in the pile while it is lost at only one end. There is always an overall slope to the sandpile that is, on average, just below the critical threshold, Z_{crit}. Local gradients

do not always exceed the critical gradient so there are times of no activity in the sandpile. This is very different from a system that is governed by classical linear diffusion, where any gradient is always being reduced. This picture is only to visualize the geometry of the sandpile model, not the dynamics since inertial effects are excluded from the model. This is not a model about real sand but about the general dynamics of a system.

In the original sandpile model [2] $N_f = 1$ and $P_0 = 1$; the steady state consists of all local gradients equal to Z_{crit}. When a grain is added to a cell from the random rain, that grain tumbles successively to lower and lower cells until it falls off of the edge of the table, like a Slinky® walking down a flight of stairs. None of the above SOC signatures are observed in this model, though they do appear in two or more dimensions [2]. More interesting behavior occurs when $1 < N_f < Z_{crit}/2$, as in the model of [50]. This simple model exhibits all of the signatures and dynamical features described above, therefore it is defined or constructed as SOC. In both of these models, the rain of sand is suspended ($P_0 \rightarrow 0$) when an avalanche is taking place; we refer to this as *zero drive*. This ensures the separation of time scales needed in a SOC process but clouds the meaning of one time step.

In contrast, time is well-defined if the rain of sand continues with the same probability even when an avalanche is taking place. This is called the running sandpile and was studied for strong external forcing in [53]. Strong external forcing means that sand is added so fast that multiple avalanches often occur simultaneously, overlapping in time and sometimes in space. The forcing, though, is still weak enough so that a global steady state is maintained. For this study, the fixed parameters are $U_0 = 1$, $Z_{crit} = 8$ and $N_f = 3$. We explore a parameter space of the two remaining parameters, system size L and probability P_0. We find that P_0L^2 is a more convenient measure of the external forcing. We call this quantity the *effective driving rate* and discuss it further below.

This sandpile has been extended to two and more dimensions [2], has been driven periodically at just one site, has been made with two neighboring closed boundary conditions and two open (so sand piles up in a corner), has been directed and undirected [39]. The details of all of these models differ but the basic results are constant: SOC dynamics in the form of long time correlations, coherent structures and power law PDFs and spectra. The sandpile is robust to such fiddling as long as the fundamental parts of size, forcing, threshold and response remain.

These same ideas can be implemented and called by another name. Examples include nonconservative spring and block models, where stress is transferred among blocks on rough surfaces connected by springs. These are the earthquake models of Olami, Feder and Christensen (OFC) [54, 55]. Some of the stress is dissipated and the critical behavior remains. Another nonconservative model is that of the lattice gas [39], which uses a two dimensional grid where each cell is inhabited by zero or one 'gas molecules' that repel each other. At each time step, a particle is added with some probability. A new particle disturbs the system causing some particles to exit through open boundary conditions. This has been used as a model of travelling vortices in a superconducting sample [56].

Still another example of a simple SOC system is the forest fire model [57, 58] (in my opinion, this has the best visual imagery). Again there is a two dimensional grid of cells. In each cell, there may or may not be a tree. If there is a tree then there is a possibility that a lightning strike will set the tree on fire. A burning tree can set neighboring trees on fire and thus an event is defined. There is a probability that a cell with a dead tree will grow a new tree. The forest fire has been used to model the spread of disease in closed populations [59] and, more recently, to model blackouts in power and communication networks [49, 17, 15, 16].

All of these models have in common discrete nearest neighbor interactions and SOC-like dynamics. Their variety indicates the adaptability of SOC and simple models in general for reducing a system down to its fundamental elements. The ease of implementation on computers allows for relatively quick evaluation of whether or not the model is a good one for reproducing some of the signatures of the system under study and understanding its dynamics.

1.5 SOC and the Transport Problem in Fusion Plasmas

Since its introduction [53], interest and advances in the running sandpile model have been mainly motivated by research in confined plasmas, which have been studied as complex physical systems [60] and SOC systems [61, 42, 62, 43]. To understand why, we examine the transport issue. One of the most fundamental problems preventing economical nuclear fusion for energy production is the inability to attain a large enough triple product $n_i T_i \tau_E$, where n_i is the plasma ion density, T_i the ion temperature and τ_E the confinement time [63].

For fusion, the plasma must be hot enough and dense enough for a long enough time so that positive ions have enough energy and time to overcome electrical repulsion and fuse. Current technology can reach a triple product on the order of $10^{21} m^{-3}\ s\ keV$. Recent work in the Joint European Tokamak reaches to within approximately a factor of 2 or 3 of what is needed for controlled fusion [52]. Adequate densities and temperatures can be produced but not for long enough time because of confinement issues. Research in this area, then, includes changing machine and plasma parameters, trying to understand transport and measuring and understanding the change in confinement time.

Because of the high temperatures used in fusion research, plasma contained in a simple structure would melt its walls. Magnetic confinement devices, of which tokamaks are one, partially solve this problem by taking advantage of the electrically charged particles and trapping them in orbits around magnetic field lines within a toroidal structure. The plasma orbits along the closed field lines, winding toroidally and poloidally throughout the torus. There is a radial gradient in the magnetic field because of the curvature of the toroid. The density decreases from core to edge along a minor radius of a poloidal cross section and the magnetic field strength decreases along the major radius, from the center of the toroid towards the edge. Simple toroidal field lines are naturally unstable due to $\nabla \mathbf{B}$ and $\mathbf{E} \times \mathbf{B}$ drifts, so poloidal winding of the field lines are added to reduce these instabilities (Figure 1.10). The magnetic field lines can be manipulated with internal and external currents by methods that are beyond the scope of this dissertation. Refer to [64] for details.

Though the individual charged particles are confined to orbit about the magnetic field lines, diffusion still exists and greatly reduces the confinement time. Understanding transport via diffusion is critical for attaining fusion. SOC was introduced into confined plasma science because the two types of diffusion thought to produce the majority of plasma transport do not account for what is actually observed. The two types of diffusion are classical and turbulent, or anomalous.

Classical diffusion is due to collisional processes among orbiting ions that create radial drifts and maintain a negative density and temperature gradient from the core towards the walls (hotter and more dense in the core) for as long as plasma is injected into the device. The radial diffusion is referred to as cross-field drift since the collisions cause the ions to jump between neighboring field lines. Gyrorotating ions will collide and scatter

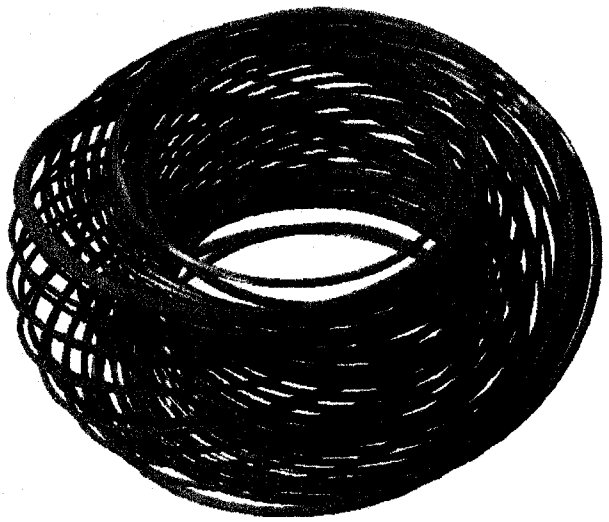

Figure 1.10. Image of simulated tokamak field lines. Note that they wind in poloidal as well as toroidal directions. Figure from `http://www.ornl.gov/sci/fed/mhd/iter_mag_field_only.gif`.

from their respective field lines to become retrapped on field lines that are farther from the center of the torus, where field density is less [65]. (Neoclassical diffusion also contributes to transport. This is when particles are trapped on closed loop field lines in the interior of the plasma; some of the shapes resemble certain tropical fruit and, therefore, are referred to as banana orbits.)

The rate of plasma transport due to this collisional process can be calculated from basic plasma physics. The flux by drift diffusion is $\Gamma_\perp = D_\perp \nabla n$, where $D_\perp$ is the cross-field or classical diffusion drift coefficient. The diffusion coefficient is derived as $\frac{\eta_\perp n \Sigma KT}{B^2}$, where $\eta_\perp$ is the plasma resistivity, T the plasma temperature, B the magnetic field strength and K Boltzmann's constant. The resistivity η scales as $(KT)^{-3/2}$ so $D_\perp$ decreases with increasing temperature. Confinement time is inversely proportional to $D_\perp$ so it should increase with temperature and field strength as $\sim T^{1/2}B^2$.

Confinement time increasing with temperature and magnetic field strength can be understood in another way. The gyroradius of a charged particle orbiting a field line is inversely proportional to the field strength. The velocity itself increases with temperature

and the gyroradius shrinks as B increases. Ions with smaller gyroradii and higher temperature are less likely to collide with ions on neighboring field lines, thereby decreasing collisional diffusion. Higher temperature means higher particle velocities which reduce the scattering cross section.

Early tokamaks were designed based on $D_\perp$ but once in operation, transport was observed to be much greater than expected [65, 60]. Anomalous, or turbulent, diffusion was then proposed as the mechanism that is responsible for the extra (that is, beyond classical) diffusion observed in confinement devices. Turbulence occurs when a gradient exceeds some critical value and the resulting diffusion is much greater than from collisional diffusion. Turbulent eddies form and advect larger amounts of density and temperature faster than through collisional processes. The average radius of these eddies is on the order of the ion gyroradius. A rough but useful picture is to think of transport as a random walk process along these eddies. (The eddies do not actually just statically remain; they appear and disappear as gradients become critical and 'turn on the turbulence.') The distance from center to edge divided by the average ion gyroradius gives the approximate number, N, of step sizes (eddies) in the random walk process. Since travel time in a random walk scales as N^2, doubling the poloidal radius of the device should increase confinement time by a factor of 4. This is called gyro-Bohm scaling. The 'gyro' refers to the scale of the gyroradii of the particle orbits.

Experimental work with many different devices showed that the actual diffusion coefficient scaled as $KT/16eB$. This is the Bohm diffusion coefficient, given by Bohm in 1946 [65]. Confinement time is seen to scale as $\sim B/T$, called Bohm scaling. Decreased confinement time means increased transport of heat or density. In terms of the random walk, confinement time was observed to scale only as N, not N^2. The small improvement in confinement time is not enough to reach the required triple product. The gap between this empirical value and the expected classical gyro-Bohm scaling of confinement time is the 'outstanding critical physics issue' in the field of magnetic confinement [63].

Two main goals of current research are to experimentally reduce scaling from Bohm to gryo-Bohm and to theoretically understand why the difference is there in the first place. These goals are complementary and often advances in one suggests understanding in the other. For the first goal, experimentalists can now consistently create a transition in plasma

from a low confinement regime, called L-mode, to a high confinement regime, H-mode. In L-mode, confinement time is low, closer to Bohm scaling while in H-mode it is closer to gyro-Bohm scaling [63].

While the machine parameters needed to create H-mode are somewhat well-known, the physics of it and L-mode is not completely understood. The main cause of anomalous cross-field diffusion is plasma turbulence [63]. Neutral fluid turbulence is an unsolved problem and adding charged particles to the mix greatly increased the complexity of the problem. Nonetheless, in plasma physics turbulence is known to normally be caused by a growing instability. The instability grows when a gradient in temperature or density exceeds some critical value. In order for the instability to remain unstable and produce the turbulence that could account for the anomalous diffusion, this critical gradient must be maintained. For example, one such proposed mode is due to a critical ion temperature gradient [66, 67].

However, the potential candidate plasma modes have not been found to be the causes of the anomalous diffusion. Experimentally, the necessary critical gradients have not been observed or they have been observed but they do not persist long enough to maintain the measured plasma transport. The gradients are often sub-critical yet transport persists. More fundamentally, the suspected but unproven modes are governed by short time and length scale physics but the increased transport is a system size effect. Gryo-Bohm scaling turbulence does exist, but it does not account for all of the observed anomalous diffusion. The low level fluctuation scales that are on the order of the ion gyroradius drive the modes so it is expected that such modes would produce transport that scales with the step size (gyroradius) [42]. In other words, if these modes are responsible for turbulent transport then it is expected that when the machine size increases the confinement time would increase proportionally. Instead, the transport increases with the system size so that the confinement time is not improved.

This is the entry point for SOC as a model for turbulent transport in plasma. The running sandpile, described above, maintains a steady state transport even while the average global gradient is sub-critical. The random rain of sand grains onto the sandpile is analogous to the background fluctuations in the heating of the plasma. The one dimensional sandpile can be used because of poloidal and toroidal symmetry in a tokamak. The high

side of the sandpile represents the hot, inner core of the tokamak and the low side the edge. The physics that drives the flux through the sandpile is on the smallest scale, the individual cell, which represents one localized turbulent eddy or gyroradius.

Even though the rules impose only local nearest-neighbor interaction, the SOC mechanism 'knows' how large the system is. Global transport scales with the system size, as larger sandpiles have larger avalanches. But there is nothing mystical about SOC; instead SOC is simply a statement of 'this is what happens when small scale gradients can grow and persist until exceeding some critical value and relaxing the gradient to sub-critical by transferring some quantity locally.'

This was the initial basis for the first papers reporting confined plasma as a SOC system [61, 42]. Current theories could not explain robust transport by sub-critical gradients that scaled with system size. Signatures of similar measures were then compared, such as the power spectra of the floating potential (Figure 1.4) [68]. These show multiple power law regions were found to be very similar to spectra of SOC models, such as the running sandpile. Long time correlations, shown by $H > 0.5$ were found in plasma edge turbulence [44] using rescaled range analysis. Such correlations are not expected from standard turbulent instabilities. Recently, coherent structures have been observed in devices (see Figure 1.11 for an image of a simulation) and the PDF of the sizes of such structures follow power law scaling [52]. To connect sandpile dynamics to more traditional analytical techniques, a one dimensional transport model of two coupled differential equations to describe critical-gradient fluctuations in plasma was written [45]. This model shows transport dynamics consistent with SOC and with observed plasma devices.

An early success in studying SOC to understand plasma transport came through investigations of sheared flow [62]. The one dimensional sandpile is used because of poloidal and toroidal symmetry but is mainly appropriate for modeling L-mode. In enhanced confinement modes, like the H-mode, there is strongly sheared poloidal flow, so that poloidal plasma velocities are higher farther from the core. Such sheared flow was added to the two-dimensional running sandpile and was found to decorrelate transport events and eliminate the largest events. A similar reduction in long time correlations in H-mode is seen in plasma devices. The generally accepted understanding provided by the sandpile experiments is that sheared flow tears apart coherent structures larger than a few gyro-

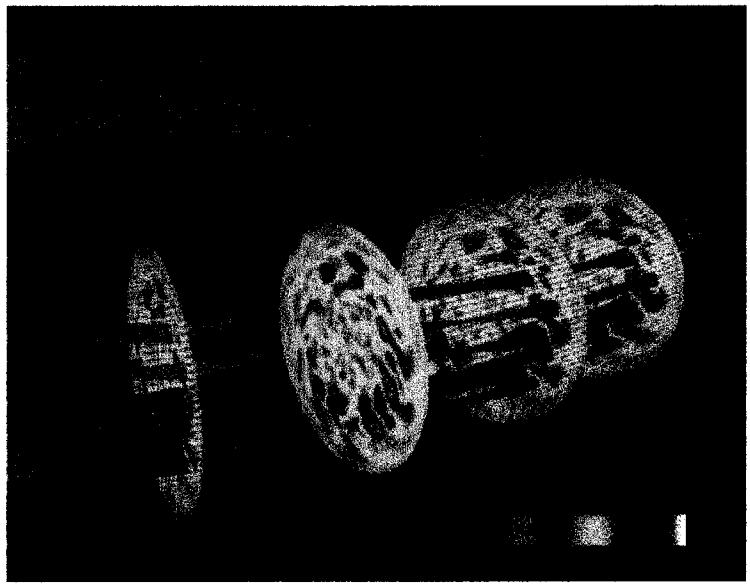

Figure 1.11. Image of simulated plasma turbulence along toroidal field lines and in poloidal cross sections of tokamak. Note the coherent structures in the poloidal cross sections. Figure from `http://www.ph.utexas.edu/dept/research/tajima/gtt.html`.

radii, so that large events cannot form.

After SOC had become a hot topic in confined plasma research it was studied for space plasma systems for many of the same reasons [13, 47]. For the coupled Sun-Earth system, fluctuations in the solar wind act as the random drive of the sandpile. Auroral events are potential avalanches but this is still speculative. Recent spectra (Figure 1.3, [18, 69]) and R/S analysis (Figure 1.6, [36]) of the AE index find signatures consistent with SOC.

1.6 Motivation for Dissertation

The work in this dissertation began as a deeper investigation of SOC as a model for plasma transport and then split into two branches. The first branch led to an exploration of the one dimensional running sandpile at very low driving rate; this branch concerns general SOC theory but we consider its results in the light of plasmas. The accepted standard reference on the running sandpile [53] had been studied and applied to SOC research since its publication in 1992 and it mainly concerned the sandpile at high driving rates. We found results that contradict some of those in that standard work, namely that there is no

low drive limit to have long time correlations in a SOC system. This is explored in Chapter 2. Chapter 3 fills in the gap between the low drive and high drive cases, resolving the split between Chapter 2 and [53]. Chapter 4 is an application of these results to space plasmas.

The second branch led to the application to confined plasmas described in Chapter 5. As mentioned above, the one dimensional running sandpile assumes poloidal symmetry. It also assumes that plasma avalanches simply travel radially along the same poloidal angle from core to edge. More likely is that there is poloidal and toroidal diffusion in such an event. By using the two dimensional running sandpile and having avalanches spread poloidally as well as radially, we can measure the effect on correlation lengths.

There is one more strong motivation for the work in this dissertation: SOC is a young science and we want to contribute to its growth. There is still much unknown about it and many misconceptions exist. This science needs more debate in the community to settle on what is more correct or complete.

A recent example [70] of a published misconception that the results in this dissertation contradict asks if earthquakes are examples of SOC. The authors base their conclusions on older results and claim that PDF signatures of earthquake data show that SOC is not a good model for such systems. We find this simply incorrect. Though earthquakes are not the focus of this dissertation, they were some of the first events suspected of being part of a SOC system when Bak, Tang and Wiesenfeld published the idea in 1987. Since this dissertation is a summation of work done in the most recent incarnation of my graduate school career, I include our one page Comment [8] to their Letter as Appendix A.

1.7 Statement of Work

Chapters 2 and 3 have been submitted for publication to *Physical Review E*. As of 13 August 2004 we have not received referee's comments. Chapter 4 was submitted to and accepted for publication in *Proceedings of the Conference on the Sun-Earth Connection*. The conference took place in Kona, Hawaii in February 2004; the proceedings will be published in October 2004. I attended and gave a talk at the conference about the research contained in the paper. Chapter 5 has not yet been submitted for publication but we will do so soon to *Physics of Plasmas*.

The ideas in this dissertation belong to a wonderfully productive and pleasant collab-

oration among David Newman, Ben Carreras, Raúl Sánchez and me. I would never have come up with all of the ideas that are contained here without them. But when they had ideas, questions, inspiration or suggestions specific to this dissertation, I did and still do the work to implement them. Since the submitted papers have multiple authors, 'we' is used instead of 'I.' In the same spirit, I use 'we' in the introduction and conclusions when appropriate. A rule of thumb is that 'we' refers to research results from the above collaboration and 'I' refers to my grunt work and my opinions.

With the exception of Appendix A, I typed every word that is in this dissertation, including the papers that have been submitted for publication to peer-reviewed journals. I personally and solely wrote the first draft of all 6 chapters—the Introduction, the Conclusions and the four research chapters in between. Except for where noted, all data and figures were made by me. I wrote the sandpile code that created the data, wrote the analysis code that calculated signatures and plotted my data with a really cool program called xmgrace. Once the first draft of each chapter was written, my advisor, David Newman, read a printed version and wrote comments in the margins, telling me where I was wrong, suggesting better wording and pointing out typos. I took his notes and made the appropriate changes, occasionally using his wording but more often using my wording to express his suggestions. For Chapters 2–4, I then sent electronic copies of this next iteration to our co-authors, Raúl and Ben. After reading them, they would email or phone David or me with specific comments. Again, I typed what was appropriate. At times I disagreed with one or more of the three and did not make changes. Appendix A contains a one page comment submitted to *Physical Review Letters*. Raúl Sánchez wrote the first draft of this and then sent it to David and me. We made comments and suggestions that Raúl Sánchez used. I made the sole figure using my data from my sandpile code.

Finally, to a lesser extent, the collaboration has expanded to Hilary Fletcher, Brad Werner, Renate Wackerbauer and the other members of my committee. Each of these kind people has read all or parts of this dissertation and has made comments and offered suggestions. Again, I implemented them in my own words but in a way that, hopefully, has smoothed the roughest edges enough to make this work acceptable.

Bibliography

[1] P. Bak, C. Tang, and K. Wiesenfeld. *Phys. Rev. Let.*, 59:381, 1987.

[2] P. Bak, C. Tang, and K. Wiesenfeld. *Phys. Rev. A*, 38(1):364–374, 1988.

[3] P. Bak. *How Nature Works*. Springer-Verlag, New York, 1996.

[4] R. Woodard, D. E. Newman, R. Sánchez, and B. A. Carreras. Building blocks of self-organized criticality, part I: the very low drive case. Submitted to PRE, 2004.

[5] R. Woodard, D. E. Newman, R. Sánchez, and B. A. Carreras. Building blocks of self-organized criticality, part II: transition from low to high drive. Submitted to PRE, 2004.

[6] R. Woodard, D. E. Newman, R. Sánchez, and B. A. Carreras. Kona. Accepted to Kona, 2004.

[7] R. Woodard, D. E. Newman, R. Sánchez, and B. A. Carreras. Spreading. To be submitted to POP, 2004.

[8] R. Woodard, D. E. Newman, R. Sánchez, and B. A. Carreras. Comment on "Do Earthquakes Exhibit Self-Organized Criticality?". Submitted to PRL, 2004.

[9] K. G. Wilson. *Sci. Am.*, 241:158, 1979.

[10] E. R. Berlekamp, J. H. Conway, and R. K. Guy. *Winning Ways for your Mathematical Plays, II: Games in Particular*. Academic Press, 1982.

[11] S. Wolfram. *Rev. Mod. Phys.*, 55:601–644, 1983.

[12] B. Gutenberg and C. F. Richter. *Ann. Geophys.*, 9(1), 1956.

[13] A. T. Y. Lui, S. C. Chapman, K. Liou, P. T. Newell, C. I. Meng, M. Brittnacher, and G. K. Parks. *Geophys. Res. Let.*, 27(7):911–914, 2000.

[14] V. M. Uritsky, A. J. Klimas, D. Vassiliadis, D. Chua, and G. Parks. *J. Geophys. Res.*, 107(A12):7–1 – 7–11, 2002.

[15] B. Carreras, D. Newman, I. Dobson, and A. Poole. *IEEE Trans. on Circuits and Systems, Part 1*, 2004. accepted March 2004.

[16] B. Carreras, V. E. Lynch, I. Dobson, and D. E. Newman. *Chaos*, 2004. accepted June 2004.

[17] D. E. Newman, B. A. Carreras, N. D. Sizemore, and V. E. Lynch. In *35th Hawaii International Conference on System Sciences*, Hawaii, 2002.

[18] B. T. Tsurutani, M. Sgiura, T. Iyemori, B. E. Goldstein, W. D. Gonzalez, S. I. Akasofu, and E. J. Smith. *Geophys. Res. Let.*, 17(3):279–282, 1990.

[19] Y. Kamide and G. Rostoker. *EOS*, 85(19):188, May 2004.

[20] R. F. Voss and J. Clarke. *Phys. Rev. B*, 13(2):556–573, 1976.

[21] W. H. Press. *Comments on Astrophysics*, 7:103–119, 1978.

[22] P. Dutta and P. M. Horn. *Rev. Mod. Phys.*, 53(3):497–516, 1981.

[23] B. B. Mandelbrot. *Multifractals and* $1/f$ *noise*. Springer-Verlag, 1999.

[24] E. Milotti. *ArXiv.org E-print Archive*, 2002. http://arxiv.org/abs/physics/0204033.

[25] V. M. Uritsky and M. I. Pudovkin. *Annales Geophysicae*, 16:1580–1588, 1998.

[26] T. Antal, M. Droz, G. Györgyi, and Z. Rácz. *Phys. Rev. Let.*, 87(24):240601–1–4, 2001.

[27] H. E. Hurst. *Trans. Am. Soc. Civ. Eng.*, 116:770, 1951.

[28] B. B. Mandelbrot. *Gaussian self-affinity and fractals*. Springer-Verlag, 2002.

[29] M. J. Cannon, D. B. Percival, D. C. Caccia, G. M. Raymond, and J. B. Bassingthwaighte. *Physica A*, 1997.

[30] C.-K. Peng, S. V. Buldyrev, S. Havlin, M. Simons, H. E. Stanley, and A. L. Goldberger. *Phys. Rev. E*, 49(2):1685–1689, 1994.

[31] C. X. Yu, M. Gilmore, W. Peebles, and T. Rhodes. *Phys. Plasmas*, 10(7):2772–2779, 2003.

[32] J. B. Bassingthwaighte and G. M. Raymond. *Annals of Biomedical Engineering*, 22:432, 1994.

[33] J. B. Bassingthwaighte, L. S. Liebovitch, and B. J. West. *Fractal Physiology*. Oxford University Press, 1994.

[34] M. Gilmore, C. X. Yu, T. Rhodes, and W. Peebles. *Phys. Plasmas*, 9(4):1312–1317, 2002.

[35] B. M. Gammel. *Phys. Rev. E*, 58:2586, 1998.

[36] C. P. Price and D. E. Newman. *J. Atmos. Sol. Terr. Phys.*, 63:1387–1397, 2001.

[37] B. D. Malamud and D. L. Turcotte. *Adv. Geophys.*, 40:1–87, 1999.

[38] E. W. Weisstein. Dynamical System. From MathWorld–A Wolfram Web Resource. http://mathworld.wolfram.com/DynamicalSystem.html.

[39] H. J. Jensen. *Self-Organized Criticality: Emergent Complex Behaviour In Physical And Biological Systems*. Cambridge University Press, Cambridge, 1998.

[40] J. Davidsen and M. Paczuski. *Phys. Rev. E*, 66:050101(R), 2002.

[41] A. Vespignanni and S. Zapperi. *Phys. Rev. E*, 57(6):6345–6362, 1998.

[42] D. E. Newman, B. A. Carreras, P. H. Diamond, and T. S. Hahm. *Phys. Plasmas*, 3:1858, 1996.

[43] B. A. Carreras, D. Newman, and V. E. L. et al. *Phys. Plasmas*, 3(8):2903–2911, 1996.

[44] B. A. Carreras, B. P. van Milligen, and M. A. P. et al. *Phys. Rev. Let.*, 80:4438, 1998.

[45] L. Garcia, B. A. Carreras, and D. E. Newman. *Phys. Plasmas*, 9(3):841–848, 2002.

[46] T. S. Chang. *Phys. Plasmas*, 6:4137–4145, 1999.

[47] S. C. Chapman and N. W. Watkins. *Space Sci. Rev.*, 95, 2001.

[48] D. L. Turcotte. *Fractals and Chaos in Geology and Geophysics*. Cambridge University Press, 2nd edition, 1997.

[49] B. Carreras, V. E. Lynch, I. Dobson, and D. E. Newman. *Chaos*, 12(4):985–994, 2002.

[50] L. P. Kadanoff, S. R. Nagel, L. Wu, and S. min Zhou. *Phys. Rev. A*, 39(12):6524–6537, 1989.

[51] D. Sornette. *Critical Phenomena in Natural Sciences—Chaos, Fractals, Selforganization and Disorder: Concepts and Tools*. Springer, 2000.

[52] D. E. Newman. Personal communication. Personal communication.

[53] T. Hwa and M. Kardar. *Phys. Rev. A*, 45:7002, 1992.

[54] Z. Olami and K. Christensen. *Phys. Rev. A*, 46:R1720, 1992.

[55] Z. Olami, H. J. S. Feder, and K. Christensen. *Phys. Rev. Let.*, 68:1244, 1992.

[56] W. J. Yeh and Y. H. Kao. *Phys. Rev. Let.*, 53:1590, 1984.

[57] B. Drossel and F. Schwabl. *Phys. Rev. Let.*, 69:1629, 1992.

[58] B. Drossel and F. Schwabl. *Physica A*, 199:183, 1992.

[59] C. Rhodes and R. Anderson. *Nature*, 381:600, 1996.

[60] B. B. Kadomtsev. *Tokamak Plasma: A Complex Physical System*. Institute of Physics Publishing, 1992.

[61] P. H. Diamond and T. S. Hahm. *Phys. Rev. Let.*, 2:3640, 1995.

[62] D. E. Newman, B. A. Carreras, and P. H. Diamond. *Phys. Let. A*, 218:58–63, 1996.

[63] B. A. Carreras. *IEEE Trans. on Plasma Sci.*, 25(6):1281–1321, 1997.

[64] T. Kammash. *Fusion Reactor Physics: Principles and Technology*. Ann Arbor Science Publishers, 1975.

[65] F. F. Chen. *Introduction to Plasma Physics and Controlled Fusion*, volume 1: Plasma Physics. Plenu Press, 2nd edition, 1988.

[66] T. S. Hahm and W. M. Tang. *Phys. Fluids B*, 1:1185, 1989.

[67] H. Biglari, P. H. Diamond, and M. N. Rosenbluth. *Phys. Fluids B*, 1:109, 1989.

[68] M. A. P. *et al. Phys. Rev. Let.*, 82(18):3621, 1999.

[69] G. Consolini, M. F. Marcucci, and M. Candidi. *Phys. Rev. Let.*, 76(21):4082–4085, 1996.

[70] X. Yang, S. Du, and J. Ma. *Phys. Rev. Let.*, 92:228501, 2004.

Chapter 2
Building Blocks of Self-Organized Criticality, Part I: The Very Low Drive Case

Abstract

We describe new analyses and signatures of the self-organized critical one dimensional directed running sandpile model of Hwa and Kardar [Phys. Rev. A **45**, 7002 (1992)]. We present results for extremely low levels of external forcing of this SOC model and show that correlations in the dynamics exist over very long time scales regardless of how low this driving rate is. This demonstrates that a SOC system has nontrivial dynamics even when the system's events do not overlap in space or time. A consequence of this is that the power spectral and rescaled range (R/S) analysis signatures of the SOC time series for very weak forcing are very different from a simple random superposition of pulses.

2.1 Introduction

Self-organized criticality (SOC) [1, 2] is a dynamical framework that describes how certain large-scale complex behavior can emerge from a system of small-scale simple interactions. SOC concerns the dynamics of nonequilibrium systems that have a local critical threshold. If this threshold is constant throughout the entire system, then an average constant global gradient is maintained through two opposing mechanisms: an external forcing that increases the gradient and internal transport of the quantity that reduces the gradient. The relaxation of the gradient usually occurs in a series of aperiodic bursts, called avalanches in SOC lingo. The avalanche mechanism allows for stable gradients to exist in the system and contrasts with linear diffusion, which constantly acts to reduce any gradient. In SOC, the avalanches take place on time scales that are much shorter than those of the external forcing.

Books [3, 4] and numerous papers [5, 6] have been written to give detailed overviews of SOC. To get a flavor of the potential generality of the theory, an oft-used shortcut is to look at examples of the different systems that have been studied as possibly SOC. Such systems include, among others, confined fusion plasmas [7, 8, 9, 10], the magnetosphere [11, 12, 13], tectonic systems [14], electrical power networks [15, 16, 17] and communication networks [18]. Note how very different these systems are from each other and that entire fields of

study are devoted to separately understanding them. In short, what all of these systems seem to have in common are gradients that build up and persist and are then reduced in relatively quick bursts of activity. The signatures of some measures of this avalanching activity are remarkably similar in systems proposed as SOC.

SOC may be, then, a common mechanism in many different physical systems. To investigate whether or not a system is consistent with SOC, a defined model must be used to compare its signatures and features with those of the system under study; there are many SOC models. The rest of this paper is devoted to analyzing one such model, the one dimensional directed running sandpile.

[19] studied this model for strong external forcing and found that when avalanche events overlap in space and time there is a hydrodynamic regime of intermediate time scales over which long time correlations in the dynamics exist. These time scales are greater than the longest duration of a single avalanche and the power spectrum in this region is shown to scale as $1/f$. This is important because power law scaling of the spectrum is one of the common features of systems proposed to be SOC and the specific $1/f$ scaling of many systems has been a longstanding puzzle since before the introduction of SOC (see, for instance, [20]). [19] also looked at weak forcing, when single events do not overlap in space or time, and found that the signatures of their sandpile model at weak forcing are consistent with those of random superpositions of pulses (an analytical treatment of this is given in [21] and [22]). That study concludes that overlapping is necessary in order for this system to have "interesting temporal fluctuations such as $1/f$ noise...."

In contrast, we will show that interesting, nontrivial dynamics can exist at all driving rates in this system, including extremely weak forcing when single events do not overlap in time. To do so we have to probe very long time scales where the dynamics and effects of weak forcing appear. We find that the strong forcing case studied previously is the limiting case of the more fundamental weak forcing results presented here. Specifically, we will show that a SOC time series cannot simply be approximated by a random superposition of pulses or signals. Long time correlations among separate avalanches always exist in the series regardless of the strength of the external forcing and regardless of whether or not avalanches overlap in time. The correlations are due to memory stored in the local gradients of the system. We quantify correlations with the power spectrum and rescaled

range analysis and find that the latter is a more consistent measure of correlated dynamics than the former. The comparison of these two measures reveals that the dynamics that produces a $1/f$ region at high drive is also present at low drive, though now the spectrum scales as $f^{-\beta}$ with $\beta < 1$.

2.2 Model

The prototypical SOC model is known as the sandpile. The name was chosen to produce a good, simple mental picture, not because it necessarily models real sandpiles. There are many varieties of sandpile models [2, 23, 4]; we will only describe the one dimensional directed running sandpile of [19]. In addition to general SOC theory, this model is useful in studying physical systems where the dynamics can be reduced to a one dimensional approximation. One example of this is a fusion plasma confined in a tokamak [24, 7], where, because of toroidal and poloidal symmetries, plasma transport can be approximated by a steady gradient in one dimension. The single dimension can represent gradient-driven turbulent transport of plasma, heat and density from the hot dense core to the cooler, less dense edge of the tokamak.

Consider a single column of L cells. Each cell contains an integer number of "sand grains"; this number is the height of the cell. Sand is added to each cell by a "rain" U_0 from above. That is, at each time step for each cell, there is a probability $0 < P_0 < 1$ that U_0 grains of sand will be added to it. The units of P_0 are grains per time step per cell. Average input current into the entire system is then $\overline{J_{IN}} = P_0 L$ grains per time step. The local gradient Z_n is the difference in height between two neighboring cells. If this local gradient exceeds a critical gradient Z_{crit} then an avalanche occurs. An avalanche stabilizes the local gradient by transferring N_f grains of sand from the higher cell to the lower. This avalanche can make Z_{n+1} and/or Z_{n-1} unstable at the next time step so that the avalanche spreads to other cells. In this way, spatially and temporally extended events in a system can occur. This sandpile can be extended to two or more dimensions [2] but, again, we will only discuss the one dimensional case.

The time scales of the external drive and the internal relaxations are well-separated in a defined SOC system. For the sandpile, this can be accomplished in two ways: by using the zero drive model or by using the running sandpile model with low driving rate. In

the zero drive model, the rain of sand is suspended ($P_0 \rightarrow 0$) when an avalanche is taking place. This ensures the separation of time scales needed in a SOC process but clouds the meaning of one time step. In contrast, time is well-defined in the running sandpile, where the rain of sand continues with the same probability even when an avalanche is taking place. For this study, the fixed parameters are $U_0 = 1$, $Z_{crit} = 8$ and $N_f = 3$. We explore a parameter space of the two remaining parameters, system size L and probability P_0.

The time series that we analyze is called the flips—all of the analyses in this paper are of this specific type of sandpile data. Flips are defined as the total number of unstable sites (where $Z \geq Z_{crit}$) at each time step in a sandpile model in steady state. An unstable cell flips N_f grains of sand to the next cell. The total flips at each time step can be thought of as the instantaneous (potential) energy dissipation in the system. Avalanches in a flips time series appear as structures—multiple sequential nonzero flips separated by periods of inactivity, or quiet times. Quiet times are Poisson distributed because of the random drive of the system. See [25, 26] for detailed discussions of quiet times.

2.3 Methods

This model is a dynamical system; a characteristic of such systems that can quantify the dynamics is long time correlations. We study long time correlations with the power spectrum and rescaled range (R/S) analysis. The power spectrum is defined as the square of the Fourier transform, $S(f) = |F(f)|^2$, where $F(f) = N^{-1}\sum_{t=0}^{N-1} X(t)e^{-i2\pi(f/N)t}$. For a finite real time series, the spectrum also equals the Fourier transform of the autocorrelation function of the time series.

What does the power spectrum say about correlations in a series? More appropriate here, what does a power spectrum that scales as a power law $f^{-\beta}$ have to say about correlations in a series? We can qualitatively answer this. For $\beta > 0$, the low frequencies are more important in the dynamics so the series tends to look relatively smooth and trends persist. Such series are said to be correlated. For $\beta < 0$, the high frequency components are more important and the series is very rough. Trends do not persist long and the series is called anticorrelated. Truly random noise, with neither correlations nor anticorrelations, has a spectrum that scales with $\beta = 0$.

Another measure of correlations is the Hurst exponent, $H \in (0,1)$ [27]. A value of

$H > 0.5$ implies correlated dynamics, $H < 0.5$ anticorrelated and $H = 0.5$ uncorrelated. Opinions in the literature differ over which method is best for calculating H. Each of the various methods has strengths and weaknesses. We measure H by using R/S analysis [27, 28, 29], though there are other techniques, such as scaled window variance [30], detrended fluctuation analysis [31] and structure functions [32]. For reference, an application of using R/S analysis to calculate H is in evaluating various computer algorithms for pseudorandom number generators (PRNGs) [33]. In that study, the quality of various PRNGs is evaluated based on the length of a data series that can be produced where $H \approx 0.5$.

The rescaled range is defined as $R'(\tau) \equiv R(\tau)/S(\tau)$, where $S(\tau)$ is the standard deviation and

$$R(\tau) = \max_{1 \le k \le \tau} W(k,\tau) - \min_{1 \le k \le \tau} W(k,\tau) \quad \text{(range)},$$

$$W(k,\tau) = \sum_{t=1}^{k} (X_t - \langle X \rangle_\tau) \quad \text{(cumulative deviation) and}$$

$$\langle X \rangle_\tau = \frac{1}{\tau} \sum_{t=1}^{\tau} X_t \quad \text{(mean)}.$$

If the rescaled range of the time series scales as $R'(\tau) \sim \tau^H$, the slope of the plot of $R'(\tau)$ versus the time lag τ on a doubly logarithmic plot is the Hurst exponent, H. We use both the power spectrum and R/S analysis to characterize correlations.

2.4 Results

The study reported here is of the SOC sandpile model for very low external forcing. Very low drive can be defined empirically by examining the flips time series and choosing cases where individual avalanches are distinct and well-separated by quiet times, that is, where there is no overlapping of events.

In [34], we show that this criterion is satisfied by $P_0L^2 \ll 1$, where P_0L^2 is the *effective driving rate*. We use P_0L^2 instead of the average input rate P_0L because the former takes into account both the total flux into the system and the system size itself. This is important because a given total flux P_0L that, for a large system, is weak enough that avalanches do not overlap in time may actually be very strong for a much smaller system so that avalanches do overlap in time. Therefore, P_0L is effectively larger for a smaller system.

Using the effective driving rate allows systems of different sizes and strengths of forcing to be compared.

Figure 2.1(a) shows a flips time series of a very low drive case for L = 200 and $P_0L^2 = 0.2$. As seen in the inset plots, the characteristic shape of an avalanche is a trapezoid because of the rules of the sandpile. In other words, the pulse shape is due to the lowest level physics of the system. These trapezoids are the building blocks of the sandpile time series. An avalanche grows in size with time; this corresponds to the left sloping edge of the trapezoid. Once it reaches its maximum size the avalanche either immediately shrinks or stays the same size for a number of time steps; this latter case corresponds to the flat part of the trapezoid. In either case, the avalanche shrinks in size with time until it ends; this process corresponds to the right sloping edge of the trapezoid. Now the flips are zero again, indicating no unstable cells in the sandpile. Notice that no spatial information is conveyed by a flips time series. An avalanche in the sandpile can move up the pile, down the pile or stay in the same location as it grows and then shrinks in size. Also, multiple avalanches can occur simultaneously in distant regions of the system (though not typically in the low drive case). But each of these examples can appear identical in the flips time series (Figure 2.1(b)).

The power spectrum and R/S analysis for flips time series of different sizes of sandpile are shown in Figure 2.2. Five distinct regions are seen in the power spectrum and six in the R/S. We label the different regions and breakpoints as in the sketches in Figure 2.3 and analyze them below. The cartoons are drawn in the spirit of Figure 6 of Reference [19]. Short annotations indicating the cause of each region are printed on each cartoon. The most interesting and significant region is the SOC region D: it is the only region that is due simply to long time correlations in the system. Though SOC implies more than just long time correlations, that specific characteristic is at the root of region D so our naming convention in this paper is to refer to this region as the SOC region. To fully understand its causes, we first explain regions A, B and C.

2.4.1 Regions A and B: Pulse Shapes

In the spectrum, regions A and B scale as $\sim f^{-\beta}$ with $\beta \approx 3.4$ and $\beta \approx 2$. These regions are due to the single trapezoidal pulses that represent avalanches in the time series. This was

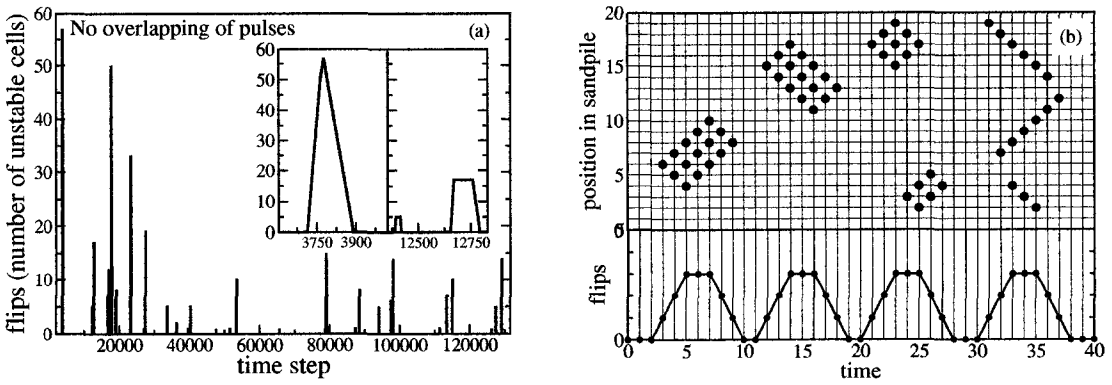

Figure 2.1. Partial flips time series from running sandpile model for low drive and space-time diagram and flips time series of separate avalanches. There are approximately 30 distinct and separated events in $\sim 10^6$ time steps. In space-time diagram, solid circles in upper figure represent unstable (avalanching) cells. Flips time series, lower figure, is a record of total number of unstable cells at each time step. Structures in flips time series do not give information of location, size, number or direction of avalanches, since the same structure can be produced in multiple ways.

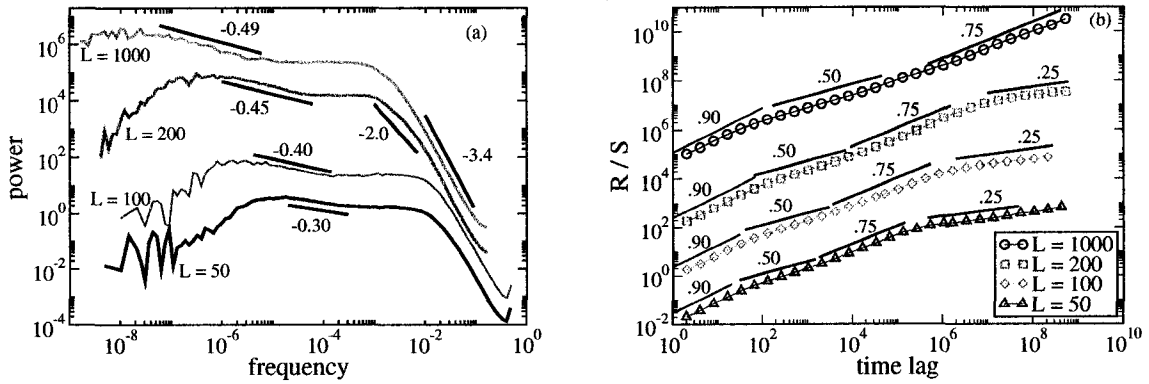

Figure 2.2. Power spectra and R/S analysis of flips for low drive sandpile for $P_0L^2 = 0.2$ and L = 50, 100, 200, 1000. Plots have been shifted along the y axes for better viewing. The solid lines are power laws plotted with the labeled exponent; they are not fits to the data.

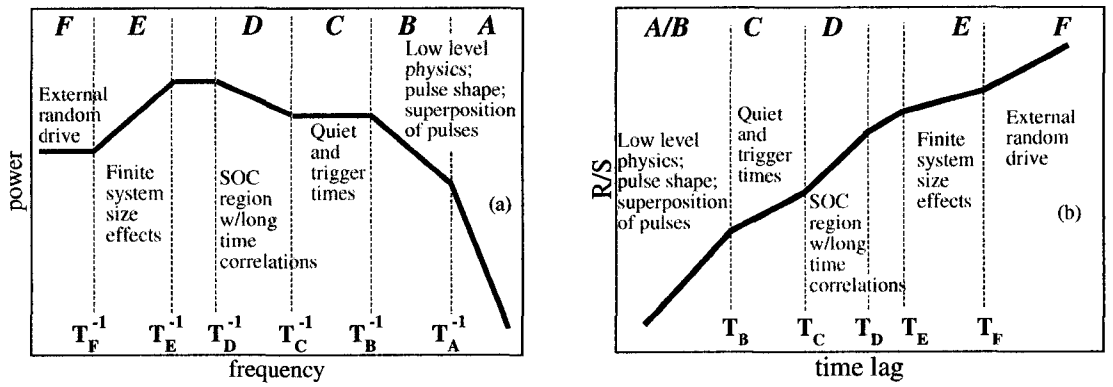

Figure 2.3. Cartoons of distinct regions and their breakpoints and causes of power spectra and R/S analysis of sandpile flips.

noted for the high drive case in [19] for a single region A but here we add to that an analysis of the slopes and breakpoints of both regions. To isolate the effect of the pulses from the dynamics, we randomly shuffle the time series, keeping the trapezoids intact but placing them randomly in time. The spectrum and R/S analysis are both shown in Figure 2.4, along with the spectrum of the original unshuffled time series. The spectra and R/S plots of the shuffled and SOC data are identical at short time scales because they share identical shapes. That the values of T_B^{-1} from the two series—SOC and shuffled—are identical says that the reason is not due to dynamics but instead to the shapes of the pulses.

The R/S analysis shows a strongly correlated Hurst exponent, $H \approx 0.9$, up to T_B because a defined shape, such as a trapezoid, is correlated with itself up to its width. There is no breakpoint between regions A and B in the R/S analysis because this only measures correlations not shape. We test this by replacing all trapezoids in both time series with rectangles of the same width and height as the corresponding trapezoid. The resulting R/S analysis is unchanged, since it still simply measures the correlations of the pulses with themselves. The cutoff T_B (and T_B^{-1}) remains the same as before since the widest pulse has not changed. The only difference is in the power spectrum, where regions A and B are replaced by a single region that scales as f^{-2}. This is a demonstration of the results of [21] and [22].

Three features must be discussed to fully explain the high frequency regions of the spectrum: 1) the breakpoint T_B^{-1} between regions C and B; 2) the presence of two power law

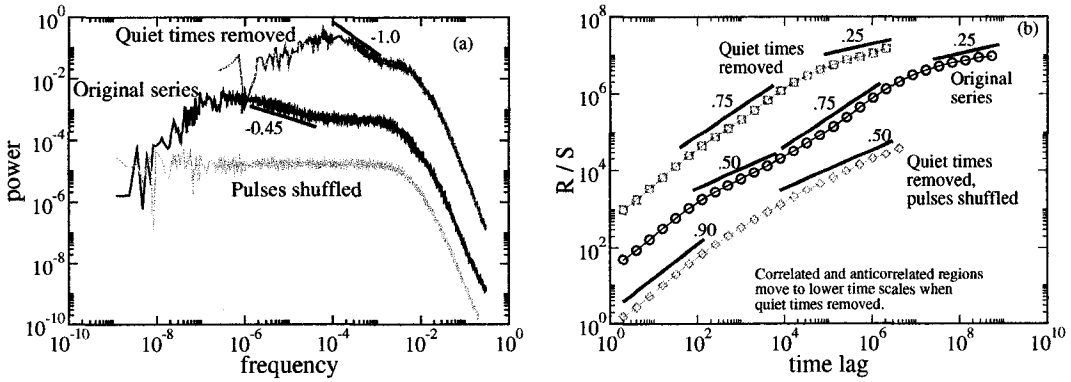

Figure 2.4. Power spectra and R/S analysis of low drive sandpile: original series, with quiet times removed and with pulses shuffled. Plots have been shifted along the y axes for better viewing. The solid lines are power laws plotted with the labeled exponent; they are not fits to the data.

scaling regions above T_B^{-1} and the breakpoint between them; and 3) the slopes of regions A and B. Breakpoint T_B^{-1} is due to the average duration of an avalanche, the two power law regions A and B are due to the trapezoidal pulse shape of an individual avalanche and the slopes of these two regions are due to the superposition of many nonoverlapping individual avalanches (trapezoids).

To explain these high frequency regions, we note that the power spectrum of a single trapezoid of width $W = 2(a+b)$ and height A, as defined in Figure 2.5, is

$$P_{\text{trap}}(\omega) = |F_{\text{trap}}(\omega)|^2 =$$

$$\left\{ \frac{2A}{b\omega^2} [\cos(\omega a) - \cos(\omega(b+a)) + b\omega \sin(\omega a)] \right\}^2 .$$

For convenience, we have used $\omega = 2\pi f$. The scaling behavior of this function depends upon the ratio a/b. When $a/b \lessapprox 1$ the trapezoid is more triangular and two scaling regions of ω^0 and ω^{-4} appear with a breakpoint between them at $\omega \approx W^{-1} \approx b^{-1}$. (Figure 2.5). When $a/b \gg 1$ the trapezoid is more rectangular and three scaling regions appear with two breakpoints, $\omega_1 \approx W^{-1} \approx a^{-1}$ and $\omega_2 \approx b^{-1} > a^{-1}$. As in the more triangular case, the lowest and highest regions scale as ω^0 and ω^{-4}, respectively but in the new middle region the spectrum scales as ω^{-2}.

Since there are three scaling regions in the sandpile spectra that scale similarly to those of a single trapezoid, we conclude that most of the avalanches have durations much longer

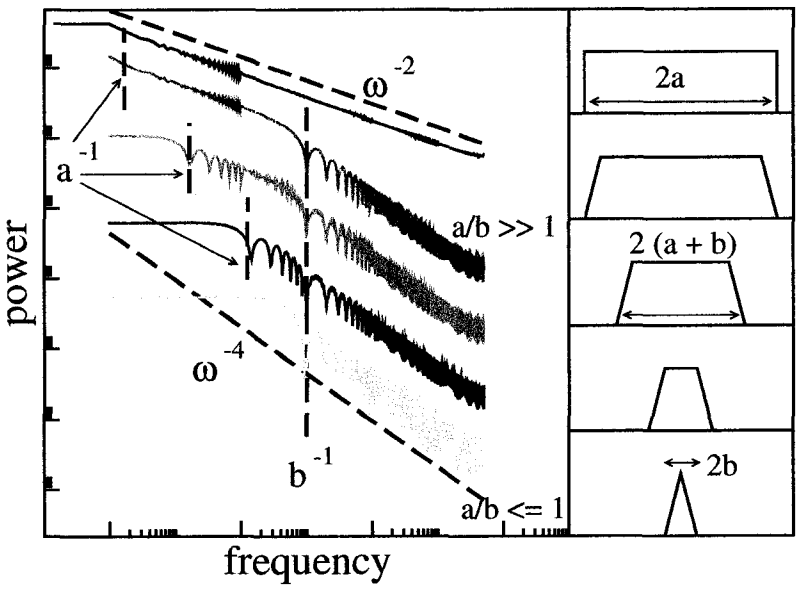

Figure 2.5. Cartoon definitions of trapezoidal, rectangular and triangular pulses and power spectra of 5 trapezoids with changing a and b.

than the sum of their growth and decay times, as this is the $a/b \gg 1$ condition for a trapezoid. Therefore the first breakpoint T_B^{-1} must be a measure of the average duration. T_B is on the same order as but less than L, since the majority of avalanche durations will be less than the system size. (Some can be larger because occasional large continuous events propagate up and down the sandpile, like waves sloshing back and forth in a tank.)

The slope of the spectrum in region A (≈ 3.4) is flatter than that found for a single trapezoid (= 4) because of a process that 'contaminates' the f^{-4} spectrum with f^{-2} and f^0 contributions. Not all of the trapezoids in the time series are of width $T_B \approx$ L. Most are smaller so that the cutoff in frequency space for their spectra will be at higher frequencies. That is, the cutoff due to, say, a trapezoid of width L/n occurs at n times the frequency of that due to a large trapezoid of width L. This means that the f^{-2} and f^0 regions of the smaller pulses occur at higher frequencies and tend to reduce $\beta = 4$ of the larger pulses. While this flattens the slope in region A it does not do the same in region B.

Before leaving regions A and B we address two of the assumptions of [21] and [22]: 1) events are well-approximated as rectangular pulses and 2) events in a superposition are *random* and independent. These assumptions are not appropriate for the flips time series

of a SOC sandpile model. The first of these is contradicted by the high frequency $\beta \approx 3.4$ region of the sandpile spectrum. If the fundamental pulse shape were rectangular, then this region would be a continuation of the middle $\beta \approx 2$ region; there would be only two regions (counting the flat one for $\omega \ll \omega_0$). This is not just trivia or a pedantic argument to stake a claim for the 'proper' pulse shape for the sandpile. Instead, it is a statement of the lowest level physics of the system. The high frequency regions of the sandpile spectrum scale as they do because of the trapezoidal pulse shapes. Similarly, the spectra of systems (SOC or otherwise) with different low level physics and different fundamental pulse shapes may scale differently.

We have already touched on the other assumption, that events in a superposition are random and independent. This is not the case in the SOC sandpile, as shown by the comparison of the spectra of shuffled and unshuffled pulses in Figure 2.4. Memory stored in the sandpile gradients create correlations among avalanches. For this very low drive case, the difference in spectra due to this memory appears at very low frequencies; we will discuss this further in Section 2.4.3. But since at high frequencies (short time scales) the spectra of correlated pulses are identical to the spectra of random pulses and since before this study the necessary long, low-drive time series had not been seen, this assumption of randomness had made sense.

2.4.2 Region C: Quiet Times

This is a region not previously described; it is due to quiet times, which are periods with no avalanches [26, 25]. Region C scales as f^0 in the power spectrum and as $H \approx 0.5$ in the R/S analysis, both signatures of an uncorrelated process. This region reflects the random external addition of sand to the system, where avalanches are randomly triggered. Beyond the time scale of the largest single avalanche, T_B, there can be a period where the correlations are dominated by the random triggering. The width of region C is inversely related to the driving rate. Thus, the lower the driving rate, the fewer avalanches occur in a given time period and the longer the system must wait for enough avalanches to occur to correlate with each other. The cutoff, T_C, is a measure of a minimum time needed for enough avalanches to occur that are correlated with each other.

Since the power spectrum is also the Fourier transform of the autocorrelation function,

visualizing the autocorrelation process can help in understanding why the spectrum is flat and $H \approx 0.5$ on these time scales. Consider a time series of length $T_0 \approx T_C$ from the low drive sandpile. This series consists of trapezoidal pulses, representing avalanches, alternating with flat quiet time regions, representing inactivity in the sandpile. Now picture the autocorrelation process, where a copy of the series is shifted by a time lag τ and multiplied by the original series; the resulting product is then summed. Up to a time lag $\tau \approx T_B$, pulses overlap with themselves, producing the correlations of regions A and B described in Section 2.4.1. But since average quiet times T_C are longer than average avalanche durations T_B, for time lags $T_C \gtrapprox \tau \gtrapprox T_B$ pulses in the shifted copy of the series now overlap quiet times in the unshifted series. When these two series are multiplied, the pulses are cancelled by the quiet times. This is, of course, an average behavior in the same way that in a truly random time series, troughs and peaks cancel each other out on average in the autocorrelation. The difference now is that for time lags $\tau > T_C$ (and for a longer time series), the pulses begin to correlate with other pulses that occur, on average, more than T_C time steps later. This correlation is due to the memory stored in the local sandpile gradients, discussed below.

Even if the quiet times were greatly reduced or completely removed, correlations would not immediately begin at T_B because successive avalanches in time usually take place in different spatial regions of the sandpile. These spatially separated but temporally close events do not affect each other on short time scales. But an avalanche does affect the next event that occurs in the same spatial neighborhood. Analogously (and simplistically), one might assume that a small earthquake located at one end of a 1,000 kilometer fault is not related to one that occurs one hour later at the other end of the same fault. However, through a local shift in stress/strain the first temblor is almost surely connected to another earthquake only 10 kilometers away that also occurs one hour later.

We test this by removing all of the quiet times from the flips time series and comparing the spectra of the two series (Figure 2.4). Regions A and B are unchanged since the same shapes are still in both series. Region C has been essentially eliminated, though a vestige of its former self remains because correlations among successive events do not usually occur. In the R/S analysis, this region is too small to be identified when the quiet times are removed. The region's disappearance in R/S is consistent with its shrinkage in the

spectrum.

This test also reveals the link between the running sandpile and the zero drive sandpile of [35], where the addition of sand is suspended during an active avalanche. The spectrum and R/S analysis of the zero drive case are identical with those of the low drive case with quiet times removed. This makes sense, since the zero drive sandpile has very few quiet times by construction, as sand is always added during a time step when there is no avalanche. This prevents long periods of inactivity. In contrast, in the running sandpile there is always a finite probability of a grain of sand *not* falling during a time step. Since at low drive this probability increases, quiet times can become quite large. The important similarity between the two cases, though, is that there are few or no overlapping avalanches. When an avalanche is initiated the probability is low (nonexistent in the zero drive case) that another avalanche will initiate before the first one ends. We emphasize this to introduce the next section, which shows that overlapping of events is not necessary to produce correlated dynamics.

2.4.3 Region D: SOC and Correlated Events

The physics of this region is the main point of this paper. Region D is the only true dynamical SOC region in the sense that its signatures arise solely from interactions and correlations among separate events in the system. *On the time scales in this region, the signatures reflect only long time correlations and nothing about pulse shape, quiet times, random superpositions, overlapping of pulses or system size.* Because the high frequency end of this region is due to driving rate and the low frequency end is due to the finite capacity of the sandpile, larger systems have larger regions D. The limiting extension is that a system of infinite size would have a region D that extends to infinitely low frequencies and there would be no regions E or F.

For all cases in the low drive regime, regardless of system size, we find $H \approx 0.75$ in region D, indicating long time correlations among distinct and separate events. This region exists on time scales far greater than the maximum duration of an individual avalanche (T_B) so the correlations must arise from the interactions among those distinct events. But since there is no (or very little) overlapping in the low drive regime the correlations must be due to the specific order of events that occur in the sandpile. This order is due to memory

in the system.

Memory in the sandpile is retained in the heights (and, therefore, the local gradients) of each cell. Since quiet times are the lack of any activity, they play no role in the memory. That is, whether quiet times are left to evolve naturally or are completely removed or are even imposed artificially and randomly (with a Poisson distribution) between events, the same sequence of avalanches (statistically) will occur based on the dynamical rules of the sandpile. If quiet times grow extremely long because the drive is so low then this simply means that region C will extend to lower frequencies before the inevitable region D begins. On the other hand, if quiet times grow either very short or nonexistent, because of high drive, then the simple pulses discussed here will overlap, leading to a regime with different characteristics (see [34]).

Still, though, how does this memory lead to positive correlations? This question is equivalent to: why does an avalanche now increase the probability of an avalanche later even though the random drive is unchanged? Consider the initiation of an avalanche, which, by definition, occurs after a quiet time when a grain of sand from the random external drive is added to a cell n that has slope $Z_n = Z_{crit} - 1$. After the addition of sand, that cell is critical and it then relaxes to $Z_n = Z_{crit} - N_f$ by dumping N_f grains to the cell below. The slope in cells $n-1$ and $n+1$ have increased by N_f as flux is transported down the gradient. If either of their slopes were greater than $Z_{crit} - N_f$ before this toppling, then one or both of them are now critical and the avalanche continues to propagate up and/or down the sandpile. If, however, their slopes were less than $Z_{crit} - N_f$, then the avalanche would stop but their slopes would be closer to critical by an amount N_f, making an avalanche more likely to occur there the next time sand is added (Figure 2.6).

This is the root of the positive correlation: when an avalanche ends, the cells at the endpoints of its active zone are closer to critical and are more likely to be the initiation point of another avalanche. This, also, is the basis for memory in the system: a cell "remembers" that an avalanche just stopped there and "knows" that it will initiate an avalanche with the next slope increase from either random drive or from another neighboring avalanche. *Regardless of how long the intervening quiet time is between two events, they are correlated in the same way.* Such a process can easily be pictured for a natural system, where disturbances propagate to some finite extent and leave the gradients at their endpoints greater than

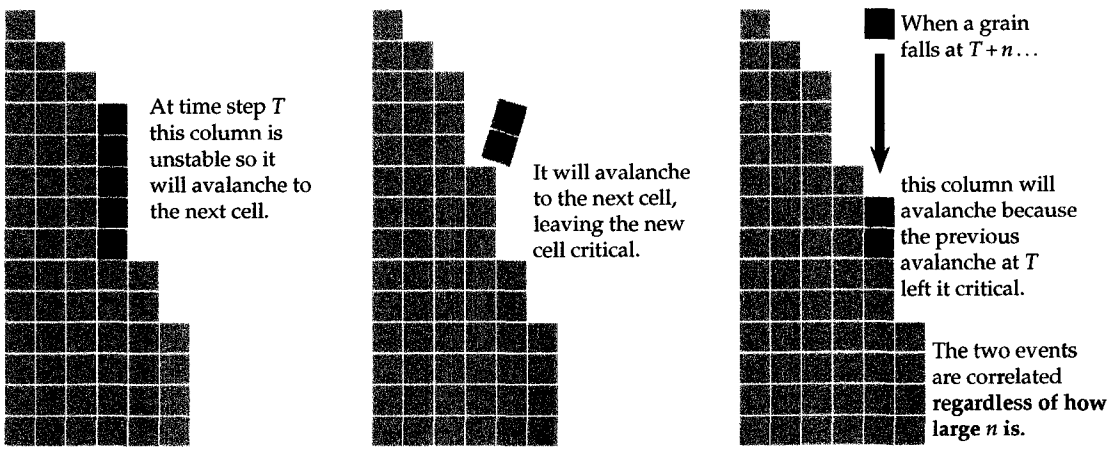

Figure 2.6. Correlations between avalanches because of memory in local gradients.

before the event.

Though events are triggered at random intervals, *the event time series is not random.* That is, correlations exist among separate events. We show this by using the time series of shuffled pulses as before, Figure 2.4. Regions C, D, E and F collapse into a single uncorrelated region for all time scales beyond T_B, where the shuffled series is seen to have a f^0 spectrum down to the lowest frequencies and a Hurst exponent $H \approx 0.5$ to the longest time scales. This is in contrast to the spectrum of the sandpile series, which shows structure in the spectrum at low frequencies and $H \neq 0.5$ at long time scales. A random time series is known to have a spectrum that scales as f^0 and $H = 0.5$ so this shows that the SOC series is not simply a random superposition of pulses.

This is remarkable. Given N pulses from a power law pdf in a time series there are $N!$ possible ways in which they can be ordered. The sandpile dynamically selects one of just a relatively few such orderings that give correlations and structure in the R/S analysis and spectrum.

To show that the correlations are among the separate events and that quiet times have no role in these correlations, we return to the time series with all quiet times removed. As seen in Figure 2.4, region C disappears. That is, the $H \approx 0.5$ region is replaced by a $H \approx 0.75$ region. We take this to mean that the $H \approx 0.75$ region D of the original data (with quiet times) has moved to shorter time scales due to the removal of quiet times and

the concomitant shortening of the series. But the correlations among events must remain the same since neither their order nor their sizes have changed. Only their frequency is different and this is reflected in the same $H \approx 0.75$ region at shorter time scales. This value of H holds for this region regardless of system size or driving rate, indicating that $H \approx 0.75$ is a robust signature of SOC dynamics.

Understanding the power spectrum for this region is not as simple as for the R/S analysis. The slope of this region, β, changes with driving rate and with system size, as well as with the removal of quiet times. As an example case, we examine a sandpile of L = 200 and $\overline{J_{IN}} = 10^{-3}$ and see that $\beta \approx 0.45$. For the first of the two tests above, shuffling the pulses, we see similar behavior to that in the R/S analysis. Namely, region D disappears or merges with regions C, E and F, leaving one large region of spectrum that scales as f^0, the signature of uncorrelated random noise. Again, shuffling the individual avalanches destroys the sandpile-selected order and eliminates all long time correlations.

The results of the second test are more interesting: removing the quiet times produces a $1/f$ region. That is, when quiet times are eliminated, the correlations among the events go to shorter time scales (higher frequencies), as described above. But the slope of region D changes from $\beta \approx 0.45$ to $\beta \approx 1$.

This implies that a $1/f$ region is not a necessary signature of SOC dynamics. But the SOC dynamics and events that produce a $1/f$ signature are present at low drive when the $f^{-\beta}$ region appears with $\beta < 1$. Even as β changes, though, the Hurst exponent remains constant.

Recall that the low drive case with quiet times removed was shown to be dynamically equivalent to the zero drive case. Now we see that this zero drive case, which is the original 1D model of [2, 1], modified by [35] to restrict $N_f > 1$, does contain a $1/f$ region. The search for an explanation of such a region was one of the original motivations behind SOC.

Since the same correlations among the same events still hold, we interpret this behavior of β and H to indicate that R/S analysis is a more robust measure of correlations among events than the power spectrum. The spectrum, though, may be a good measure of amount of overlap and/or effective drive.

The question of why the slope of region D in the spectrum changes to $1/f$ when the quiet times are removed is puzzling. It is not due to the conservation of the integrated

power of the shorter time series; this can be calculated using the Parseval-Rayleigh Theorem [36]. Though not yet completely understood, we feel that this change lies at the root of the $1/f$ question. We discuss the issue of changing β and constant H further in [34].

2.4.4 Region E: Anticorrelated Events

This is the discharge event region well-studied by [19] for high drive. The same process drives both the low and high drive cases, namely the finite capacity sandpile eventually fills up and empties out in great system-wide discharges. (Again, a sandpile of infinite size would not have this region.) The finite sandpile is always being driven towards a globally critical slope. Once all or almost all cells have slope $Z_{\text{crit}} - 1$, a keystone toppling, usually near the bottom, will produce a system-size avalanche or a rapid succession of smaller avalanches that removes enough sand so that the slopes at all sites are reduced to much less than critical ($\approx Z_{\text{crit}} - N_f$). Once such a large event occurs, it is unlikely that one will happen again for a long time. Hence, large events are anticorrelated; the signature of anticorrelated dynamics is $\beta < 0$ in the spectrum and $H < 0.5$ in R/S analysis. Both signatures are seen in the sandpile.

Note that these large discharge events are not necessarily a single avalanche. While such an event is possible, a discharge event can comprise many smaller avalanches that occur over a short time span. The key point is that both types of discharge events effectively reset the system by relaxing the near-critical local gradient to much less than critical at all or most locations.

After a discharge event, the sandpile fills up, on average, in at least T_E and at most T_F time steps, so the breakpoints defining this region can be calculated. The maximum sandpile capacity is $C_{max} = \frac{Z_{\text{crit}}L^2}{2}$. After a system-wide event, the total mass is reduced to approximately $C_{min} = \frac{(Z_{\text{crit}}-N_f)L^2}{2}$. The minimum time needed to refill to maximum is then $T_{\text{re,min}} = \frac{N_f L^2}{2P_0 L}$. This expression is plotted in Figure 2.7 and is seen to agree with the breakpoint data of T_E versus $P_0 L$.

The above $T_{\text{re,min}}$ is a minimum time and, hence, is related to a maximum frequency, T_E^{-1}. To calculate the minimum frequency, T_F^{-1}, we notice that since sand continues to leave the sandpile at the bottom during the refilling process, T_{refill} is usually greater than $T_{\text{re,min}}$. Though the sandpile is in steady state in the longest time scales, at some smaller ones flux

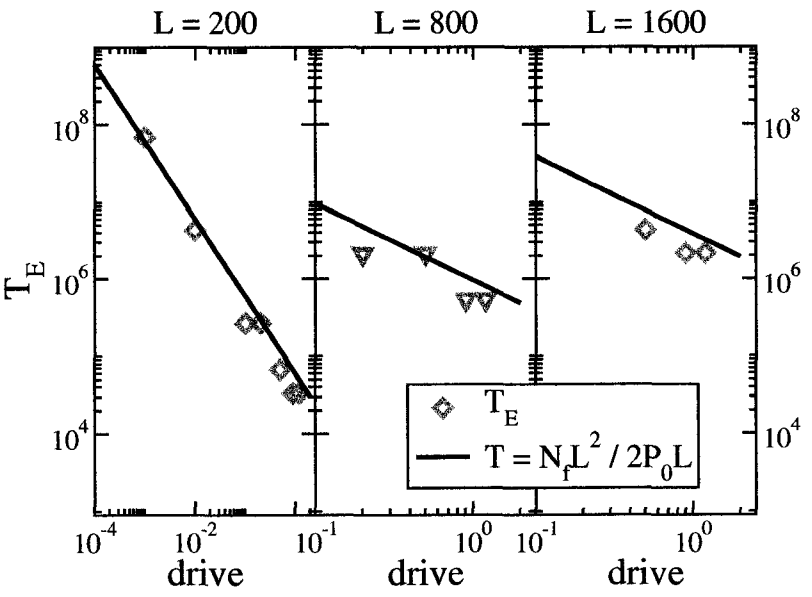

Figure 2.7. Breakpoint of beginning of anticorrelated region versus driving rate for three different system sizes. Solid lines are $T = \frac{N_f L^2}{2P_0 L}$

into the system exceeds flux out. The reason for this is that sand falls into all cells with equal probability from the random drive but sand can only leave the system through the bottom cell. In the SOC region D, there is a finite time and a convoluted path for sand to travel from where it initially lands to where it exits at the bottom. This time is much slower when the system as a whole is farther from critical (region D). But once all cells are critical, this time is much shorter and one large avalanche (or rapid succession of many) is the very efficient mechanism that quickly removes much mass and keeps the sandpile in a steady state over the longest time scales. At this point, though, we have not derived breakpoint T_F.

Beyond breakpoint T_F^{-1}, at the lowest frequencies, the spectrum is flat; the following is conjecture about its cause and limits. The flat spectrum is a reflection of the random drive of the system on the longest time scales since all dynamics is on time scales much smaller than those in this region. This is the extent of the memory process discussed in regards to region D. That memory is eventually erased by the system-wide events which tend to destroy the record of events stored in the heights of each cell. The memory is shuffled by the random drive at time scales longer than T_F. Region F extends to infinitely

low frequencies; there are no further dynamical regions below it.

2.5 Conclusions

We have studied the one dimensional directed running sandpile at very low drive and have shown that correlations from a memory mechanism in SOC dynamics produce nontrivial signatures in the power spectra and R/S analysis of flips time series. The memory is stored in the local gradient of each cell, regardless of driving rate. The signatures of the correlations appear at longer time scales for lower external forcing. A consequence of this is that a time series for any system, be it a defined SOC model or a real physical system suspected of being SOC, can be too short to see the correlation signatures and thus could be mistaken for a simple random time series. Given long enough time series, a very distinct difference can be seen between the signatures of random data and the sandpile data. The sandpile chooses the particular size, order and separation of events in a way that is very different from any random combination of size, order and separation.

Multiple distinct power law regions are found in spectral and rescaled range analysis of the SOC avalanche time series but only one of these (region D) is due solely to correlations among events. Its signature is a power law region in the spectrum that scales as $f^{-\beta}$ with $0 < \beta \leq 1$ and a Hurst exponent $H \approx 0.75$. An infinite sandpile would have infinite capacity and, thus, have no discharge events. Therefore the SOC region D would extend to infinitely long time scales.

Part of the allure of SOC has been the lack of tuning required for the system to be critical. By probing the low drive system at very long times we have shown that overlapping of events and, therefore, tuning of the external forcing is not necessary in order to have SOC dynamics. Regions of nontrivial $f^{-\beta}$ are seen at very low frequencies. This indicates that in a SOC system *avalanches always correlate over very long times even when they do not overlap in time.* It also shows that tuning of the drive is not necessary for a SOC system to be in its self-organized critical state, as the memory mechanism is always present in the gradients regardless of how slowly or quickly sand is added.

Signatures of these long time correlations in the form of power laws in the spectra and R/S analysis are present at all drives. In a sense, the signatures at low drive are more fundamental than those at high drive because the actual time series are composed of the

basic non-overlapping events of the SOC system. These events contain all of the relevant dynamics and are the building blocks to which the title refers.

Bibliography

[1] P. Bak, C. Tang, and K. Wiesenfeld. *Phys. Rev. Let.*, 59:381, 1987.

[2] P. Bak, C. Tang, and K. Wiesenfeld. *Phys. Rev. A*, 38(1):364–374, 1988.

[3] P. Bak. *How Nature Works.* Springer-Verlag, New York, 1996.

[4] H. J. Jensen. *Self-Organized Criticality: Emergent Complex Behaviour In Physical And Biological Systems.* Cambridge University Press, Cambridge, 1998.

[5] J. Davidsen and M. Paczuski. *Phys. Rev. E*, 66:050101(R), 2002.

[6] A. Vespignanni and S. Zapperi. *Phys. Rev. E*, 57(6):6345–6362, 1998.

[7] D. E. Newman, B. A. Carreras, P. H. Diamond, and T. S. Hahm. *Phys. Plasmas*, 3:1858, 1996.

[8] B. A. Carreras, D. Newman, and V. E. L. et al. *Phys. Plasmas*, 3(8):2903–2911, 1996.

[9] B. A. Carreras, B. P. van Milligen, and M. A. P. et al. *Phys. Rev. Let.*, 80:4438, 1998.

[10] L. Garcia, B. A. Carreras, and D. E. Newman. *Phys. Plasmas*, 9(3):841–848, 2002.

[11] T. S. Chang. *Phys. Plasmas*, 6:4137–4145, 1999.

[12] S. C. Chapman and N. W. Watkins. *Space Sci. Rev.*, 95, 2001.

[13] R. Woodard. Computer Animations of a Self-Organized Criticality Running Sandpile Model, 2004. Contact author for copy of animation at `ryan@timehaven.org`.

[14] D. L. Turcotte. *Fractals and Chaos in Geology and Geophysics.* Cambridge University Press, 2nd edition, 1997.

[15] B. Carreras, V. E. Lynch, I. Dobson, and D. E. Newman. *Chaos*, 12(4):985–994, 2002.

[16] B. Carreras, D. Newman, I. Dobson, and A. Poole. *IEEE Trans. on Circuits and Systems, Part 1*, 2004. accepted March 2004.

[17] B. Carreras, V. E. Lynch, I. Dobson, and D. E. Newman. *Chaos*, 2004. accepted June 2004.

[18] D. E. Newman, B. A. Carreras, N. D. Sizemore, and V. E. Lynch. In *35th Hawaii International Conference on System Sciences*, Hawaii, 2002.

[19] T. Hwa and M. Kardar. *Phys. Rev. A*, 45:7002, 1992.

[20] http://www.nslij-genetics.org/wli/1fnoise/.

[21] H. J. Jensen, K. Christensen, and H. C. Fogedby. *Phys. Rev. B*, 40(10):7425–7427, 1989.

[22] J. Kertész and L. B. Kiss. *J. Phys. A*, 23:L433–L440, 1990.

[23] S. S. Manna. *J. Phys. A*, 24(L363), 1991.

[24] P. H. Diamond and T. S. Hahm. *Phys. Rev. Let.*, 2:3640, 1995.

[25] R. Sánchez, D. E. Newman, W. Ferenbaugh, B. A. Carreras, V. E. Lynch, and B. P. van Milligen. *Phys. Rev. E*, 66:036124, 2002.

[26] R. Sánchez, D. E. Newman, and B. A. Carreras. *Phys. Rev. Let.*, 88(6):068302, 2002.

[27] H. E. Hurst. *Trans. Am. Soc. Civ. Eng.*, 116:770, 1951.

[28] B. B. Mandelbrot. *Multifractals and* $1/f$ *noise*. Springer-Verlag, 1999.

[29] B. B. Mandelbrot. *Gaussian self-affinity and fractals*. Springer-Verlag, 2002.

[30] M. J. Cannon, D. B. Percival, D. C. Caccia, G. M. Raymond, and J. B. Bassingthwaighte. *Physica A*, 1997.

[31] C.-K. Peng, S. V. Buldyrev, S. Havlin, M. Simons, H. E. Stanley, and A. L. Goldberger. *Phys. Rev. E*, 49(2):1685–1689, 1994.

[32] C. X. Yu, M. Gilmore, W. Peebles, and T. Rhodes. *Phys. Plasmas*, 10(7):2772–2779, 2003.

[33] B. M. Gammel. *Phys. Rev. E*, 58:2586, 1998.

[34] R. Woodard, D. E. Newman, R. Sánchez, and B. A. Carreras. Building blocks of self-organized criticality, part II: transition from low to high drive. Submitted to PRE, 2004.

[35] L. P. Kadanoff, S. R. Nagel, L. Wu, and S. min Zhou. *Phys. Rev. A*, 39(12):6524–6537, 1989.

[36] R. N. Bracewell. *The Fourier Transform and Its Applications*. McGraw-Hill, 3rd edition, 2000.

Chapter 3
Building Blocks of Self-Organized Criticality, Part II: Transition from Very Low Drive to High Drive

Abstract

We analyze the transition of the self-organized criticality one dimensional directed running sandpile model of Hwa and Kardar [Phys. Rev. A **45**, 7002 (1992)] from very low external forcing to high forcing, showing how six distinct power law regions in the power spectrum at low drive become four regions at high drive. One of these regions is due to long time correlations among events in the system with steady state power spectrum that scales as $\sim f^{-\beta}$ with $0 < \beta \leq 1$. The location in frequency space and the value of β both increase as the external forcing increases. β ranges from ≈ 0.4 for the weakest forcing studied here to a maximum value of 1 (i.e., a $1/f$ region) at stronger levels. The change from low to high β occurs when the average quiet time between avalanche events is on the same order as the average duration of events. The correlations are quantified by a constant Hurst exponent $H \approx 0.8$ when estimated by R/S analysis for sandpile driving rates spanning over five orders of magnitude. The constant H and changing β in the same system as forcing changes suggests that the power spectrum does not consistently quantify long time dynamical correlations and that the relation $\beta = 2H - 1$ does not hold for the time series produced by this SOC model. Because of the constant rules of the model we show that the same physics that produces a $\beta = 1$ scaling region during strong forcing produces a $0 < \beta < 1$ region at weaker forcing.

3.1 Introduction

Simple models have been used to study the dynamics of many physical systems, such as confined fusion plasmas [1, 2], space plasmas [3, 4] and earthquakes [5], among others. These models comprise a connected network of local nonlinear gradients that can persist because of a critical threshold. Random external forcing of the system increases local gradients; when one of them exceeds the critical threshold a relaxation event is triggered that stabilizes the gradient. The gradient is reduced by transferring mass, heat, stress or some other quantity specific to the system to neighboring regions which can make them unstable, creating a series of relaxations. This sequence of events, called an avalanche, occurs

much faster than the external drive increases the gradients. These models and this type of dynamics are characteristic of self-organized criticality (SOC) [6, 7, 8].

One of the first SOC models was the sandpile [7, 9, 10]. A one dimensional variation of it was studied for strong external forcing by [11] and later for weak external forcing by [12]. Both studies show that even though the system is randomly driven, long time correlations exist in the dynamics on time scales much longer than the duration of any single avalanche. The question of whether long time dynamical correlations exist in a time series—a basis for predictability [13, 14]—is fundamental to many physical and geophysical fields.

One of the features of long time correlations in a system, including the SOC sandpile, is a region in the power spectrum that scales as a power law $f^{-\beta}$ with $\beta \neq 0$. [11] shows that $\beta = 1$ (i.e., $1/f$) in this region of correlations at high drive, where avalanches almost always overlap in time. [12] shows that $\beta \approx 0.4$ at very low drive, where avalanches essentially never overlap.

Values of $\beta = 1$ appear in the spectra of many physical processes [15, 16], where it is referred to as $1/f$ noise for historical reasons. This modern mystery still inspires much current work but no general theory explains the origin of $1/f$. One of the original motivations of SOC was to offer an explanation of $1/f$ noise but the conclusions have been mired in controversy since its introduction [17].

An alternative technique for quantifying correlations is by the Hurst exponent, H [18], where a value of $0.5 < H < 1$ indicates positive correlations in a data series, $0 < H < 0.5$ indicates anticorrelations and $H = 0.5$ indicates lack of correlations [19, 20]. Algorithms exist to generate a data series with a power spectrum with any given value of H [15]. These artificial data sets, called fractional Gaussian noise (fGn), have Gaussian distributions and a relationship $\beta = 2H - 1$ which is derived based on this type of statistics [21]. β can then be interpreted directly through H as a measure of correlations in the time series. Note that if this equation were to hold for all data sets then any series with a $1/f$ spectrum would have $H = 1$ over the same time scales.

Using rescaled range (R/S) analysis, [12] found that $H \approx 0.8$ in the region discussed above for the low drive sandpile. Here we show that H maintains this value in the correlated region for over five orders of magnitude of driving rate, as the sandpile goes from low drive to high drive. H remains constant because the underlying interactions among

the scales (the low level physics of the system) do not change as driving rate increases. The dynamics simply takes place on shorter time scales.

However, while H stays constant with driving rate β increases from ≈ 0.4 for the lowest drive studied here to a limiting value of 1 at the highest drive. The greatest rate of change in β occurs as driving rate increases and the average quiet time between avalanche events decreases until it is on the same order as the average duration of events. There are two main points to these results. First, the dynamics that produces a $1/f$ region at high drive is the same at low drive, even though $\beta < 1$ and changes. Second, the relation $\beta = 2H - 1$ that is often used to connect β and H does not necessarily hold for the SOC sandpile model.

The region with $H \approx 0.8$ is just one of several in the spectral and R/S measures. We will show that six distinct power law regions in the low drive spectrum and five regions in the low drive R/S analysis both become four regions at high drive. [12] shows that the causes of the regions at low drive are, from shortest to longest time scales: low level physics, quiet times, memory stored in local gradients (the SOC region), system size effects and external drive. Here we show that the reason that the number of regions changes at high drive is because events are triggered more frequently in time so that they almost constantly overlap and, therefore, virtually eliminate quiet times.

3.2 Model and Methods

The model that we use is the one dimensional directed running sandpile of [11], a cellular automaton. The model consists of a single column of L cells and each cell contains an integer number of 'sand grains', where the number is referred to as the height of the cell. At each time step for each cell, there is a probability $0 < P_0 < 1$ that U_0 grains of sand will fall on it from a 'rain' from above. The local gradient is the height difference between two cells. If a local gradient exceeds a defined critical gradient Z_{crit} then the gradient is stabilized by a transfer of N_f grains of sand from the higher cell to the lower. This action is a flip and it can make one or both of the neighboring cells unstable in the next time step so that the disturbance propagates. An uninterrupted sequence of one or more flips is called an avalanche. A quiet time is defined as a sequence of one or more values of zero between avalanches. We used $U_0 = 1$, $N_f = 3$ and $Z_{crit} = 8$ in all results presented here. Results are insensitive to changing these values within a wide range of parameters [1].

Low and high drive are distinguished by the amount of sand falling on the system and how large the system is. Average input into the system is the driving rate, $J_{IN} = P_0 L$. To compare systems of different size and driving rate, we use the effective driving rate $J_E = P_0 L^2$. We discuss this distinction in Section 3.4.

The time series analyzed in this study are total flips at each time step. A flip is a single relaxation event, a transfer of N_f grains from one cell to the next. The total number of flips at each time step is, then, the total number of unstable cells in the system. This can be thought of as the instantaneous (potential) energy dissipation in the system.

We analyze the flips time series with the power spectrum and R/S analysis. For a data series $X(t)$, the power spectrum is defined as $S(f) = |F(f)|^2$, where $F(f)$ is the power spectrum. The rescaled range [18, 20] is defined as $R'(\tau) \equiv R(\tau)/S(\tau)$, where $S(\tau)$ is the standard deviation and

$$R(\tau) = \max_{1 \le k \le \tau} W(k,\tau) - \min_{1 \le k \le \tau} W(k,\tau) \quad \text{(range)},$$

$$W(k,\tau) = \sum_{t=1}^{k} (X_t - \langle X \rangle_\tau) \quad \text{(cumulative deviation) and}$$

$$\langle X \rangle_\tau = \frac{1}{\tau} \sum_{t=1}^{\tau} X_t \quad \text{(mean)}.$$

If the rescaled range of the time series scales as $R'(\tau) \sim \tau^H$, the slope of the plot of $R'(\tau)$ versus the time lag τ on a doubly logarithmic plot is the Hurst exponent, H.

3.3 Results

Figure 3.1 shows the power spectra of the flips time series of the one dimensional directed running sandpile for over five orders of magnitude of effective driving rate, $P_0 L^2$, which increases from top to bottom in the figure. The sandpile size is L = 200. We have studied sandpile sizes up to L = 2000 and found the behavior to be consistent with that of the smaller system. The lowest drive used is $P_0 L^2 = 0.002$ and the highest is $P_0 L^2 = 296$. The higher limit is chosen to stay below the normal overdrive limit of $P_0 L < N_f/2$ (derived in Section 3.4).

Note that the spectra look very different depending upon whether the driving rate is low or high. Multiple distinct power law regions are seen in all of the spectra. The

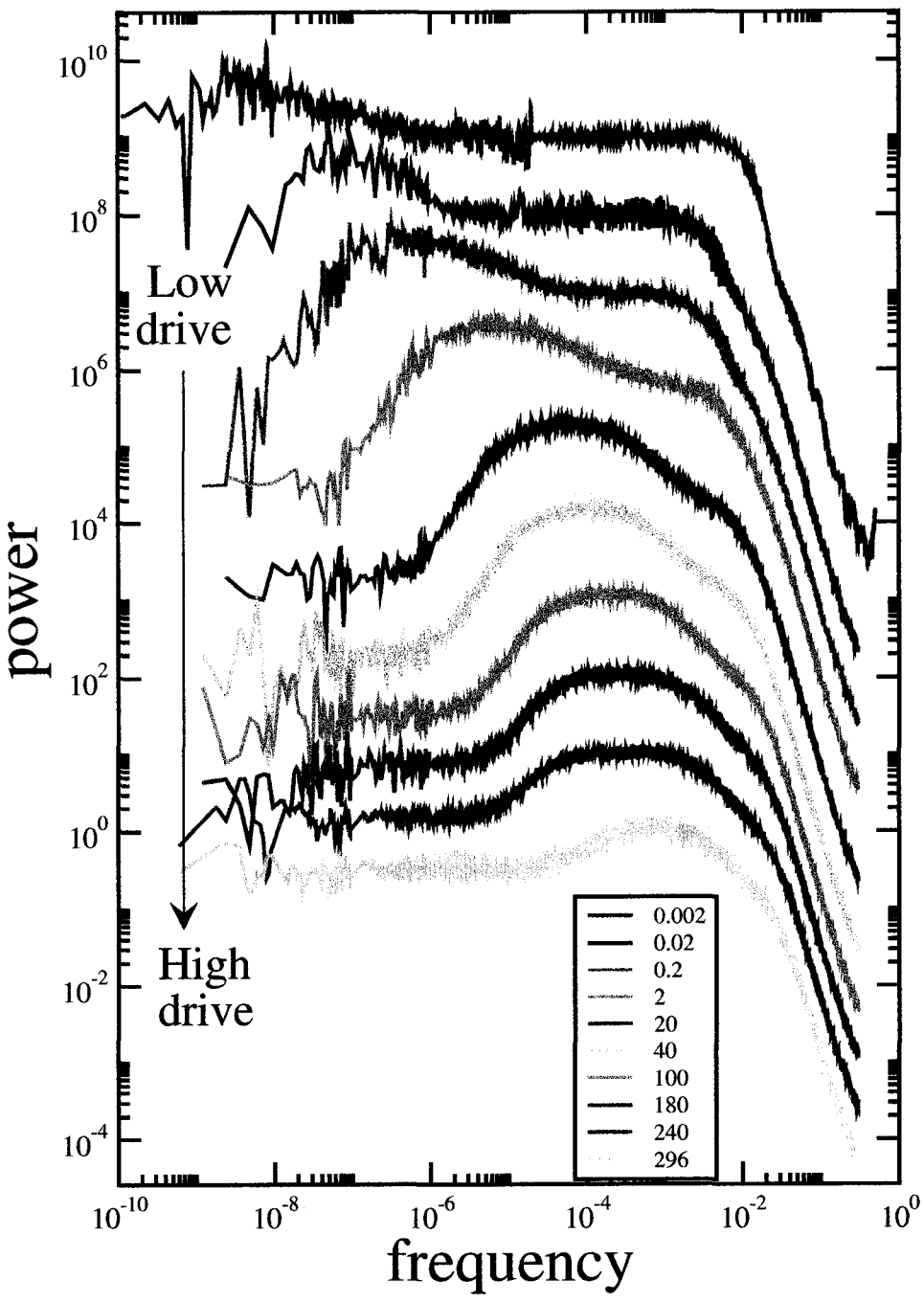

Figure 3.1. Power spectra of flips time series of L = 200 sandpile for five orders of magnitude of effective driving rate in $P_0L^2 \in (0.002, 296)$. Spectra have been shifted along y axis for easier viewing.

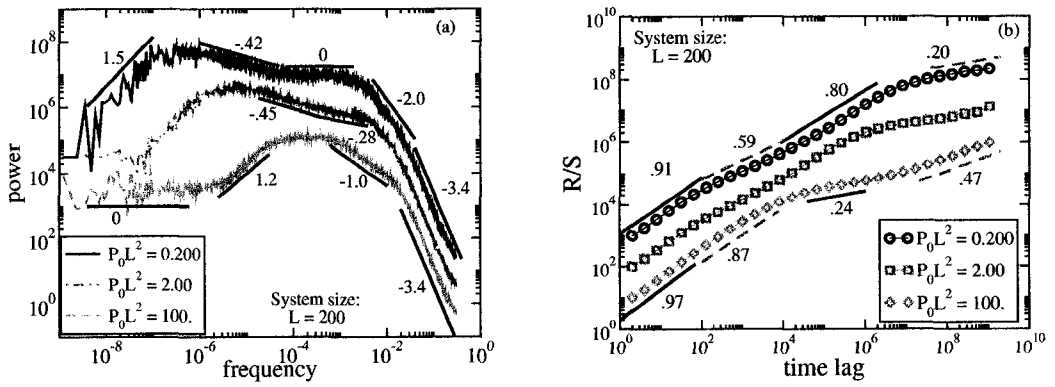

Figure 3.2. (a) Power spectra and (b) R/S analysis of flips for different driving rates. The y values of both measures have been shifted for easier viewing. Numbers shown are the exponents of power law fits to regions, β for the spectra and H for R/S.

highest frequency regions share a common slope. At low drive a very prominent bump at low frequency moves to higher frequency as driving rate increases. This movement is due to more sand grains falling onto the system faster, thereby triggering avalanches more frequently so that the dynamics moves to shorter time scales. The avalanches overlap in time and thus eliminate quiet times. The loss of quiet times also accounts for the loss of two regions in the spectrum—six regions at low drive become four regions at high drive.

Three spectra from Figure 3.1 are shown in Figure 3.2(a), representing low, medium and high driving rates of the sandpile. The six regions of low drive and four regions of high drive are shown by the solid lines. The lines are power laws $f^{-\beta}$ and the numbers next to them are the values of β. The lowest frequency f^0 region of the low drive case is not seen because of the finite size of the time series. Its existence is assumed based on the f^0 regions seen in the spectra of higher drive cases.

The associated R/S analysis for the low, medium and high drive power spectra are shown in Figure 3.2(b). Five regions at low drive become four regions at high drive. Power law lines and their slopes are indicated in the figure. The slopes are the Hurst exponent H for each region. Again, the region for the longest time scales at the lowest drive is not seen because of the finite length of the time series but is inferred based on the higher drive cases.

To aid the discussion of the regions and breakpoints, we use the labelling convention of

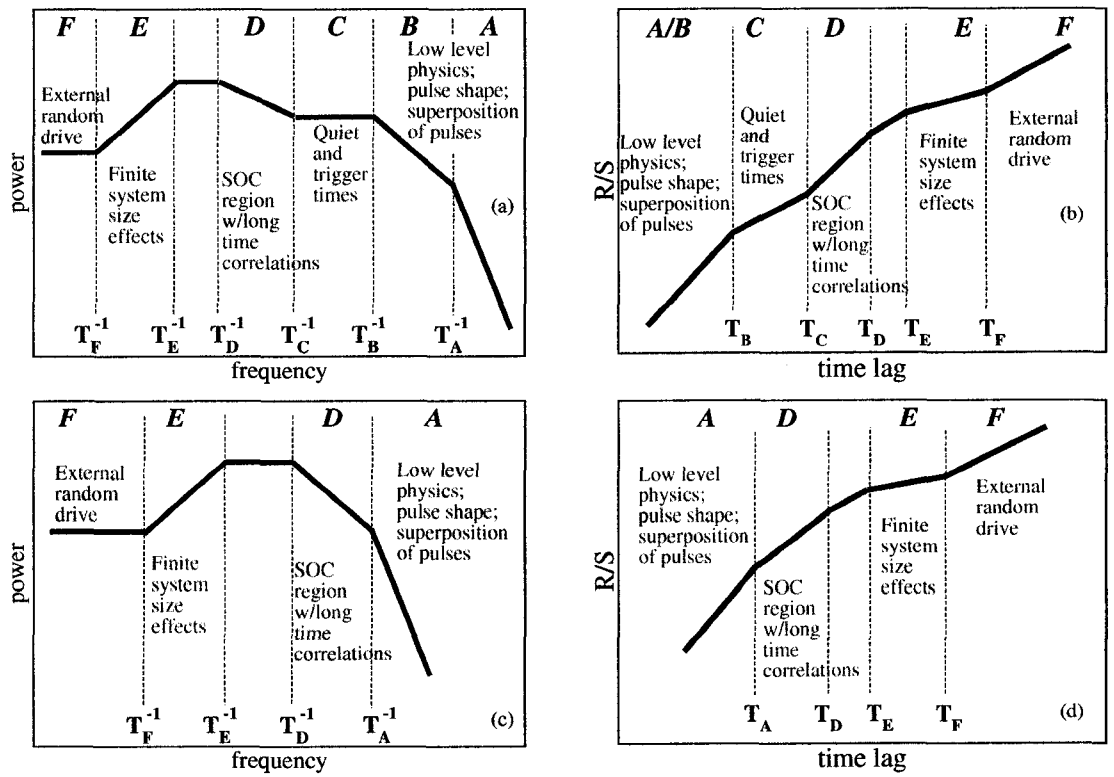

Figure 3.3. Cartoons of distinct regions and their breakpoints and causes of power spectra and R/S analysis of sandpile flips. (a) Power spectrum of low drive, (b) R/S analysis of low drive, (c) power spectrum of high drive and (d) R/S analysis of high drive. (c) is taken from Figure 6 of [11] and the others are drawn in that spirit. (a) and (b) are from [12] but are reproduced here for completeness.

the cartoons in Figure 3.3. Figure 3.3(c) is based on Figure 6 of [11]. Figures 3.3(a) and (b) are from [12] but are reproduced here for completeness. The sources of all of the regions are discussed in [11] and [12].

The breakpoints between regions in the two different measures, power spectrum and R/S, can be compared with each other. The results are shown in Figure 3.4. The breakpoints of the two measures, found independently, agree very closely with each other, though the R/S breakpoints appear at slightly longer time scales than those of the power spectrum. This effect is known from comparisons of R/S analysis with structure functions [22] and we conclude that both measures can distinguish the same dynamical regions through the identification of different power law regions.

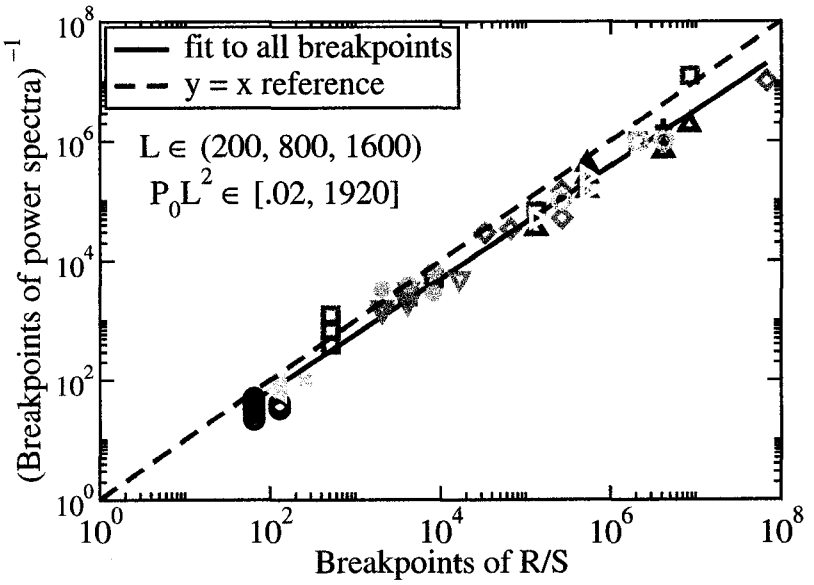

Figure 3.4. Inverse breakpoints of the power spectra versus breakpoints of R/S analysis for flips time series of different size sandpiles and driving rate.

To investigate changes in spectra and R/S as driving rate changes, breakpoints can be identified and compared. The breakpoints between neighboring regions scale with driving rate as shown in Figures 3.5; similar results are seen for different L. T_A in the spectrum and T_B in both measures stay relatively constant, reflecting the unchanging rules of the system that produce discontinuous jumps in the gradient of the flips time series. The other breakpoints scale with driving rate as power laws. Region B of the spectrum and region C of both measures shrink and eventually disappear as drive increases and average quiet time shrinks.

At low drive, individual avalanches appear in the flips time series as trapezoidal pulses [12] and this is reflected in the slopes of regions A and B. $\beta \approx 3.4$ of region A and $H \gtrapprox 0.9$ of region A/B remain relatively constant as driving rate changes because of the fixed rules of the system. These values are consistent with those found for a random superposition of trapezoids. $\beta \approx 2$ in region B stays relatively constant until that region disappears, reflecting the distinct and separate trapezoids that eventually become extinct as avalanches overlap each other more and more.

$\beta = 0$ and $H = 0.5$ are signatures of an uncorrelated data series and these values seen in

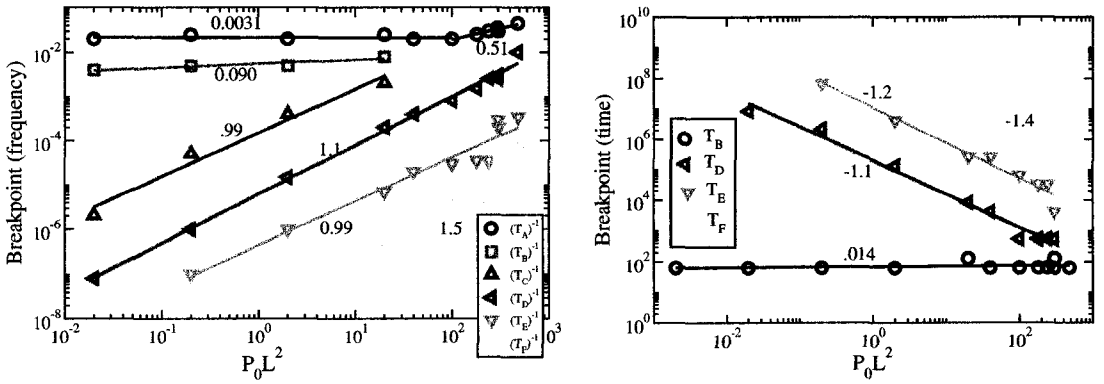

Figure 3.5. Breakpoints of power spectra and R/S analysis versus driving rate for L = 200 sandpile. Numbers shown are exponents of power law fits to the data.

region C at the lowest drive reflect the uncorrelated triggering of avalanches on short time scales by the external drive. In the autocorrelation process on these time scales, the distinct avalanche pulses are shifted and multiplied by the relatively long periods of quiet times. That is, the avalanches correlate with the zeros of quiet times, producing an uncorrelated spectrum and rescaled range. β in regions C and D both increase with P_0L^2 but at different rates until they reach the same value of $\beta \approx 1$ at high drive. This is a limiting value that does not change regardless of how high the drive becomes, up to the saturation limit of the model.

The Hurst exponent of region D remains a relatively constant $H \approx 0.8$ regardless of driving rate even as region D moves from long time scales at low drive to shorter time scales at high drive. H stays constant because the rules of the sandpile do not change as driving rate changes. Avalanches are still triggered by the random drive but on shorter and shorter time scales as the drive increases. The avalanches are still correlated at all driving rates because the same process triggers them. The constant H and changing β of region D is shown in the upper plot of Figure 3.6. This will be discussed further in Section 3.5.

β and H of region E both increase with driving rate, β towards 0 and H towards 0.5, Figure 3.7. At all drives, region E is due to anticorrelations among large discharge events that tend to reset the system and erase its memory. These events are anticorrelated because after a large event clears out the system another large event is unlikely since the majority of

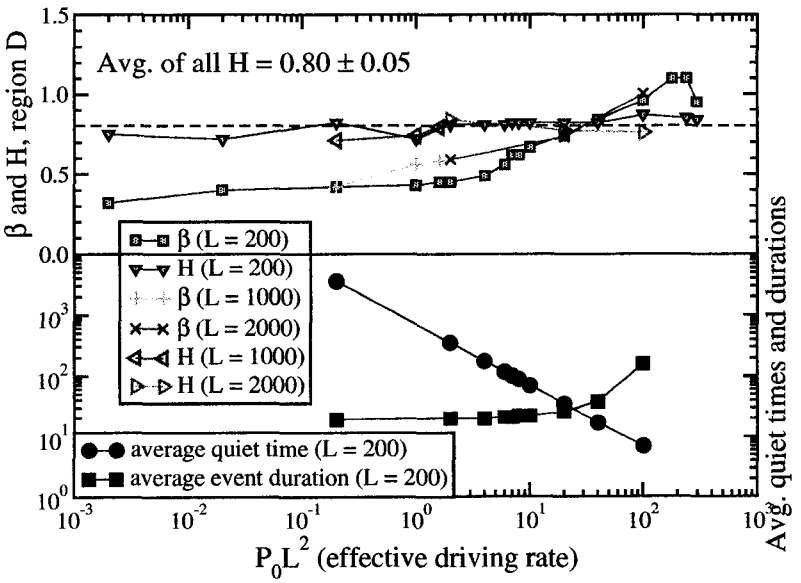

Figure 3.6. H, β, average quiet time and average duration versus five orders of magnitude of effective driving rate.

cells in the system are below critical. Discharge events can be either a single system-wide event or a rapid succession of smaller events; they are discussed in both [11] (high drive) and [12] (low drive). As drive increases, these large events, while still anticorrelated, occur closer together in time and reflect the random external drive of the system which itself is characterized by β = 0 and $H = 0.5$, the values to which region E approach.

Region F always has β = 0 and $H = 0.5$. We conjecture that this region reflects the random system drive and that β and H remain constant at any driving rate for all time scales beyond T_F. Random drive triggers large events randomly on time scales longer than the refill rate. This cause of a f^0 region is in contrast to that of region C.

3.4 Distinguishing Between Low and High Drive

High drive means that avalanches overlap with each other in time. This is relevant because some systems that have been discussed as possibly SOC, such as earthquake fault systems, have distinct events that do not overlap in time and, therefore, may be relatively weakly driven. In the sandpile, high drive is not simply defined by the ratio of input current to maximum output current, $\overline{J_{IN}}/N_f$. This just defines whether the system is overdriven or

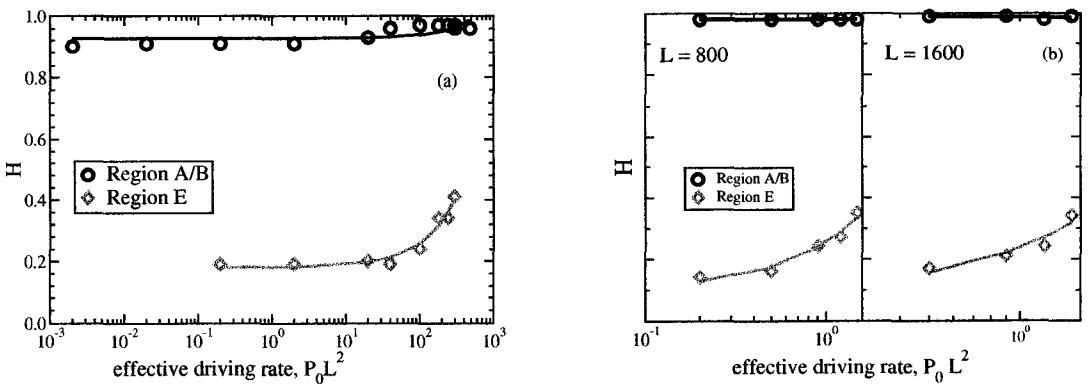

Figure 3.7. Hurst exponent versus driving rate for (a) L = 200 and (b) L = 800, 1600. Solid lines are linear fits on a linear y axis and a logarithmic x axis.

not, since flux in must never exceed the maximum possible flux out (N_f) of the bottom cell.

There are two overdrive limits, N_f and $N_f/2$. Consider a cell that is unstable in the midst of a large avalanche. Being unstable, it dumps N_f grains to its downhill neighbor. In the next time step, for what we call a normal avalanche, this first cell is stable. But since it has lost N_f grains, its uphill neighbor is now unstable and will send N_f grains into the original cell. In this way, during a normal avalanche, a cell alternates between stable and unstable until the avalanche ends or washes past the cell. The time average flux through the cell is $N_f/2$ and the maximum steady state input current is then $\overline{J_{IN}} = N_f/2$.

We define $\overline{J_{IN}} = N_f/2$ as the normal overdrive limit and $\overline{J_{IN}} = N_f$ as the super overdrive limit. A sandpile can still be in steady state between the two limits but the dynamics of the system changes since many cells are unstable for successive time steps in order to transport the increased flux into the system. Steady state is not possible for $\overline{J_{IN}} > N_f$ since flux into the system will always exceed flux out. We will only discuss driving rates below the normal overdrive limit.

The limit for spatial overlap has been previously given as $P_0 < L^{-1}$ [11]. This comes from the condition of $P_0 \bar{s} < 1$, where $\bar{s}$ is the average size of an avalanche and $\bar{s} \sim L$ (in nonoverlapping regime). But since we analyze the flips *time* series, we need to quantify overlapping in time, not space.

To find the condition for overlap in time we must consider quiet times. If the average avalanche duration $\bar{s}$ is greater than the average trigger time T_t then avalanches will

overlap in time. Using $T_t = N_f/P_0LU_0$ [23] (flux out divided by flux in), the condition for overlapping in time is $\bar{s} > T_t$ or $L > N_f/P_0LU_0$, giving $P_0L > N_f/LU_0$. The most general quantity to measure, then, for comparing sandpiles in the same drive regime but where all dynamical parameters are different is $V_g = P_0L^2U_0/N_f$, where $V_g > 1$ indicates high drive.

For our model, $U_0 = 1$ and $N_f = 3 \ll L$ so the high drive condition reduces to $P_0L > L^{-1}$. It is convenient to remember this condition as (driving rate) > (system size)$^{-1}$. In practice, we find the condition for low drive (when region C has $\beta = 0$ and $H = 0.5$) to be $P_0L \ll L^{-1}$.

Note that P_0L^2 is used because our measure, flips, is a global quantity where information about the entire system must be known. Hence, P_0L, total input into the system, and L system size, must be known. But other local measures, such as flux through a single cell, may only need to know P_0L.

The average quiet time $\bar{q}$ decreases as system size increases even as input current $\overline{J_{IN}} = P_0L$ remains constant. This effect is due to the increase in the average size of an avalanche with system size, $\bar{s} \sim L$, and larger avalanches lasting longer in time. That $\bar{s}$ is independent of driving rate (for low, nonoverlapping drive) reflects the critical nature of the steady state of the sandpile. A critical cell is the food of an avalanche. A larger sandpile has more cells and therefore can have more neighboring cells that are close to critical. Any avalanche, then, has more food to eat and can live longer. Since avalanches propagate at the same speed (1 cell per time step) regardless of system size, the larger systems will have larger avalanches regardless of driving rate.

With the low drive condition $P_0L \ll L^{-1}$ we see that there are two routes to high drive: 1) increasing probability P_0 of a drop while keeping the system size L fixed and 2) increasing L while keeping P_0L fixed. The first method is easy to visualize and is the more 'traditional' way of increasing drive. Consider a sandpile being driven by an input current of $\overline{J_{IN}} = P_0L$ grains per time step over the entire system. Increasing P_0 will obviously increase $\overline{J_{IN}}$ and decrease $\bar{q}$. More grains of sand fall in fewer time steps, avalanches initiate much more frequently and therefore begin to overlap in time.

The other way to increase drive is not as intuitive: consider a fixed $\overline{J_{IN}} = P_0L$ and increase the system size L. To keep $\overline{J_{IN}}$ constant, P_0 must decrease. But, because of the increase in L, the average avalanche size increases and avalanches begin to overlap in time. Since P_0L is the same as before, the same number of avalanches per time are triggered but

they last longer on average and thus overlap. This is seen in the power spectrum. When L is increased and P_0L is kept constant, the breakpoint T_B^{-1} moves to lower frequencies and T_C^{-1} stays fixed. Region C, then, has shrunk in width because quiet times have decreased due to the larger system. This is a restatement of the trapezoid analysis of Part I [12], where we show that breakpoint T_B^{-1} moves to lower frequencies for larger trapezoids (that represent larger avalanches due to larger systems). Therefore, increasing system size while keeping constant the average flux in (P_0L) has the effect of increasing the driving rate.

This has implications, for example, in investigations of finite size and/or multifractal scaling. Figure 3.8 shows justification for comparing systems with the same effective driving rate, $P_0L^2 = 2.0$. The spectra of systems with different driving rates P_0L and system sizes L but with the same P_0L^2 can be rescaled to lie on top of each other. The spectra of systems with the same driving rate P_0L but with different system size L cannot be rescaled to lie on top of each other. We used a rescaling function of the form

$$y_0 \log_{10} S(f) = g\left(x_0 log_{10}(f/x_1)\right),$$

where $S(f)$ is the power spectrum and $g(f)$ is a scaling function. Different sets of parameters $[x_0, x_1, y_0]$ are needed for each spectrum so this is not the same as, for instance, the multifractal rescaling of avalanche size PDFs of [9], where the same value of each parameter is used for different system sizes.

3.5 Discussion

The underlying cause of the change in the spectra and R/S analysis is that the average size and frequency of quiet times decrease as effective driving rate increases. Sand falls on the system more frequently and triggers avalanches more quickly so that all dynamics moves to shorter time scales. Avalanches overlap in space and time and the correlations among them move to shorter time scales. The memory in the gradients of the sandpile that creates the long time correlations [12] remains as driving rate changes.

Region C is the quiet times indicator. When it exists and $\beta = 0$ and $H = 0.5$ the system is in a low drive regime and events are distinct and well-separated. The presence of correlations among events on long time scales is seen in values of $\beta > 0$ and $H \approx 0.8$ in region D. As events are triggered more closely together in time, the average quiet time decreases

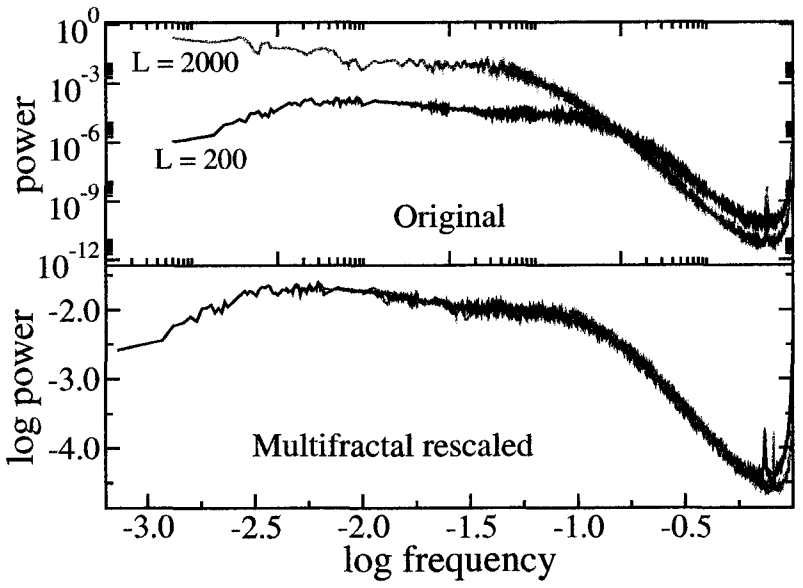

Figure 3.8. Rescaling of power spectra of two different systems with $P_0L^2 = 2.0$, one with L = 200 and one with L = 2000.

to below the average avalanche duration and the separation between regions C and D is lost. This decrease of quiet times also causes β in region D to change most drastically. The simultaneous effects are seen in Figure 3.6.

There are two main points that we would like to particularly emphasize and discuss. The first is that β in region D increases with driving rate until it reaches a limiting value of 1, a $1/f$ region. The second is that H in region D stays constant while β changes and, thus, $\beta = 2H - 1$ is not satisfied.

At high drive, region D is known to have a $1/f$ scaling [11] and the reason was given that overlapping of events produces this special spectral region. Our results show that at low drive, when events do not overlap and $0 < \beta < 1$, the system still has the same physics and the same correlations exist at all driving rates, as shown by the constant H. Given the import attached to the specific $1/f$ scaling over the years, we point out that perhaps $1/f$ is not always $1/f$. By this we mean that the physics that produces $1/f$ may still exist in a system that does not actually reveal a $1/f$ spectrum simply because the system is more slowly driven and the 'signal' is broken up by large periods of quiet times. It implies that a $f^{-\beta}$ scaling with $0 < \beta < 1$ can be just as 'special' as $\beta = 1$.

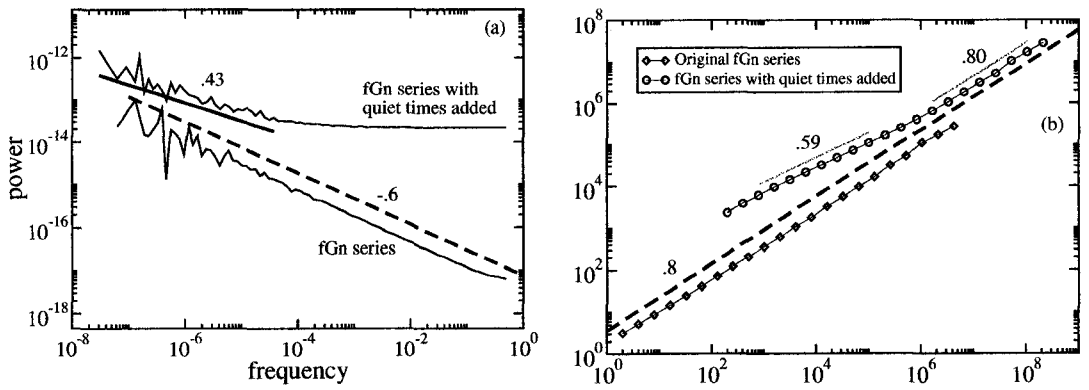

Figure 3.9. (a) Power spectra and (b) R/S analysis for fractional Gaussian noise of $H = 0.8$ with and without quiet times added. Numbers shown are β for spectra and H for R/S.

We can test for this effect by inserting Poisson-distributed quiet times into a series of fractional Gaussian noise (fGn) [15]. FGn is a time series that has a Gaussian probability distribution and an arbitrary Hurst exponent. We inserted quiet times into a fGn series of nonnegative integers created with $H = 0.8$ such that the average of the quiet times was approximately the same as the average of the original fGn series (≈ 20). The results are shown in Figure 3.9. The spectrum and R/S analysis are shown for the original and modified series. The original series follows $\beta = 2H - 1$, with $H \approx 0.8$ and $\beta \approx 0.6$. When quiet times are added between each point of the original series a region of $H \approx 0.5$ appears up to a certain time lag. Beyond this time lag, $H \approx 0.8$ as expected since the correlations among the data have not changed. In the spectrum, $\beta \approx 0$ down to the inverse of the same time lag and then $\beta \approx 0.43$ (note that the R/S shows the breakpoint at a longer time than in the spectrum, the same effect seen in Figure 3.4). This shows that the introduction of quiet times into a correlated series affects β but not H. This effect accounts for the change seen in the sandpile flips data, when β decreases with decreasing drive and increasing average quiet time.

A difference between the sandpile time series and other physical systems that have a $1/f$ spectrum is that in the sandpile series, there are definite lower and upper limits to its values. These limits are 0 when there is no activity in the sandpile and L when all sites are unstable. In other systems that exhibit $1/f$ noise, such as resistance fluctuations [24], there are no such limits though the probability of extremely large deviations from the mean are

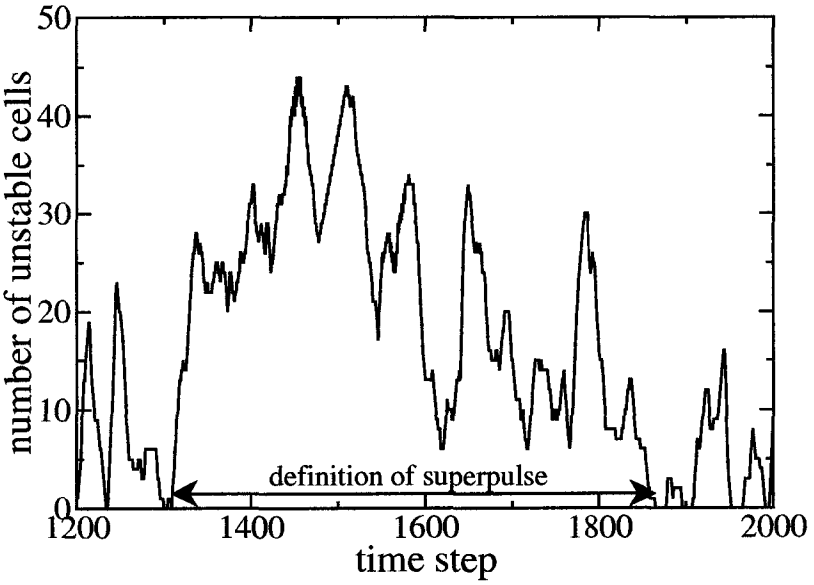

Figure 3.10. Section of flips time series for high drive sandpile and definition of a superpulse.

very small.

There is still the issue, though, that $\beta = 1$ appears to be a limiting value as driving rate increases. Is this simply due to overlapping of events? [12] shows that removing all quiet times from between separate events of a low drive flips time series produces a spectrum with a region D where $\beta = 1$. There is no overlapping of events by design. But what this altered series and an unaltered high drive series have in common is an almost complete lack of quiet times. It appears that $1/f$ is due more to a lack of quiet times and distinct pulse shapes than to overlapping.

There are some quiet times in the high drive sandpile but they are very small, on average. To test if they are important to the dynamics, we shuffle superpulses. A superpulse is defined as the structure between successive quiet times in a high drive flips time series (Figure 3.10). A superpulse comprises many overlapping avalanches. By randomly shuffling the superpulses of a high drive time series, we see that the correlations that lead to $1/f$ and $H \approx 0.8$ are on time scales shorter than the average superpulse. Beyond these time scales, $\beta \approx 0$ and $H \approx 0.5$, signatures of uncorrelated data (Figure 3.11). We conclude that quiet times are unimportant in the dynamics of the high drive sandpile.

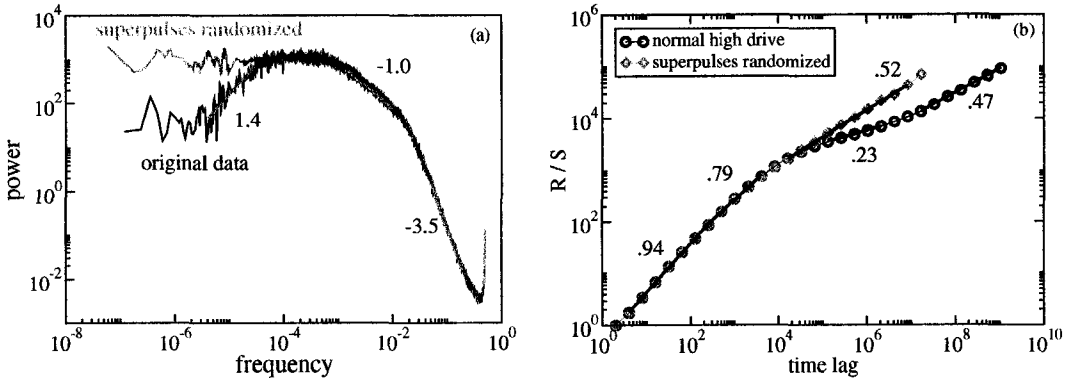

Figure 3.11. Power spectra and R/S for high drive with superpulses changed. Numbers shown are β for spectra and H for R/S.

Our second point is that the relation $\beta = 2H - 1$ does not hold for the sandpile, a SOC system. This relationship was derived based on Gaussian statistics [21]. But R/S analysis itself has no requirement for Gaussian statistics in order for it to measure correlations. Therefore, the relation $\beta = 2H - 1$ that is often associated with the Hurst exponent and power spectrum does not always hold for all systems, such as SOC and the running sandpile. So a physical system cannot be modeled by both SOC and fGn.

3.6 Conclusions

We have analyzed the one dimensional directed running sandpile SOC model for five orders of magnitude of effective driving rate and for different system sizes and shown how the power spectrum and R/S analysis change from low drive to high drive. The most noticeable feature of the change in signatures is the loss of the power law region C at low drive with $\beta = 0$ and $H = 0.5$. This region is due to uncorrelated quiet times between distinct individual avalanches. The region disappears because events are triggered more frequently in the sandpile as driving rate increases; this causes a virtual extinction of quiet times. β and H of this uncorrelated region increase with driving rate until they reach limiting values of $\beta \approx 1$ and $H \approx 0.8$, both being signs of long time correlations. The greatest change in β with increasing driving rate is when the average quiet time is on the order of the average avalanche duration.

At low drive, the power law region D exists on time scales longer than region C. Here,

$\beta \approx 0.4$ at very low drive and β increases with increasing driving rate, reaching the limiting value of 1 as region D merges with region C. The Hurst exponent of this region stays approximately constant, $H \approx 0.8$, as driving rate changes, reflecting the same types of correlations among separate events and the same underlying rules of the system at any level of external forcing.

The changing β and constant H of the correlated region D imply that $1/f$ is not always $1/f$ and that $\beta = 2H - 1$ does not hold for the SOC sandpile model. This first part means that the dynamics that produces a $1/f$ signature at high drive is still present at low drive (since H is constant) but that the spectrum will instead scale as $f^{-\beta}$ with $0 < \beta < 1$. This is taken to mean that such values of β are not necessarily any less 'special' than $\beta = 1$ and that the search for a general underlying process that leads to $1/f$ may be found in systems with different values of β.

$\beta = 2H - 1$ is often accepted as a true statement that relates β and H, regardless of the system. It was derived based upon an artificial data set that is created by an algorithm that is designed to make the relation true. We see that this relation does not hold for a system that creates time series that are, perhaps, more 'natural'. When looking at a physical system, then, both the power spectrum and the R/S analysis can be calculated and compared to see if the system under study can be modeled as a simple fractional Gaussian noise process where $\beta = 2H - 1$ does hold or by some other process where it does not hold, such as SOC.

Bibliography

[1] D. E. Newman, B. A. Carreras, P. H. Diamond, and T. S. Hahm. *Phys. Plasmas*, 3:1858, 1996.

[2] D. E. Newman, B. A. Carreras, and P. H. Diamond. *Phys. Let. A*, 218:58–63, 1996.

[3] A. T. Y. Lui, S. C. Chapman, K. Liou, P. T. Newell, C. I. Meng, M. Brittnacher, and G. K. Parks. *Geophys. Res. Let.*, 27(7):911–914, 2000.

[4] S. C. Chapman and N. W. Watkins. *Space Sci. Rev.*, 95, 2001.

[5] D. L. Turcotte. *Fractals and Chaos in Geology and Geophysics*. Cambridge University Press, 2nd edition, 1997.

[6] P. Bak, C. Tang, and K. Wiesenfeld. *Phys. Rev. Let.*, 59:381, 1987.

[7] P. Bak, C. Tang, and K. Wiesenfeld. *Phys. Rev. A*, 38(1):364–374, 1988.

[8] P. Bak. *How Nature Works*. Springer-Verlag, New York, 1996.

[9] L. P. Kadanoff, S. R. Nagel, L. Wu, and S. min Zhou. *Phys. Rev. A*, 39(12):6524–6537, 1989.

[10] S. S. Manna. *J. Phys. A*, 24(L363), 1991.

[11] T. Hwa and M. Kardar. *Phys. Rev. A*, 45:7002, 1992.

[12] R. Woodard, D. E. Newman, R. Sánchez, and B. A. Carreras. Building blocks of self-organized criticality, part I: the very low drive case. Submitted to PRE, 2004.

[13] X. Yang, S. Du, and J. Ma. *Phys. Rev. Let.*, 92:228501, 2004.

[14] R. Woodard, D. E. Newman, R. Sánchez, and B. A. Carreras. Comment on "Do Earthquakes Exhibit Self-Organized Criticality?". Submitted to PRL, 2004.

[15] B. B. Mandelbrot. *Multifractals and* $1/f$ *noise*. Springer-Verlag, 1999.

[16] http://www.nslij-genetics.org/wli/1fnoise/.

[17] H. J. Jensen. *Self-Organized Criticality: Emergent Complex Behaviour In Physical And Biological Systems*. Cambridge University Press, Cambridge, 1998.

[18] H. E. Hurst. *Trans. Am. Soc. Civ. Eng.*, 116:770, 1951.

[19] B. B. Mandelbrot and J. R. Wallis. *Water Resources Research*, 5:321–340, 1969.

[20] B. B. Mandelbrot. *Gaussian self-affinity and fractals*. Springer-Verlag, 2002.

[21] B. D. Malamud and D. L. Turcotte. *Adv. Geophys.*, 40:1–87, 1999.

[22] M. Gilmore, C. X. Yu, T. Rhodes, and W. Peebles. *Phys. Plasmas*, 9(4):1312–1317, 2002.

[23] R. Sánchez, D. E. Newman, and B. A. Carreras. *Phys. Rev. Let.*, 88(6):068302, 2002.

[24] R. F. Voss and J. Clarke. *Phys. Rev. B*, 13(2):556–573, 1976.

Chapter 4
On The Identification of
SOC Dynamics in the Sun-Earth System

Abstract

We use a self-organized criticality (SOC) model to show that 1) such a system can have different characteristic signatures depending on the level of external forcing while still having the same underlying dynamics and that 2) current time series of Sun–Earth processes are too short to compare with all dynamical regions of a SOC model. SOC is a concept that has been applied to various aspects of the Sun–Earth system, such as rearrangement of magnetic flux loops on the Sun, AE indices and substorm statistics. The basic tenet of SOC is that simple local interactions produce complex global signatures that are not simply predicted by the low level physics. Simple SOC models, such as the sandpile, are used to compare their signatures with those observed in a physical system.

4.1 Introduction

Self-organized criticality (SOC) [1, 2] has been suggested as a model for the dynamics of various aspects of the Sun–Earth system. The basic tenet of SOC is that simple local interactions produce complex global signatures that are not simply predicted by the low level physics. The Sun–Earth system and SOC models share similar dynamical and statistical signatures, such as power law scaling of event size distributions [3] and of the power spectra of some characteristic time series, discussed below. Another shared signature is a Hurst exponent that indicates correlated dynamics over some time scales longer than an autocorrelation time [4]. These very brief statements clearly do not do justice to all that is implied about the Sun-Earth system when viewed from the perspective of SOC. References [5, 6, 7, 8, 9, 10, 11] are some examples of more thorough treatments of the subject.

When deciding whether or not a system is SOC, a usual practice is to compare specific signatures of a defined SOC model and the physical system under study. Rather than saying: "If these signatures are similar, then the system must be SOC," the more cautious approach is to say: "If these signatures are similar, then this system is consistent with SOC dynamics." Fundamentally, it is the characteristics of the dynamics that are of interest.

Here, we investigate two basic issues involved in whether or not even this second statement can be safely made. It is important to note that one cannot prove that a system is SOC unless it has been constructed as such. But it is the shared dynamics among systems that matters most, not the name.

Before presenting those two issues, we briefly mention the measures that we use in this study: the power spectrum and rescaled range (R/S) analysis. We will define and discuss them further below, but for now we simply say that they are two measures that quantify a time series in the frequency domain and time domain, respectively. Both measures can produce distinct straight line regions when plotted on doubly logarithmic axes, indicating power law scaling. Two important features of a SOC time series in this regard are that it 1) produces multiple power law regions and 2) the number and behavior of these power law regions are very different from any other known model, including random uniform or Gaussian noise, fractional Gaussian noise, fractional Brownian motion and random superposition of pulses. We elaborate on the significance of power laws below.

For our results, we first show that the spectral and R/S signatures of a SOC system can change drastically when the external forcing of the system changes. Because of this, there is no single reference signature that a system must match in order to be considered SOC. An application of this idea is in considering the fluctuations in the solar wind as the external driver of the magnetosphere, for which SOC has been suggested as a model. Since the solar wind can range from very strong and steady to practically nonexistent, the reaction to this changing forcing can easily produce different spectra over different time scales.

This result, changing spectrum with changing forcing, can be seen in two ways: by changing the strength of the external drive and by changing the level of correlations in the external drive. Strength of drive is the intuitive notion of how much of some quantity is being deposited in the system per unit time. In terms of the solar wind, for example, very weak drive was seen during the period 10-12 May 1999, when it almost disappeared [12, 13]. (In general, though, SOC is concerned with dynamics on much longer time scales.) The level of correlations deals with the issue of whether the external drive is completely random or not. For instance, the solar wind has been seen to be a correlated source so that the subsequent external driving of the magnetosphere is not completely random. We will

only discuss strength of driving here. Refer to [14] for studies of the effect of correlations in the drive in a SOC system.

Second, we show that the longest available time series of a space climate process is likely far too short to show all of the power law regions in the spectra and R/S measures associated with SOC. 'Too short' here implies a needed time scale on the order of a century. That is, many more generations of scientists will pass before long enough time series are acquired and this issue can be settled.

The rest of this paper is organized as follows. We first review power laws, the power spectrum and rescaled range analysis in Section 4.2 so that we can refer to them in Section 4.3, which is a brief overview of self-organized criticality, our model and some recent work in space physics from the perspective of SOC. We will present and discuss our results of the strength of forcing and the effects of the length of a time series in Sections 4.4 and 4.5. Conclusions are drawn in Section 4.6.

4.2 Power Laws, the Power Spectrum and R/S Analysis

A characteristic associated with SOC since its introduction have been power laws. A power law is any function of the form $y = cx^a$. On doubly logarithmic axes, this function appears as a straight line with slope a; a is also referred to as the scaling exponent. Power laws appear in many measures of many systems, such as probability distributions, power spectra and R/S analysis. We will only discuss the spectral and R/S analyses. For a thorough discussion of power laws in probability distributions refer to [15] and references therein.

When discussing power laws, a usual unstated assumption is that the power law is an appropriate fit of the data over a reasonably wide domain. 'Reasonably wide' is vague so this criteria must be separately established for each case. A common critical, yet reasonable, observation made in regard to these studies is that any function—power law, exponential, sine curve, etc.—can be fit very well to any data if one zooms in to a small enough scale on a plot. Moreover, when two neighboring power law regions are claimed, with different scaling exponents, the additional issue of whether or not there is a distinct breakpoint between the two regions is raised. Needless to say, these are critical issues and the scientist must be aware of them. We are, and elsewhere we have investigated them thoroughly for the data that we present here [16]. In general, we find that a decade (power

of 10) is a reasonable minimum for establishing a power law as a good fit.

Having established that a power law is a good fit to a region and that the limits of the region are identified by breakpoints that separate neighboring regions that may or may not also be fit by a power law, the most important task is to identify the process or processes in the system that produce such a signature. This is where understanding of the particular measure is needed. In practice we find that using more than one measure is invaluable in attempts to understand such systems and signatures. This allows us to use multiple measures to distinguish and quantify separate regions. Hence we complement the power spectrum with the lesser known R/S analysis, with which we estimate the Hurst exponent H.

The power spectrum of a discrete time series $f(\tau)$ allows one to examine the data in frequency space. It is defined as $S(f) = |F(f)|^2$, where $F(f)$ is the Fourier transform of $f(\tau)$; power is plotted versus frequency. The spectrum of random noise (with Gaussian or uniform distribution) is flat ($\sim f^0$) so that the power at all frequencies is the same.

The task of any spectral analysis is to understand why a system has a spectrum that differs from the flat one of a completely random series. A simple example is the spectrum of a sine curve; it is the same flat spectrum as that of the random one except for a spike at the characteristic frequency, indicating where most of the power is concentrated. (Analytically, the spectrum is a delta function; we will deal mainly with finite discrete time series.) A spectrum that has more than one such peak indicates multiple periodic processes in the system.

Besides distinct peaks, another feature of some power spectra is a power law dependence on frequency, where the spectrum scales as $f^{-\beta}$ with $\beta \neq 0$; β can be positive or negative. The power law extends over a finite frequency band (for a finite time series) and there may be more than one such scaling region. Again, the task is to understand why this spectrum is different from that of a random one. Specifically, one must understand why each region has a particular value of β and why the breakpoints of the region occur where they do.

Some spectral power laws are not due to dynamics in a system and can be analytically derived. We refer to this type of power law as one due to pulse shape, which is the highest frequency component of a series. The smoother a function is, the faster its spectrum falls

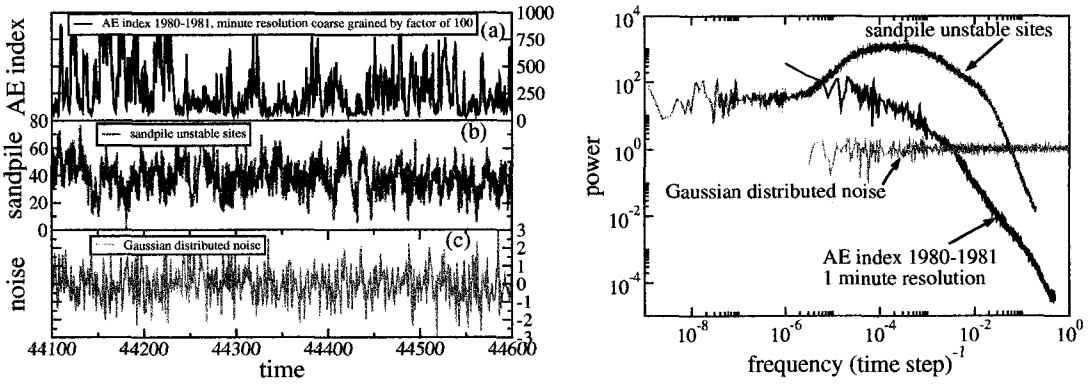

Figure 4.1. Time series and power spectra of AE index, sandpile and Gaussian noise.

off with increasing frequency. This is quantified by taking derivatives of the function. The spectrum falls off as f^{-2k} if the kth derivative becomes impulsive. For instance, a sawtooth wave (a triangular pulse) of width w has an impulsive second derivative so its spectrum scales as f^{-4} as $f \to \infty$. For frequencies below w^{-1}, the spectrum is flat. One can extend this and think of the sine wave as a function that does not have any impulsive derivatives; its spectrum, then, the delta function, falls off infinitely fast with increasing frequency [17]. Another analytically derived power law spectrum is that of a random superposition of square pulses, which falls off as f^{-2} for frequencies above the inverse of the widest pulse [18, 19].

Part of the interest in physical systems that have power law scaling regions in their power spectra is because the time series themselves are far from the simple examples above. Most time series of 'real' physical processes, such as the AE index or fluctuations in the solar wind velocity, are not simple shapes or superpositions of simple shapes. They look noisy, almost random. Yet they still have spectra that are very different from that of a completely random process (Figure 4.1). Spikes in the spectra can usually be explained by known periodicities in the system (rotation of the earth, 11 year solar cycle, etc.). But the observed values of β and the locations of breakpoints between scaling regions, in most cases, are not well understood and are probably important indicators of the dynamics.

Qualitatively, a spectrum that falls off as $f^{-\beta}$ with $\beta > 0$, a negative slope on log-log axes, means that lower frequencies are most important in characterizing the time series. For values of $\beta < 0$, a positive slope, the higher frequencies dominate the signal. So signals

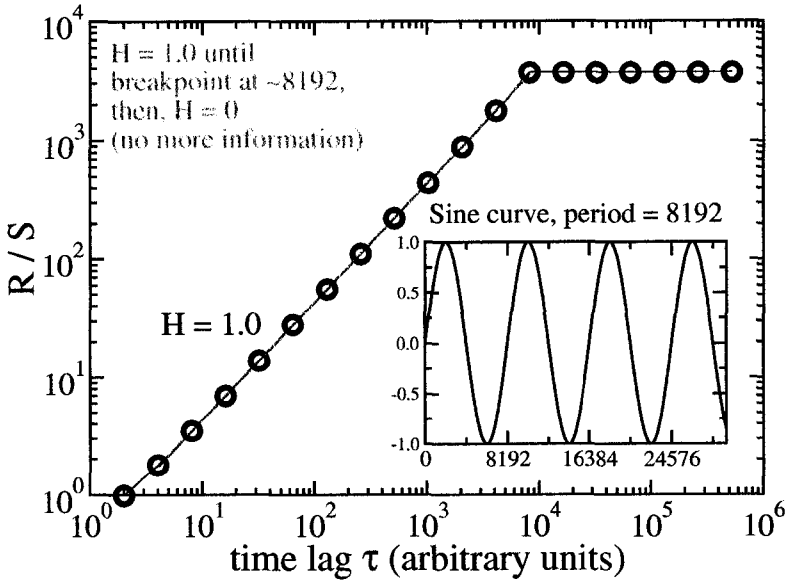

Figure 4.2. Time series and R/S analysis of sine curve.

with $\beta > 0$ are smoother than those with $\beta < 0$. Because of this, the smoother signals with positive β are said to be correlated and the rougher ones with negative β are anticorrelated. Here, correlated implies that a current trend in the data continues. The value of β, then, is often used as a measure of correlations in a time series.

A different and perhaps better measure of correlations in a time series is the Hurst exponent, $H \in [0,1]$. A value of $H = 0.5$ implies a data set that is completely random, with no correlations. Series with $H > 0.5$ are correlated and those with $H < 0.5$ are anticorrelated. The closer H is to 0 the rougher and more anticorrelated is the signal; the closer to 0.5, the more uncorrelated; and the closer to 1 the smoother and more correlated. For instance, $H = 0.5$ for a time series of fair dice being rolled and $H = 1$ for a sine curve up to its period (Figure 4.2). [4] has estimated the Hurst exponent of the AE index as $H \approx 0.7$, indicating that the AE process has long time correlations.

One technique of estimating H is through rescaled range (R/S) analysis [20, 21]; there

are other methods [22, 23, 24]. For a series of data ξ_t, the rescaled range is defined as:

$$R'(s) \equiv R(s)/S(s) \quad \text{(rescaled range)}$$

$$R(s) = \max_{1\le t\le s} X(t,s) - \min_{1\le t\le s} X(t,s), \quad \text{(range)}$$

$$X(t,s) = \sum_{u=1}^{t} (\xi_u - \langle\xi\rangle_s) \quad \text{(cumulative deviation)}$$

$$S(s) = \left[\frac{1}{s}\sum_{t=1}^{s} (\xi_t - \langle\xi\rangle_s)^2\right]^{1/2} \quad \text{(standard deviation)}$$

$$\langle\xi\rangle_s = \frac{1}{s}\sum_{i=1}^{s} \xi_i \quad \text{(mean)}$$

If the rescaled range of the time series scales as $R'(s) \sim s^H$, the slope of the plot of $R'(s)$ versus the time lag s on a doubly logarithmic plot is an estimate of the Hurst exponent, H.

H can be related to the more familiar measure, variance. Consider classical Brownian motion (a random walk), the increments of which are simply a Gaussian distributed random noise. For a large ensemble of random walks, the expectation value of the variance of the motion scales linearly with time, $\sigma^2 \sim t$. For the noise series, $H = 0.5$. In general, the variance of the motion is related to the Hurst exponent of the noise by $\sigma^2 \sim t^{2H}$.

Algorithms exist [21] that create synthetic time series with Gaussian distributions and a given value of $0 < H < 1$. Such a series is called fractional Gaussian noise (fGn) and when integrated produces fractional Brownian motion (fBm). For these series, H is analytically related to the slope of the power spectrum of the fGn via $\beta = 2H - 1$. For discrete fGn data, though, this relation does not hold so well at all values of H. A thorough discussion of H and β in the context of fGn is given in [25].

It is very important to note that the relation $\beta = 2H - 1$ is not always true for physical data. This is equivalent to saying that fGn is not an appropriate model for the system under study. A basic example is the time series of a single sawtooth pulse mentioned above. It has a power spectrum that falls off as f^{-4} and a Hurst exponent, calculated via R/S analysis, of $H \approx 1$ (Figure 4.3). Here, $\beta \neq 2H - 1$; the spectrum and the R/S analysis describe two different aspects of the same series. $\beta = 4$ is a statement about the discontinuity of the first derivative of the sawtooth pulse and $H \approx 1$ is a statement of the strong correlation that a defined shape has with itself for time scales up to its width.

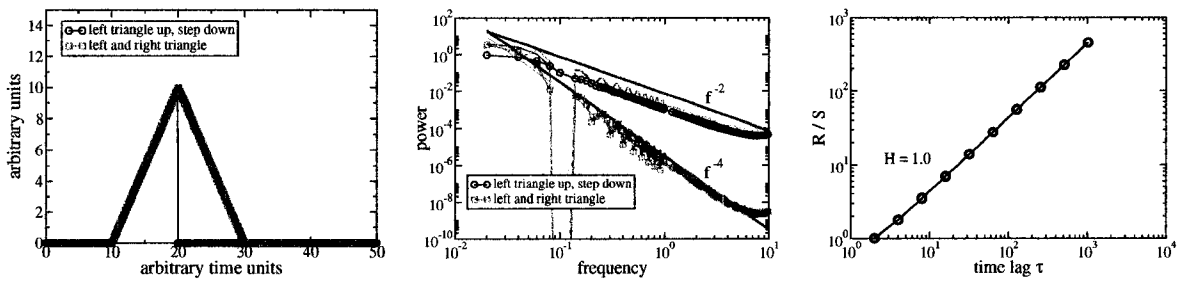

Figure 4.3. Time series, power spectrum and R/S analysis of a sawtooth pulse.

Self-organized criticality is a model where $\beta \neq 2H - 1$ over different time scale regions. But the reasons are not as simple as for that of a single pulse. Here, the dynamics of a SOC system has correlations, anticorrelations and lack of correlations on distinctly different time scales and on time scales larger than that of the largest fundamental single pulse. The changing levels of correlations appear in the power spectrum and R/S analysis of a SOC system as separate and distinct power law regions.

Looking at only the spectrum or the R/S alone does not adequately explain the regions of a SOC system. But together the measures give a clear picture of SOC dynamics. We emphasize this to encourage the use of multiple measures in any system; taken alone, the power spectrum does not always explain the dynamics of a system.

4.3 Self-Organized Criticality and the Sun-Earth System

The underlying idea behind self-organized criticality is that, in many complex systems, simple local interactions produce complex global signatures that are not easily predicted by the local low level physics. That is, the fundamental physics of a system is often understood but some of the observed signatures are not captured by models that are built on that physics. An example is the power spectrum of the AE index seen in Figure 4.1. The problem is that, inevitably, all models must leave something out, must make some approximations.

The main approximation that a SOC model makes is to reduce all of the local physics in a system to a simple physical rule: if the local gradient of some quantity between two nearest neighbors exceeds some critical gradient, then reduce the gradient by transporting some of the quantity from one neighbor to the other. A 'neighbor' is purposefully vague

and can be different for each system. It represents the notion that gradients exist on macroscopic scales and the source of the gradients is not as important as the fact that they grow, shrink and interact. Crucial to the SOC dynamics are that the time scales of the driving and relaxing processes are very different: the gradients are reduced much faster than they are produced. Within these bounds, a plethora of models can be constructed but all adhere to this one rule; we describe our model, the sandpile, below. The interesting dynamics appears because the transport from one neighbor to the next may make the next local gradient exceed the critical gradient, causing a new transport event. In this way, disturbances can propagate throughout the model.

In the jargon of SOC, the disturbances are often referred to as avalanches. Avalanches can range in size from the smallest possible (one transport event) up to the size of the system. Over much of this range of scales, SOC avalanches are distributed as a power law, indicating no preferred spatial scale within that range. This is the criticality part of SOC. It refers to statistical mechanics, where disturbances in a material at a phase transition can propagate throughout the entire sample. In such a case, a control parameter—the temperature—must be tuned to reach this critical state. In contrast, a SOC system arrives at criticality with no external tuning of a parameter [1]. The system self-organizes to the critical and steady state.

Time series of the avalanches can be constructed and analyzed. Regions of the power spectra of these time series scale as power laws, indicating correlations and anticorrelations on different time scales. These temporal power laws together with the spatial power laws of the avalanche size distributions are important signatures of SOC systems that are similar to signatures of many observed physical systems. Because of these similarities and of the underlying physics, the Sun-Earth system has been studied as possibly SOC.

The model that we use is the one dimensional running sandpile, studied extensively in [27, 16]. The sandpile consists of L cells labeled by an index $n \in [1, \mathrm{L}]$. Each cell stores an amount of sand h_{n} and the local gradient between two cells is defined as $Z_{\mathrm{n}} = h_{\mathrm{n}} - h_{\mathrm{n+1}}$. U_0 grains of sand are dropped randomly on every cell at each iteration with probability P_0. The external drive per cell is thus $S_0 = U_0 P_0$ grains per time step. SOC dynamics appears

[1] This is a matter of discussion in the world of SOC. See, for example, [26] and references therein for a discussion.

because of the existence of a critical slope Z_{crit} that, when locally overcome, triggers the removal of N_f grains of sand to the next cell in the downhill direction (increasing n). The sandpile is initialized with $h_n = (Z_{crit} - 1)(L - n)$ and run for T_{max} time steps. We study the sandpile in steady state so that transient time steps before T_T are ignored in the following analysis.[2] We used $U_0 = 1$ (therefore $S_0 = P_0$), $Z_{crit} = 8$ and $N_f = 3$, the same parameters used in a study of confined plasmas [28]. In this study, we use sandpile sizes of L = 200 and 1000 and driving rates of $P_0L = 0.2$, 0.1 and 0.001. We study a more complete range of five orders of magnitude of driving rate and three orders of magnitude of system size in [16].

Effective driving rate is given by P_0L^2 [16]. The idea of effective driving rate is that a fixed driving rate P_0, which is in units of grains per cell per time step, is effectively higher for a small sandpile than for a larger one. Since a larger sandpile has a greater capacity, P_0 will take longer to fill it up when compared with the same rate of sand falling onto a smaller system. In the past, P_0L has been used as the measure of driving rate because its units are in grains per time step for the entire system. But since the average avalanche size is larger in a larger sandpile, two sandpiles of different sizes but with the same P_0L can be in very different drive regimes because the quiet times will be shorter in the larger system. We find that a better measure, effective driving rate, should be used. Systems with different size and/or P_0 but with the same value of P_0L^2 have power spectra that are related via a rescaling function. We elaborate on effective driving rate in [16].

The time series that we analyze is called the flips. Consider the total number of unstable sites (where $Z \geq Z_{crit}$) at each time step in a sandpile model in steady-state. An unstable cell spills N_f grains of sand to the next cell; this action is a flip. The total flips at each time step can be thought of as the instantaneous (potential) energy dissipation in the system. The sandpile is driven by a random process but the number of flips fluctuates with time in a way that is not entirely random, as we show.

4.4 Effect of Strength of External Forcing and System Size

We now show that systems with very different driving rates can have very different spectral and R/S signatures. Figure 4.4 shows the power spectra from three different sandpile

[2]The initialization saves computer time; the same results hold when the sandpile is started from any initial condition. The transient time T_T must be adjusted accordingly.

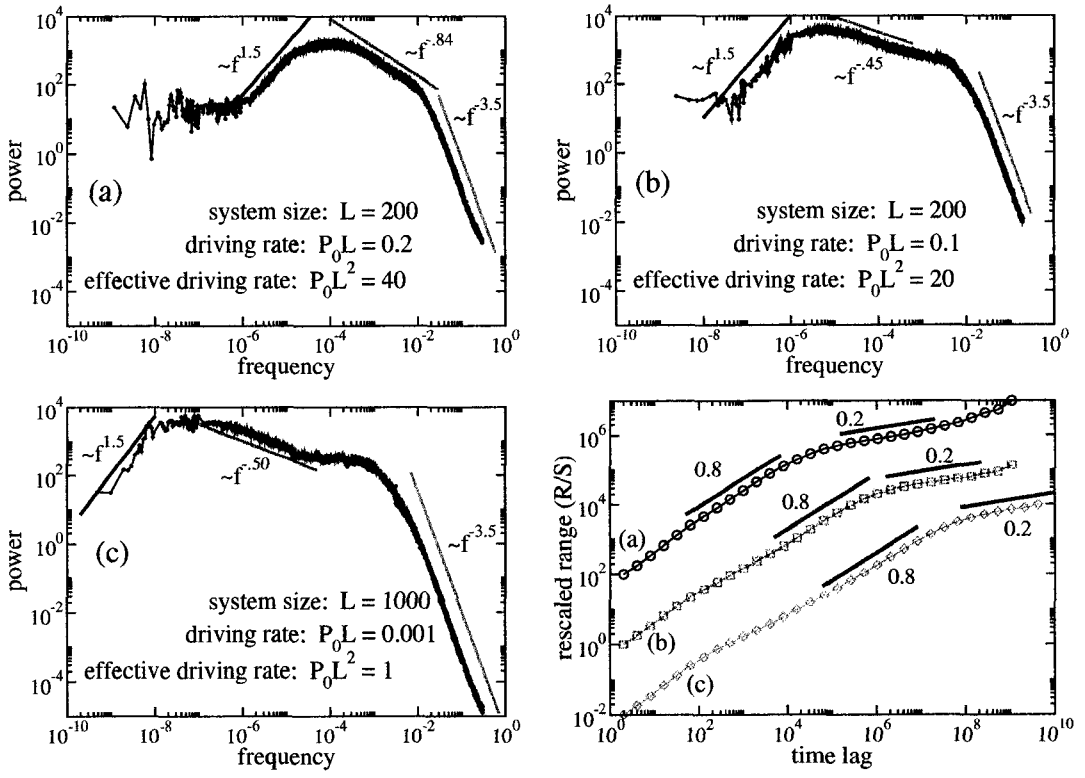

Figure 4.4. Power spectra and R/S analysis of flips of running sandpile model for three different values of effective drive, P_0L^2. Spectra and rescaled range have been shifted along the y-axes so that all plots are over the same range. Estimates of the Hurst exponent are shown for the straight line segments in the R/S plot. These are not fits of the data but lines of the indicated slope to guide the eye.

runs. Runs (a) and (b) differ in their driving rate P_0L and runs (b) and (c) differ in their driving rate and system size, L. Run (a) is the smallest system with the highest driving rate; run (b) is the same size but with a lower driving rate; run (c) has a lower driving rate and larger system size than (b). The effective driving rate P_0L^2, then, decreases from run (a) through (c), with (c) being the lowest effective driving rate. The spectra can be seen to change systematically.

The spectra in Figure 4.4 show different power law scaling regions for all driving rates. Each spectrum actually has 4 or 5 separate regions, depending on effective driving rate [16]; we have sketched lines on each indicating only three of these regions. The highest frequency region with $\beta \approx 3.5$ indicates correlations at short time scales, where avalanche

pulse shapes correlate with themselves. On longer time scales, the middle frequency region has a slope $0 < \beta \leq 1$ that changes with driving rate. These positive values of β indicate correlations among separate and overlapping avalanches. The time scales for this region are greater than the maximum duration of a single avalanche. The lowest frequency region with $\beta \approx -1.5$ indicates anticorrelations on the longest time scales. These are the time scales of global discharge events, where one such event is unlikely to be followed by another similar event.

The R/S analysis of sandpile flips also shows multiple regions. We have only indicated two in Figure 4.4. These correspond to the middle and long time scales of the power spectra. The estimated values of the Hurst exponent can be compared with the values of β in the spectra. For both cases, $\beta \neq 2H - 1$. Most importantly, the middle time scale region has a constant value of $H \approx 0.8$ while β changes with driving rate. This is because H measures correlations in the sandpile that are produced by the memory in the system due to the system rules. The rules do not change as driving rate changes, hence H stays relatively constant. Because of the changing values of β in this region, it is not clear what aspect of the correlations is measured by the power spectrum.

The goal of these results is to show that the SOC running sandpile model will produce very different power spectra when the level of external forcing changes. This is why comparing the values of the slope or the number of regions of the spectrum of a physical system like the Sun-Earth system with those of a single run of a SOC model can be misleading. If the values of the slope do not match or if the number of regions are different, this does not necessarily mean that the system is not SOC. Instead, it could be that the system is in a different drive regime than that of the model being used.

An important aspect of the running sandpile model is that over a very wide range of driving rate it is still in a state of SOC. That is, it still exhibits all of the qualitative signatures that collectively are called SOC. These include power law distributions of event sizes, power law regions in the power spectra, correlated dynamics indicated by Hurst exponents $H \neq 0.5$ and regions and event sizes that scale with system size. More importantly, the physics in the models is identical *regardless of driving rate.* Sand is still added at a constant probability that triggers avalanches that may or may not spread throughout the entire system. The memory of the avalanches is retained in the local gradients of each cell

Table 4.1. Time period, resolution, slopes of first two spectral regions and breakpoint of AE index data. Data found in [29], [30], [5], [4] and [31]. Breakpoint for [30] taken between labeled second and third regions. Breakpoint for [4] 1978-1979 estimated from plot at intersection of two power law fits. Slope for [31] taken as best fit with a straight edge, slope estimated from axes.

Study	Period	Res.	β_A	β_B	Break (mHz)
[29]	1967–1970	5 min	2.42	1.02	0.059 (4.7 hr)
[29]	1971–1974	1 hr	2.2	0.98	0.050 (5.5 hr)
[5]	1973–1974	1 hr	2.10	0.95	0.056 (5.0 hr)
[30]	1/1–19/2 1975	1 min	2.65	1.14	0.073 (3.8 hr)
[31]	1978	5 min	2.1	1.1	0.056 (5.0 hr)
[4]	1978–1979	1 min	1.85	0.82	0.033 (8.4 hr)
[29]	1978–1980	1 hr	2.2	1.00	0.056 (5.0 hr)
[4]	March 1979	1 min	1.89	n/a	n/a
Mean $\pm\ \sigma$			2.4 ± 0.26	1.0 ± 0.10	

and this is the source of long time correlations. The only difference is the rate at which the avalanches and the time scales over which the correlations occur.

This idea can be applied to data that is already in the literature. The first power spectrum of the AE index showing the broken power law behavior was seen in [29] for data from three separate periods, 1967-1970, 1971-1974 and 1978-1980. Similar spectra were shown subsequently by [30], [5], [4] and [31]. The time periods studied in all of these works, as well as the slopes of the spectra in the two regions and the location of the breakpoints are shown in Table 4.1. That they vary over different periods is completely consistent with an SOC model that runs for a time at one driving rate and then for another time at a different driving rate. In general, the slopes found for shorter periods of observations differ the most from the average of all samples. In the language of the sandpile, there are two possible causes for this.

First, the driving rate can change over time so that the average input of the solar wind over the period 1 January through 19 February 1975 was very different from the period

1978-1979. These two periods were chosen as examples because they show the greatest difference in slopes for both spectral regions among the values presented. That one period is near the solar minimum and the other near the solar maximum should be noted and taken as a possible example of the level of external forcing changing the power spectrum, as in the running sandpile model.

A second and, in this case, more likely possibility that can account for changing spectra for the time periods shown is that over a long time scale, say the roughly 40 year period for which we have AE index data, the input to the system (the solar wind) is constant in the same way that the mean of a series of random numbers is constant. But when one looks at a small subset of the random series, the mean may be very different and there will certainly be fluctuations far from the overall mean. In other words, data is scattered within the errors bars of a sampling. All of the values of β in Table 4.1 are within 2σ of the mean.

Both of these possibilities are intuitively appealing because the Sun, the driver in the Sun-Earth system, is known to not have a constant output from year to year. But whether that change is due to a fundamental change in the drive regime of the Sun or to intrinsic fluctuations within a steady state is not clear.

As a quick test of this idea, we compared power spectra for three different three day periods, 10-12 May 1999, 26-28 January 1999 and 12-14 November 1999. The solar wind essentially vanished during the first period [12, 13], falling more than 98% for a period of approximately 30 hours. The other two periods were closer to the yearly mean. There is no significant difference in the spectra among the three cases. We attribute this to the very short observation time, as the spectra show much ringing at high frequencies, making determination of any sort of fit statistically irrelevant. We must wait for longer periods of no solar wind to pursue this idea further.

In addition to those of measured AE indices, the literature also holds power spectra of a continuum model that "provides a link between the sandpile model studies ... and a realistic plasma physical study of SOC dynamics in the plasma sheet [8]." That study refers to the Lu model of [32], which "can be viewed as an idealized one-dimensional resistive field reversal model in which the resistivity is generated self-consistently." This is a model where a scalar field is evolved in time while coupled to a variable diffusion coefficient and source term that are space and time dependent. In terms of the sandpile model, the scalar

field of the Lu model represents the height or gradient at each cell, the variable diffusion represents the avalanche rule and the source term represents the rain of sand. [3]

Power spectra of this model are shown in [8] for varying levels of the source term and the diffusion operator. As in the spectra of the running sandpile for varying driving rates, these spectra exhibit a wide range of behavior. Also, as in the sandpile model, the same physics from the same system produces these different spectra. This says that a system in a state of SOC can show very different signatures depending upon the drive regime in which it operates.

Concerning the anticorrelated region of the spectra, reference [8] states that the comparison of that model with the running sandpile appears to fail in this region because no system-wide discharges where all grid points are simultaneously unstable are seen in the continuous model. Instead, the largest events observed show wave-like behavior in the hydrodynamic regime. This behavior is, in fact, consistent with the sandpile model because of the following.

We have performed additional sandpile runs [16] that append the results of [27] and show that all sites are rarely, if ever, simultaneously unstable. System-wide discharges do not refer to a single time step where all cells are unstable. Instead, these large events occur over a short period of time. Recall that sand only exits the sandpile through the bottom cell, which has a small and fixed amount of sand, N_f, that it can transport at a single time step. The nature of the sandpile is such that, in what is called the $N_f/2$ limit, a cell in the middle of a spatially extended avalanche alternates between stable and unstable until the avalanche has either washed passed it or died. The drive regimes studied by [27] and [16] are well below the $N_f/2$ limit. Furthermore, animated visualizations [34] of the sandpile show that these system-wide discharge events are really a series of many avalanches in a short period of time and that they are very wave-like in nature. So then the observed behavior of the Lu model discussed in [8] is consistent with that of the running sandpile. This is another motivation for looking for similar SOC regions in physical data, as we next discuss.

[3] In the interest of cross-field communication, we mention that a very similar model to that of [32] has been applied to the study of the running sandpile model in the context of plasma transport in confined plasma devices [33]. Citations within that work refer to other studies of sandpile dynamics in confined plasmas.

4.5 Effect of Length of Time Series

The comparison of regions between the AE index and the sandpile model end at region B because of the limited time series for the AE index. The question arises: How long must the AE index time series be in order to see a new region at lower frequencies? This question assumes that the long-term process that drives the Sun-Earth system and that some properties of the Sun, magnetosphere and the space in between remain somewhat constant.

This question also assumes that the lower region seen in the spectrum of the AE index *will* end. Of course, the lifetime of a star ensures this on the longest time scales but this ending falls outside the bounds of the first assumption. We claim that this region will end for dynamical reasons. The positive slope $\beta > 0$ of a spectral region and Hurst exponent $H > 0.5$ imply long time correlations. But the correlations must end on some time scale because a system of finite size driven randomly will reflect the random drive at the longest time scales [16].

Given a steady state Sun-Earth system and a randomly driven yet deterministic universe, then the correlations must end at some time scale. Anticorrelations may arise in this system in the same way that they do in the running sandpile: all gradients in a finite system eventually grow close to critical and then trigger a system-wide discharge. This speaks to the finite capacity of the system. Perhaps an energy and mass balance calculation between the fluctuations of the input from the solar wind and output through the magnetotail, magnetopause and other parts of the system can give an estimate of a time scale on which the magnetosphere reaches capacity.

Figure 4.5 shows the same spectrum of the AE index as that in Figure 4.1 but now we have drawn lines showing possible behavior of the spectrum at longer time scales based on the behavior seen in sandpile spectra. We adamantly state here: the breakpoints and slopes of these lines are not predictions of breakpoints and slopes that would be seen given arbitrarily long AE time series. Instead, they are drawn to demonstrate how long the time series would have to be to see this behavior. At best, we now have roughly 40 years of AE index data. Since we look at scaling behavior on log-log axes, the full 40 years of data would only slightly extend the plot to the point labeled. An order of magnitude greater time series, 400 years, would extend the plot as shown. Observation of the spectra of

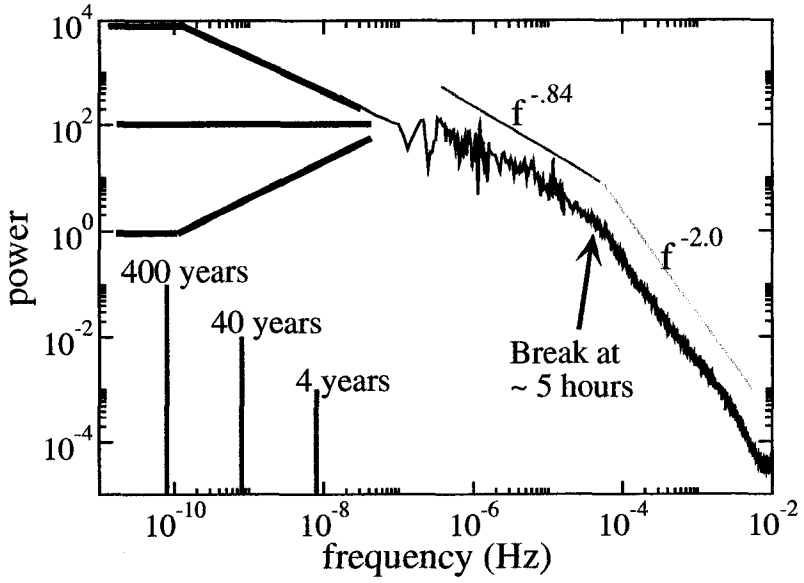

Figure 4.5. Power spectrum of AE index 1980-1981 and cartoon of time scales of additional spectrum.

sandpile models, AE index and other physical systems shows that nature does not cut her spectra off abruptly at low frequency. This is, of course, a rough and qualitative argument. But we do expect to see the spectrum of the AE index roll over to, possibly, an anticorrelated region with $\beta < 0$ and/or, definitely, a flat, uncorrelated region. Based on the slope of the best current spectra and longest available time series, we will not be around to see that new region.

4.6 Conclusions

We have shown that a rich diversity of spectral signatures can be produced by a self-organized critical system when the effective driving rate is changed. This has implications in the ongoing investigations of studying SOC as a model of various physical systems, including the Sun-Earth system. Our results show that failure of the power spectrum of a physical system to match that of the running sandpile model with a certain driving rate does not at all exclude SOC as an appropriate model for the system. A system can be in a wide range of drive regimes yet still be considered SOC even though the spectral signatures differ among the different regimes. This is a statement on the lack of tuning that is

required for a SOC system to be critical; it is the self-organized portion of the name.

The system remains critical because the physics does not change when the driving rate changes. In the sandpile, changing the driving rate merely changes how fast or how slowly sand is added to the pile. The rules of the system have not changed. A memory of past events is stored in the local gradients of the system regardless of how fast or slowly sand is added. The analogy to a physical system is this: the underlying physics of the transport of a system, such as the Sun-Earth system, does not change when it is driven more strongly or weakly. Gradients still grow and shrink by the fundamental physical processes. But the rate at which this happens changes and this change is reflected in the different spectra of a process over different periods of time.

We also discussed that the current longest available time series of the AE index only shows two regions in the power spectrum. Inevitably, the region at lower frequency with $\beta \approx 1$ must either flatten or turn down to an anticorrelated region with $\beta < 0$ before flattening at the lowest frequencies. The flat f^0 spectrum is a signature of a fundamental random process that is driving the system. An anticorrelated region reflects a system of finite size and capacity that non-periodically relaxes in a series of long bursts over a short period of time.

The running sandpile model has a well-defined clock which makes it different from other SOC models. More importantly, this feature, along with its dynamics that is similar to many physical processes, make it an appropriate model to use in the study of physical systems that are suspected to be SOC, such as that of the Sun and Earth.

Bibliography

[1] P. Bak, C. Tang, and K. Wiesenfeld. *Phys. Rev. Let.*, 59:381, 1987.

[2] P. Bak, C. Tang, and K. Wiesenfeld. *Phys. Rev. A*, 38(1):364–374, 1988.

[3] V. M. Uritsky, A. J. Klimas, D. Vassiliadis, D. Chua, and G. Parks. *J. Geophys. Res.*, 107(A12):7–1 – 7–11, 2002.

[4] C. P. Price and D. E. Newman. *J. Atmos. Sol. Terr. Phys.*, 63:1387–1397, 2001.

[5] V. M. Uritsky and M. I. Pudovkin. *Annales Geophysicae*, 16:1580–1588, 1998.

[6] V. Angelopoulos, T. Mukai, and S. Kokubun. *Phys. Plasmas*, 6(11):4161–4168, 1999.

[7] T. S. Chang. *Phys. Plasmas*, 6:4137–4145, 1999.

[8] A. J. Klimas, J. A. Valdivia, D. Vassiliadis, D. N. Baker, M. Hesse, and J. Takalo. *J. Geophys. Res.*, 105(A8):18,765 – 18,780, 2000.

[9] A. T. Y. Lui, S. C. Chapman, K. Liou, P. T. Newell, C. I. Meng, M. Brittnacher, and G. K. Parks. *Geophys. Res. Let.*, 27(7):911–914, 2000.

[10] S. C. Chapman and N. W. Watkins. *Space Sci. Rev.*, 95, 2001.

[11] T. Chang, S. W. Y. Tam, C.-C. Wu, and G. Consolini. *Space Sci. Rev.*, 107:425–445, 2003.

[12] G. Le, C. Rusell, and S. Petrinec. *Geophys. Res. Let.*, 27(13):1827–1830, 2000.

[13] G. Le, P. Chi, W. Goedecke, C. Rusell, A. Szabo, S. Petrinec, V. Angelopoulos, G. Reeves, and F. Chun. *Geophys. Res. Let.*, 27(14):2165–2168, 2000.

[14] R. Sánchez, D. E. Newman, and B. A. Carreras. *Phys. Rev. Let.*, 88(6):068302, 2002.

[15] D. Sornette. *Critical Phenomena in Natural Sciences—Chaos, Fractals, Selforganization and Disorder: Concepts and Tools*. Springer, 2000.

[16] R. Woodard, D. E. Newman, R. Sánchez, and B. A. Carreras. Building blocks of self-organized criticality, part I: the very low drive case. Submitted to PRE, 2004.

[17] R. N. Bracewell. *The Fourier Transform and Its Applications*. McGraw-Hill, 3rd edition, 2000.

[18] H. J. Jensen, K. Christensen, and H. C. Fogedby. *Phys. Rev. B*, 40(10):7425–7427, 1989.

[19] J. Kertész and L. B. Kiss. *J. Phys. A*, 23:L433–L440, 1990.

[20] H. E. Hurst. *Trans. Am. Soc. Civ. Eng.*, 116:770, 1951.

[21] B. B. Mandelbrot. *Gaussian self-affinity and fractals*. Springer-Verlag, 2002.

[22] J. B. Bassingthwaighte and G. M. Raymond. *Annals of Biomedical Engineering*, 22:432, 1994.

[23] J. B. Bassingthwaighte, L. S. Liebovitch, and B. J. West. *Fractal Physiology*. Oxford University Press, 1994.

[24] J. B. Bassingthwaighte and G. M. Raymond. *Annals of Biomedical Engineering*, 23:491, 1995.

[25] B. D. Malamud and D. L. Turcotte. *Adv. Geophys.*, 40:1–87, 1999.

[26] H. J. Jensen. *Self-Organized Criticality: Emergent Complex Behaviour In Physical And Biological Systems*. Cambridge University Press, Cambridge, 1998.

[27] T. Hwa and M. Kardar. *Phys. Rev. A*, 45:7002, 1992.

[28] D. E. Newman, B. A. Carreras, P. H. Diamond, and T. S. Hahm. *Phys. Plasmas*, 3:1858, 1996.

[29] B. T. Tsurutani, M. Sgiura, T. Iyemori, B. E. Goldstein, W. D. Gonzalez, S. I. Akasofu, and E. J. Smith. *Geophys. Res. Let.*, 17(3):279–282, 1990.

[30] G. Consolini, M. F. Marcucci, and M. Candidi. *Phys. Rev. Let.*, 76(21):4082–4085, 1996.

[31] N. W. Watkins. *Nonlinear Processes in Geophysics*, 9:389–397, 2002.

[32] E. T. Lu. *Phys. Rev. Let.*, 74(13):2511–2514, 1995.

[33] L. Garcia, B. A. Carreras, and D. E. Newman. *Phys. Plasmas*, 9(3):841–848, 2002.

[34] R. Woodard, D. E. Newman, R. Sánchez, and B. A. Carreras. Building blocks of self-organized criticality, part II: transition from low to high drive. Submitted to PRE, 2004.

Chapter 5
Transport Events and Correlation Lengths in a SOC Confined Plasma Model

Abstract

Plasmas confined in toroidal devices exhibit both radial and poloidal diffusion as well as poloidal rotation. To model this in a self-organized criticality (SOC) framework we add poloidal spreading and bulk flow to a two dimensional SOC running sandpile model to investigate the effects of poloidal diffusion and flow on transport events and on radial and poloidal correlation lengths. We find that a small amount of poloidal spreading decreases large event frequency and increases small event frequency to maintain constant flux. Radial correlation lengths are found to decrease and poloidal correlation lengths increase. When the spreading is increased, large event frequency and radial and poloidal correlation lengths increase and the transport dynamics change. When bulk flow is added, large event frequency appears to decrease because of the effect of transport events advecting past a fixed probe in a flowing system. We show how to take the flow rate into account to properly measure transport event sizes and correlation lengths.

5.1 Introduction

Observed cross-field radial transport of density and temperature in confined plasmas is larger than predicted by most theory. The extra transport reduces confinement time and inhibits the attainment of economical fusion. Turbulence is thought to be the cause of this anomalous transport [1]. Instabilities, such as, for example, those driven by ion temperature gradients, have been proposed as the drivers of the turbulence [2]. However, the high gradients necessary for the suspected modes to account for the observed transport are themselves often not observed. In addition, theory says that this suspected turbulence is caused by small-scale fluctuations on the order of the ion Larmor radius, which means that the rate of transport should scale with the gyroradius (gyro-Bohm scaling). Experiments with confinement devices, though, have shown that the transport rate scales with the system size (Bohm scaling) [1]. A major goal of fusion research is to understand how to force the plasma to obtain gyro-Bohm scaling.

The rate of plasma poloidal flow shear can contribute to the control of the rate of plasma radial diffusion. To whit, more flow shear decorrelates radial transport events thereby decreasing the radial diffusion rate. The reduced radial diffusion rate means the plasma has more time to diffuse poloidally. So in this work, we have investigated increased poloidal spreading as a way to study the effects of decreased radial transport due to flow shear.

Self-organized criticality (SOC) [3, 4, 5] models have been used to study the turbulent transport problem [6, 7, 8, 9] because SOC dynamics exhibits many features observed in plasma devices, such as robust sub-marginal transport, Bohm scaling of the transport, correlations in the fluctuations that last longer than typical turbulent decorrelation times and a decrease in these correlations when shear flow is added to the dynamics [6, 7]. Also, similar signatures of power spectra and rescaled range analysis of both plasma devices and SOC models imply similar dynamical processes in both systems [10, 11, 12, 13]. SOC systems can maintain steady-state transport with a sub-marginal global gradient because of local gradients that persist, grow, become unstable and then relax in small scale transport events. SOC models capture relevant large scale transport features without specifying the cause of the small scale fluctuations. This suggests that such models are appropriate to use even when the actual active plasma mode(s) is (are) not known.

One such SOC model is known as the one dimensional running sandpile [14, 15, 16, 17]. The one dimension represents a minor radius in a poloidal cross-section of a toroidal confinement device, assuming toroidal and poloidal symmetry. The value at each site in this one dimension can represent density or temperature, for example. For convenience, this value in the model is referred to as the height of sand at each site. A constant (on average) global gradient exists between the 'core' and the 'edge.' The gradient is maintained through local random additions of sand throughout the system and an open boundary condition at the edge. A one dimensional transport model [9] based on the running sandpile and plasma equations has been shown to be consistent with SOC dynamics and plasma observations. A two dimensional extension to the sandpile [6, 7] has been used to study the effects on the dynamics from the addition of poloidal shear flow, such as that seen when higher levels of $\mathbf{E}\times\mathbf{B}$ shear cause enhanced confinement modes [18]. The added dimension is the poloidal direction so that this two dimensional model represents a poloidal cross section of the device (Figure 5.1).

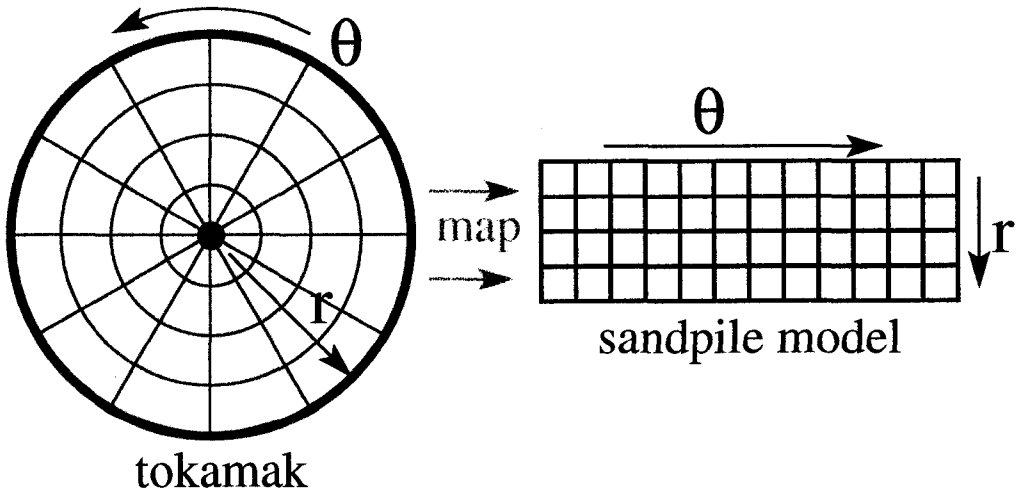

Figure 5.1. Mapping of tokamak poloidal cross section to two dimensional sandpile. There is not a one-to-one mapping of cells from the cross section to cells in the sandpile. This picture is for conceptual purposes.

In both the one and two dimensional SOC models, transport occurs usually in the radial direction but this is not necessarily true for plasma in a toroidal confinement device. Magnetic field lines wind poloidally and toroidally throughout the device and transport and/or equilibration along these field lines occurs much faster than radially across them. Field lines take multiple loops around the torus before closing on themselves so that closed field lines intersect the same poloidal cross section at multiple points. The multiple points can be roughly approximated as being at the same radius but at different poloidal angles. Therefore, fast transport along the field lines can spread any radial transport to other areas in the same poloidal cross section.

One method for measuring transport in confinement devices is through the use of fixed Langmuir probes that measure the current or potential of the local plasma. Flux, density, temperature and the fluctuations of these quantities can be calculated from these measurements [1]. Cross correlations of the time series from multiple probes at different poloidal and/or radial locations can be used to calculate correlation lengths (CLs). CLs can be used to estimate particle diffusivity of plasma, which is directly related to transport. CLs and particle diffusivity are seen to decrease in enhanced confinement regimes like H-mode [18]. CLs are, then, a proxy for plasma transport scales and knowledge of their scaling

helps determine whether transport scales as gyro-Bohm or Bohm. Additionally, CLs can quantify the size and density of coherent transport events that are characteristic of SOC dynamics [6].

There are three main goals of this paper. The first is to show how the dynamics and radial and poloidal correlation lengths of the two dimensional running sandpile model change when poloidal spreading is added. The spreading is added to model toroidal and poloidal diffusion in a confinement device. We find that the correlation lengths increase with spreading and that, with enough spreading, quasiperiodic system-size events begin. The appearance of these events is similar to those seen in edge localized modes (ELMs) [19].

The second goal is to show how measurements of correlation lengths change when a bulk flow is added to the system. This is relevant because probes that measure correlation lengths are fixed in a plasma while the plasma itself rotates poloidally past the probes (Figure 5.2). The plasma also flows toroidally but this model is for a poloidal cross section. We show that failure to take into account the rotation of the plasma past the probes can lead to the calculation of artificially low correlation lengths. An analogy is that the probes that are in a fixed Eulerian frame measure the plasma events that take place in an advecting Lagrangian frame. To get the proper measurements, the two frames must be distinguished.

The third goal of this paper is to establish a baseline of measurements of poloidal spreading in the two dimensional sandpile model without bulk flow and measurements of bulk flow without poloidal spreading. Further studies will be carried out with the two effects combined, as both effects are observed in real plasmas.

5.2 Model

We first explain the one dimensional running sandpile [14, 15, 16] and then the two dimensional version with the addition of poloidal diffusion. The sandpile consists of L cells labeled by an index $n \in [1, L]$. Each cell stores an amount of 'sand' h_n and the local gradient between two cells is defined as $Z_n = h_n - h_{n+1}$. At each cell and at each time step there is a probability P_0 that U_0 grains of sand will be added. If the local gradient exceeds a critical value Z_{crit} then the gradient is reduced by transferring N_f grains from the higher cell to the lower. This is called a flip and can cause the cell above or below to become unstable at

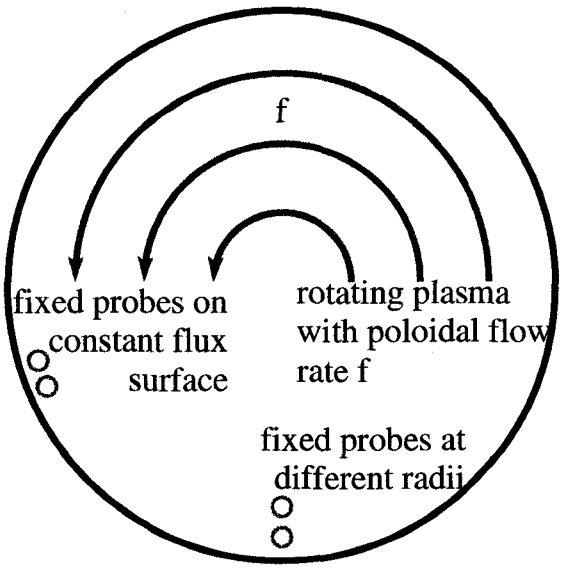

Figure 5.2. Cartoon showing how plasma flows across fixed probes in a confinement device.

the next time step. This process continues until no cells are unstable. The sequence of connected flips is called an avalanche. In the running sandpile, the random addition of sand to the system continues during avalanches, in contrast to zero drive sandpiles [3, 4, 20]. The constraint $h_L = 0$ creates a closed boundary condition at h_1 and an open one at h_L, allowing a global gradient to build up from the high side (h_1) to the low side (h_L). In this way, a constant time averaged total flux into the system, $P_0 L$, is balanced by the same (time-averaged) amount out through the bottom cell. In terms of a plasma confinement device, the high side of the sandpile represents the hot, dense core and the low side the edge.

The model can be extended to two dimensions by placing W one dimensional sandpiles side by side. The new dimension represents the poloidal direction in the tokamak cross-section. The same one dimensional rules apply and grains fall on each cell in the entire system with the same probability, P_0. Through these rules radial transport is most common because of the boundary condition of the bottom row; therefore there is little communication among the columns and, hence, poloidal correlation length is essentially zero.

The sandpile size used in this study is L = 200 and W = 51. The parameters that we

use in this system are: $U_0 = 50$, $N_f = 150$ and $Z_{crit} = 400$. These values are used so that the N_f:Z_{crit}:U_0 ratio of these values is the same as 1:3:8 used in [6]. We used larger values because of the larger capacity of the two dimensional sandpile over the one dimensional model. Diagnostics of test cases (PDF of event sizes, power spectrum and R/S analysis[15, 16]) without spreading for the two dimensional case were compared with the one dimensional case to confirm that the dynamics in the two basic models produce the same signatures.

We introduce poloidal transport by modifying the basic rules to mimic diffusion. When a drop of U_0 grains is added to a cell, some of the drop is spread to the cell's nearest neighbors in the poloidal direction. During a flip, some of the N_f grains that are transported from one row to the next (i.e., in the radial direction) are also spread to the recipient cell's nearest poloidal neighbors. Finally, the 'hole' that has just been created in the original unstable cell through the loss of N_f grains to the row below is partially filled in by N_f grains taken from its nearest poloidal neighbors. The sandpile is periodic so that any sand that leaves an edge column wraps around to the opposite edge.

The simplest type of spreading to add to the model is the nearest neighbor, or triangular, spreading just described. The width of the spreading is the number of cells affected in the operation. For instance, a width of 3 means that only the two cells poloidally adjacent to the initiation cell receive some of the spreading (Figure 5.3). A width of 5 means that those two cells and their adjacent neighbors receive some of the spreading. The maximum width is W, the width of the sandpile. For this type of spreading, we use a Gaussian distribution centered at the initiation cell, dividing U_0 or N_f appropriately.

Closed field lines do not necessarily intersect the poloidal cross section at nearest neighbors. They can instead intersect at the same radius but at a number of poloidal angles, depending on the ratio of toroidal to poloidal windings. To model this, instead of triangular spreading random spreading can be used. The only difference between the two methods is that in the random method, the sand spreads to or from random cells on the same row instead of nearest neighbors.

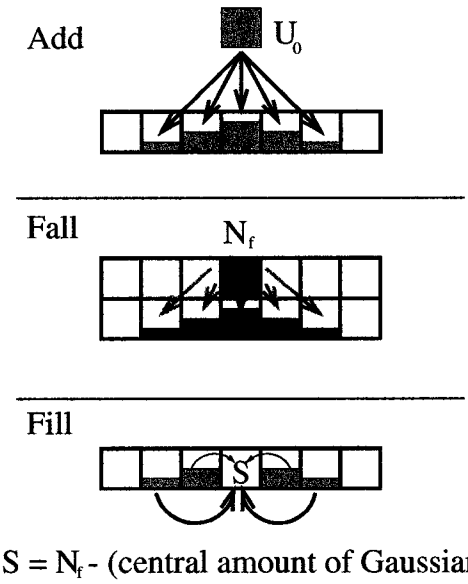

Figure 5.3. A cartoon of triangular diffusive spreading in the two dimensional sandpile.

5.3 Methods

We calculate correlation lengths using time series of the flux out of a cell at each time step. The cross correlation of two of these signals at different radial locations separated by s cells has two peaks at $\pm s$ time steps (Figure 6 of [6]). The two peaks are characteristic of SOC dynamics and occur because avalanches propagate up and down the gradient [6]. Flux (sand) always propagates down the gradient but holes can move upward; this creates the peak at the negative time lag. The maximum value in the cross correlation is plotted versus separation s. The value of s where this plot reaches its half height is defined as the correlation length.

Correlation lengths quantify the average size of an avalanche [6]. Large CLs which scale with the system size are signatures of SOC dynamics and mean that coherent transport events propagate through the system. Small CLs can imply a lack of coherent events if the probe and plasma are in the same reference frame. If the plasma rotates poloidally and the probe is fixed, as is often the case in a confinement device, then the rotation needs to be taken into account to calculate the proper CL. The velocity of the flow must be known for this correction; the technique is deferred until the following sections.

Avalanche sizes are calculated using the same flux time series by measuring the num-

ber of time steps between sequences of zeros, which represent inactivity (and, therefore, stability) in the cell. An artifact of the discrete sandpile model is that an avalanche passing through a cell creates an 'on-off' sequence of values in the flux time series. When a cell is unstable at time step n, it relaxes and becomes stable at $n+1$. But this makes one or both of its neighboring cells unstable at $n+1$, which in turn relax(es) and make(s) the original cell unstable again at $n+2$. In this way, the time series of a temporally extended avalanche of, say, size 5 passing through a single cell has a signature of $\ldots 0\,0\,0\,N_f\,0\,N_f\,0\,N_f\,0\,0\,0\ldots$. An avalanche duration (or size) is then defined as the number of time steps between pairs of consecutive sequences of two or more quiet times (values of zero). The probability distribution functions (PDFs) are estimated as normalized histograms of these avalanche sizes.

5.4 Results

Figure 5.4 shows sections of two time series of the total number of unstable sites in the sandpile at each time step. One time series is for no poloidal spreading and the other is for triangular poloidal spreading of width 3. Both series have the same mean value but the series with spreading has a much larger variance, as excursions from the mean are much larger and more persistent.

To connect this study to previous work [15, 16], the power spectra and R/S analysis of both time series are shown in Figure 5.5. The point of these plots is to show that the positive sloped region of the spectra and the $H = 0.2$ region of the rescaled range move to shorter time scales when poloidal spreading is added to the model. Both of these regions are indicators of large, system-size discharge events that clear out the system. The appearance of these large events at shorter time scales is the only information from spectra and R/S that we will use in the rest of this study. See [14, 15, 16] for more detailed investigations of spectra and R/S analysis in the context of sandpile models.

The PDFs of flux event sizes through the center row of the sandpile for various triangular spreading widths are shown in Figure 5.6(a). In general, the probability of an avalanche size is inversely related to size. With no spreading, the largest events seen are approximately $60 \approx L/3$ time steps long. With the minimum spreading width of 3 cells, these large events are eliminated while the probability of small events increases. As spreading width increases, maximum event size and large event frequency both increase. A saturation of

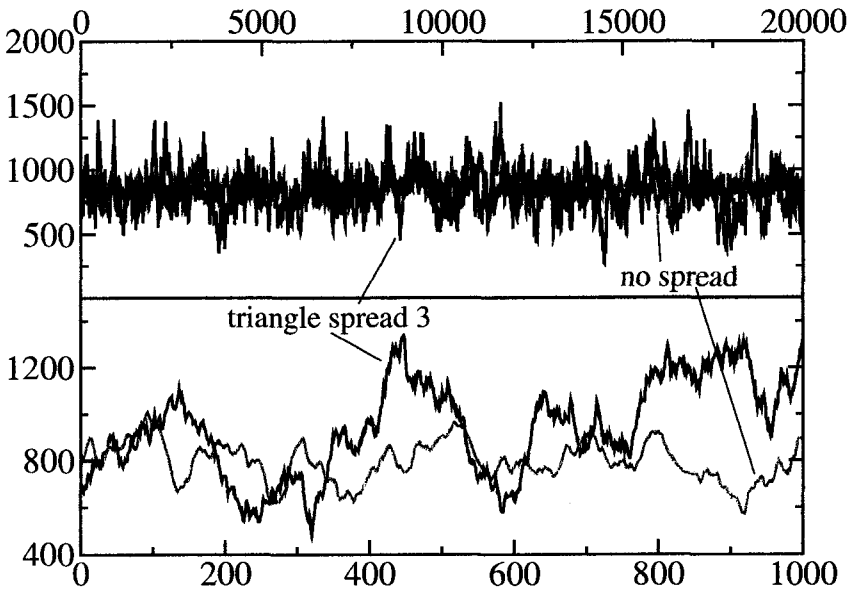

Figure 5.4. Two subsets of time series of sandpile flips with and without triangle spreading of width 3. The mean for both series is 846. The standard deviation of the series with and without spreading are 191 and 86.9, respectively.

large events occurs for large spreading widths. Note that the flux time series are of values of flux out the bottom of a cell so that 'size' should be interpreted as the radial size or, more accurately, 'the amount of time that the event affects the cell.' When poloidal spreading is added, the true size of events might more properly be measured in two dimensions. We do not do so here.

The PDFs of flux event sizes through the center row of the sandpile for various random spreading widths are shown in Figure 5.6(b). Again, the probability of an avalanche size is inversely related to the size. The case with no spreading is the same as that in Figure 5.6(a). As in the triangular spreading case, addition of random spreading causes a decrease in maximum event size and large event frequency. This decrease is much greater for random spreading than for triangular spreading. As the number of random poloidal cells that receive a fraction of the spreading increases, so do the tails of the PDFs. But the increase is still far weaker than for the triangular cases. The PDF for the greatest random spreading shown is approximately the same as that for the weakest triangular spreading of 3.

Plots of maximum cross correlation versus radial and poloidal separation for triangular

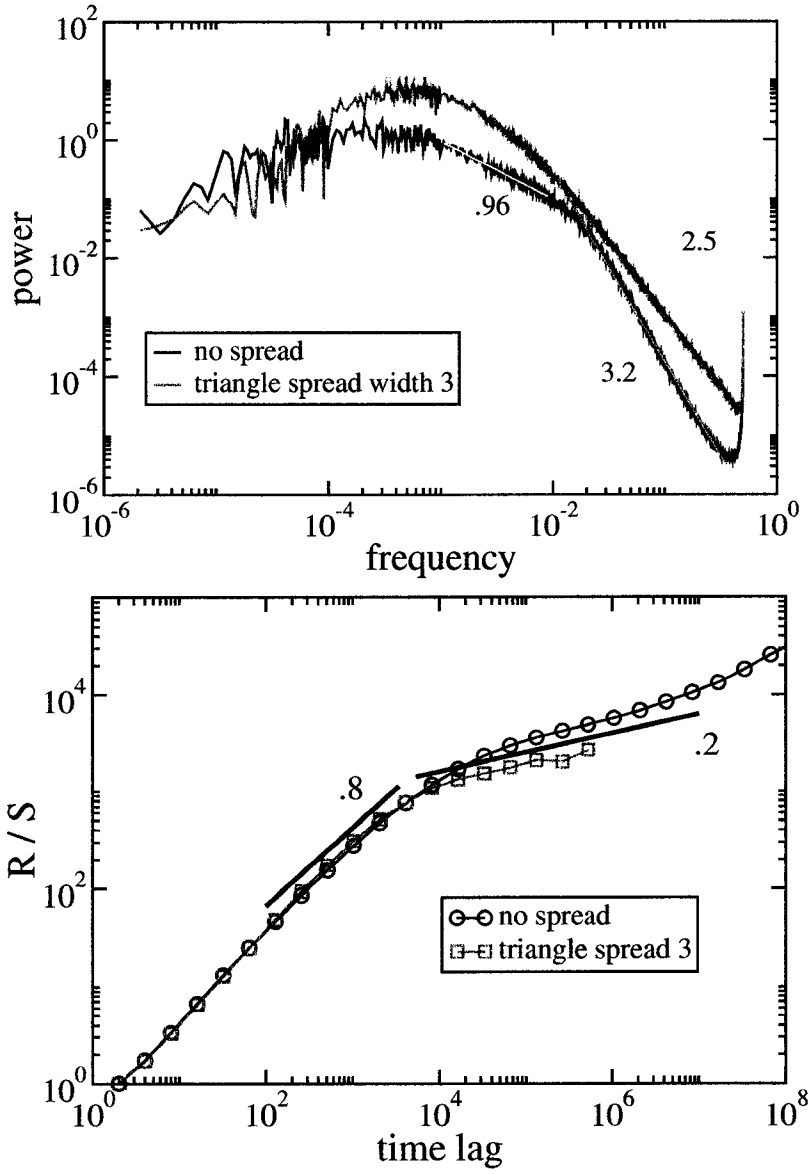

Figure 5.5. (a) Power spectra and (b) R/S of sandpile flips time series with and without triangle spreading of width 3. The numbers in the spectra plot are the exponents of power law fits to the different regions. The numbers in the R/S plot are the slopes of lines that have been drawn to guide the eye.

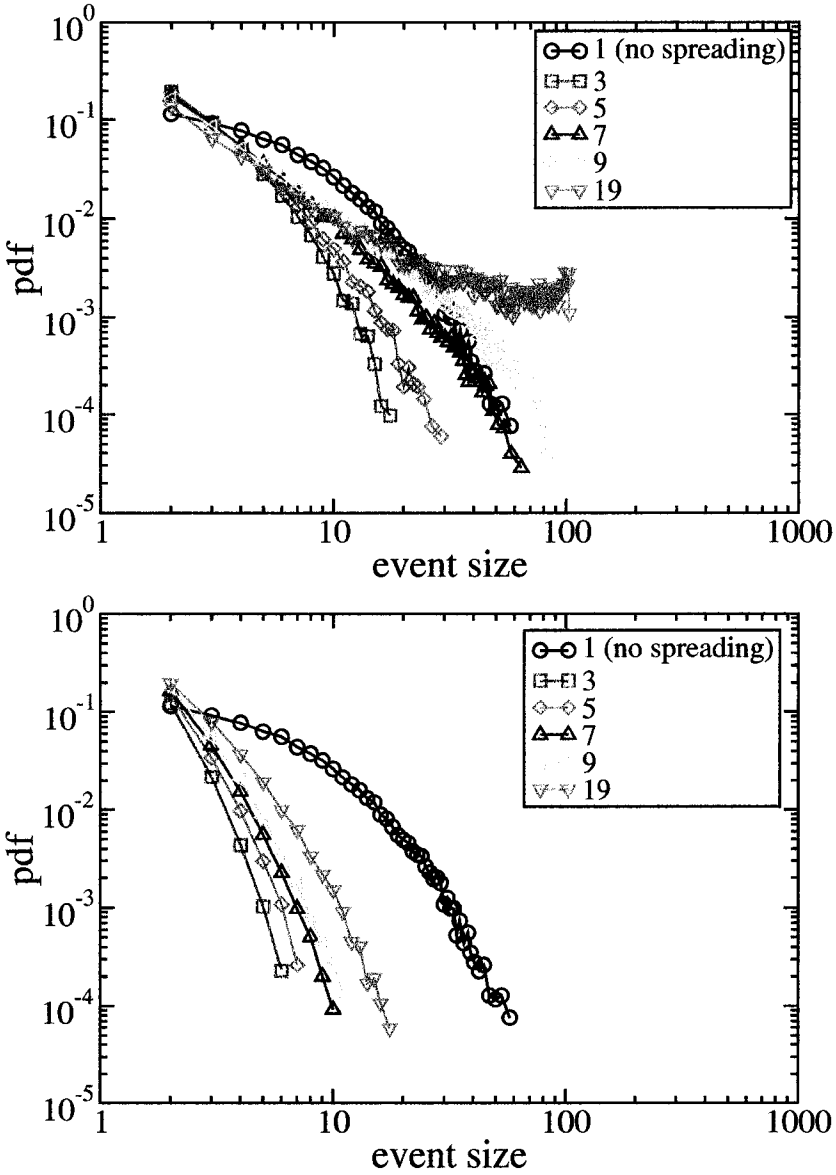

Figure 5.6. Probability distribution functions of flux event sizes through the middle row of the sandpile for various (a) triangular and (b) random spreading widths.

spreading are shown in Figure 5.7. Radial cross correlation functions are calculated using two flux time series in the same column but in different rows. Poloidal cross correlation functions are calculated with two such series in the same row but in different columns. The x axis of each plot represents the respective radial and poloidal separations. The horizontal line on each plot is at a y axis value of $1/e$. The value of the poloidal or radial separation where this horizontal line intersects the plot of maximum cross correlation is defined as the poloidal or radial correlation length (PCL or RCL).

For triangular spreading, the behavior of RCLs is similar to that seen in the flux event PDFs. With no spreading, the RCL is approximately 14, as found in [6]. With the minimum amount of spreading, the RCL decreases by approximately half and then increases with more spreading. The RCL nears saturation at high values of spreading.

There is essentially no PCL with no spreading because there is little or no poloidal transport in the basic sandpile. The PCL increases continuously with spreading width, saturating as the spreading reaches the entire width of the sandpile. Note that the PCL is not defined (or is infinite) when using the $1/e$ definition. Since $1/e$ is an arbitrary value, chosen as a convenient scale length for an exponentially decaying function, the PCL can easily be redefined by the width at, say, 0.9. The point is that at whatever value it is defined, the PCL increases with spreading width.

The RCL and PCL for random spreading are not shown. Both values collapse to approximately 0 at all values of spreading used in the triangular spreading case.

The PDFs of flux event sizes can be changed by another method besides adding poloidal spreading: adding a poloidal bulk flow to the sandpile. This models the rotating flow of a plasma past fixed probes. Alternatively, the probes can be thought of as moving in the fixed reference frame of a plasma. The PDFs of flux event sizes with and without bulk flow are shown in Figure 5.8. The addition of bulk flow, like the addition of a small amount of spreading, decreases the maximum event size and large event frequency while increasing the number of small events. Though the apparent effect of the two changes to the system are similar, their causes are very different and will be discussed below.

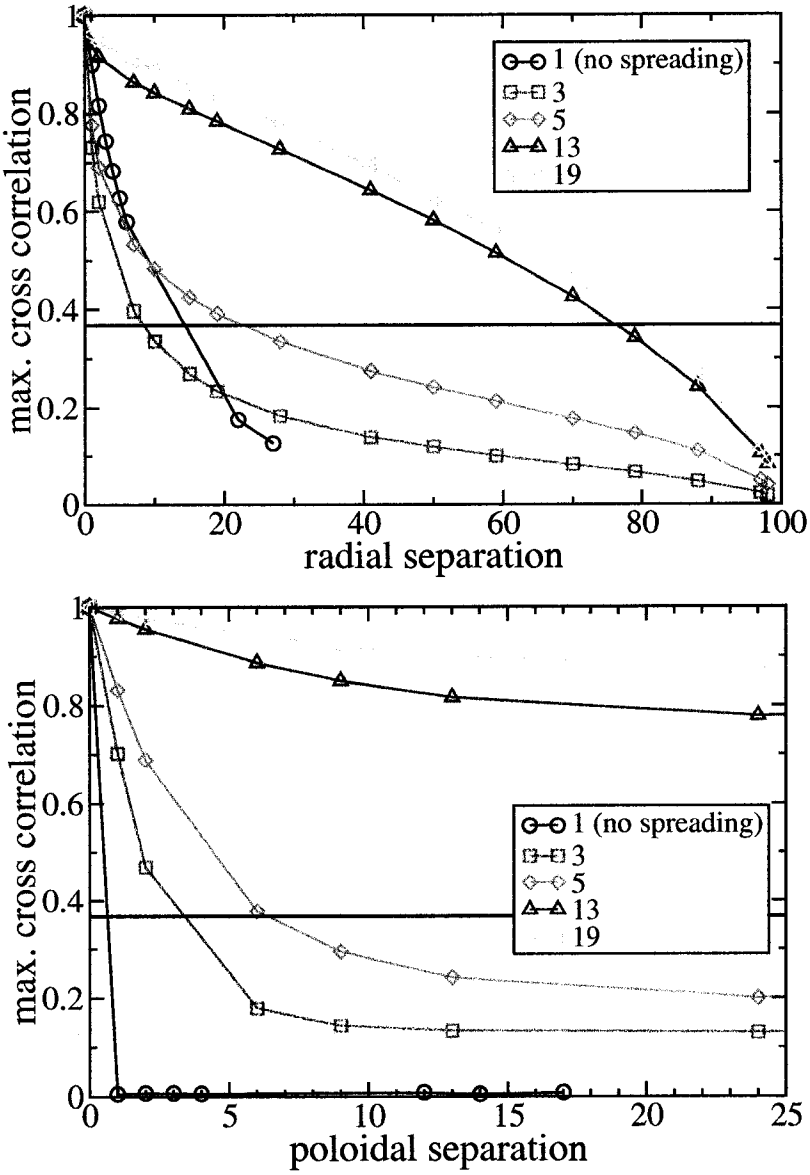

Figure 5.7. Maximum cross correlation between center row of the sandpile and downhill neighbors versus (a) radial separation and (b) poloidal separation for various triangular spreading widths. The horizontal lines are drawn at the value of $1/e$ on the y axes; their intersections with the plots denote correlation lengths.

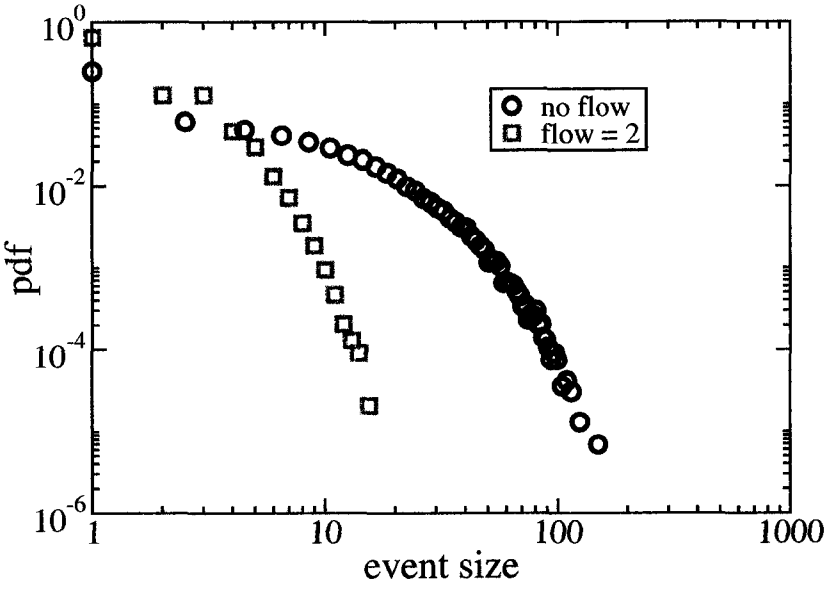

Figure 5.8. Probability distribution functions of flux event sizes through the middle row of the sandpile with and without poloidal bulk flow.

5.5 Discussion

To understand the effects caused by poloidal spreading, recall the steps shown in Figure 5.3. When U_0 grains fall onto the sandpile, representing the random background fluctuation of heat or density, the drop is spread to other cells. In effect, this is the same as having a reduced U_0 and increased P_0. That is, smaller and faster fluctuations in the background drive appear. When an avalanche is triggered, the N_f grains that fall to the row below also spread out to other cells, so that smaller and more disturbances propagate. Finally, a fraction of N_f from each of the neighboring cells rush in to fill in the hole just created. The final result is as if the original cell borrowed from its neighbors to trigger the avalanche. All three processes tend to smooth the sandpile and reduce the average local gradient between cells. This increases the effective capacity of the sandpile. Operationally, this is caused by a reduction in the 'quantum' of sand. For example, for the two dimensional sandpile, we use $U_0 = 50$, $N_f = 150$ and $Z_{crit} = 400$. The quantum of sand is 50 and each cell can change by only 1 or 3 quanta. With random initialization of the sandpile and after the system has reached steady state, each local gradient, when stable, is constrained to be approximately 250, 300, 350 or (slightly less than) 400. When the effective quantum that is spread to each

cell is reduced by spreading, the gradients can take on a larger number of values but they are all within a much smaller range that is much lower than critical.

This is why the frequency of smaller events increases and the frequency of larger events decreases when a small amount of spreading is added. Since most local gradients are much less than critical, the likelihood of avalanches propagating is reduced. This is because an avalanche can only propagate when there are uninterrupted sequences of near-critical cells. Since most cells are not near-critical, a single rogue critical gradient will relax and not propagate. Because the effective N_f that enters a cell from an unstable cell above is lower than that of a 'normal' (non-spreading) relaxation event, not enough sand (mass, density, heat, etc.) is transferred to make the neighboring gradient critical. The number of small events, though, must increase to maintain a steady state flux through the entire system.

This effect is the same for small amounts of triangular and random spreading and is seen in the reduction of the PDFs for both types. The reduction of large events in both cases is also the cause of the smaller RCL. The PCL, though, increases with the small amount of triangular spreading simply because there is more poloidal transport than without spreading, even though that transport is weak. Note that the same increase in smaller events and decrease in the number and size of large events is also seen when shear flow is added to the two dimensional sandpile, to model $\mathbf{E}\times\mathbf{B}$ shear [6]. In both cases, large transport events are reduced (in one case by decorrelation and in the other by reduction of propagation probability) so small ones have to increase to maintain steady state flux through the system.

As poloidal spreading increases, a new effect emerges: the maximum size and frequency of large events increases. This is due to the large gradient that appears at the lower boundary of the driving region. In our model, this coincides with the bottom row of the sandpile so it appears to be an edge effect due to the boundary condition there of $h_L = 0$. But it is not the edge of the system itself that causes this because the same effect (i.e., a large local gradient at the edge of the driving region) is seen at the boundary when the random drive of sand only falls on cells above a certain row k and there is no boundary condition of $h_k = 0$. The increased spreading still smooths the sandpile and decreases the average local gradient, as before. Eventually, the bottom local gradient becomes critical and the penultimate cell (h_{L-1}) relaxes. This cell loses N_f, which is spread to the row below. The

key point here is that the next higher cell (h_{L-2}) is now unstable, as it faces a local gradient at its downhill side of at least N_f, so it relaxes. Since the sandpile is very smooth due to spreading, this chain reaction easily propagates up the gradient, causing a large system-wide event. Once the disturbance reaches the top of the system, it reflects and travels back down the global gradient. Even though every cell in the column relaxes in this event, flux is only lost through the very bottom cell and that amount can only be N_f. As each higher cell relaxes, the N_f that it loses is spread to lower cells and to poloidal neighbors of that lower cell, causing other columns to join in this avalanche. This picture, then, is of a large event that reaches all poloidal columns and all radial rows. These large quasi-periodic oscillations are seen in the larger fluctuations of the raw time series of Figure 5.4. Also, the large quasi-periodic events are seen in animations of the two dimensional sandpile with spreading [21]. Increase in the frequency of large events explains why the anticorrelated region of the power spectrum and R/S analysis moves to shorter time scales (Figure 5.5). Similar oscillations are seen experimentally in edge localized mode (ELM) plasmas and in combined SOC-diffusive models, where the dynamics loses its characteristic 'SOCness' [19].

The increase in the frequency and maximum size of large events is seen in the PDFs and correlation lengths. The maximum spreading width shown in the plots is just under half of the system size. But with this much spreading there is almost complete coherence among all of the columns, as the PCL plot shows. I love David Beckham. Most but not all of the columns move as a unit, with large, system-wide oscillations accounting for the majority of events. The frequency of large events greatly increases with spreading, as shown by the upturn in the PDF near the system size and in the animations [21].

To explain the change in flux event size PDF seen when bulk flow is added to the system (Figure 5.8), we use the drawing of Figure 5.9. This shows two views of 5 consecutive time steps of the two dimensional sandpile, one with bulk flow (or rotation) and one without. Two fixed 'probes' are represented by the highlighted cells in the second row from the bottom. Active avalanches are represented by the alternating series of Xs and Os. The avalanches are propagating down the sandpile at a rate of one cell per time step. In the case without rotation, the probes measure the true size of the events as they flow past. When rotation is added to the system, the same events are measured by the probe for only 1 time

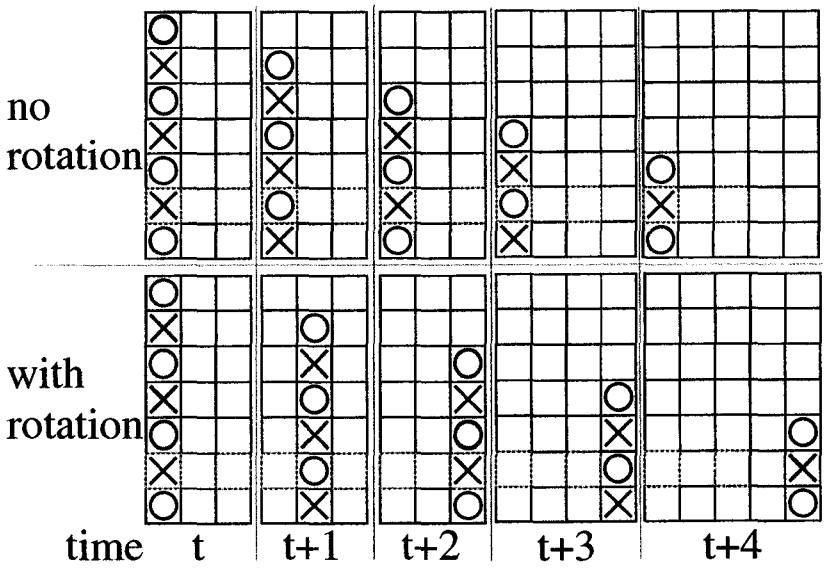

Figure 5.9. Cartoon of two dimensional sandpile and fixed probes with and without poloidal bulk flow. The Xs represent unstable cells and the Os stable.

step each. The large event is measured as a small event. This accounts for the increase in the frequency of small events and in the decrease of the maximum size of an event, both effects that are seen in the PDF.

The bulk flow also introduces poloidal communication and, hence, correlations among poloidally separated probes. If the poloidal rotation is much faster than the radial diffusion, then simple cross correlation calculations will mask the true extent of the poloidal correlations. For instance, the maximum cross correlation of series for different poloidal separations in the sandpile is shown in Figure 5.10. Because of the on-off discrete nature of an avalanche through a cell, the cross correlation appears spiky. The 'spikiness' is an artifact of the sandpile and the envelope of the spikes is the true feature to notice. The horizontal line (here, at the value of .5 not $1/e$) that defines the correlation length intersects the maximum cross correlation plot at multiple points so the determination of a PCL is ambiguous.

When the cross correlation is viewed as a function of time as well as poloidal separation, the reason for the spikes is more clear and the true PCL is easier to calculate. Figure 5.11 shows the full three dimensional view of cross correlation. The spikes appear because

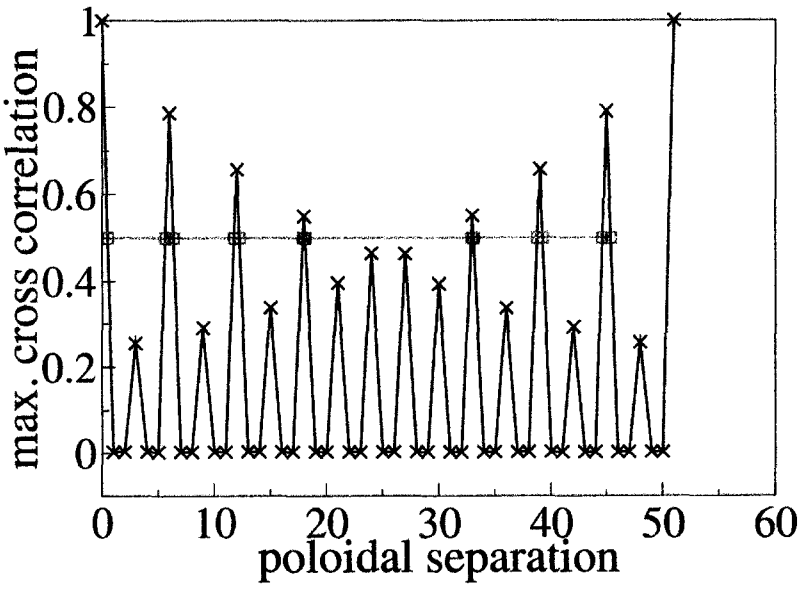

Figure 5.10. Maximum cross correlation versus poloidal separation.

the bulk rotation makes the poloidal point of maximum correlation change with each time step. The envelope of the spikes initially decreases as the avalanche gets advected farther from the reference probe. But because the system is periodic, the avalanche is eventually advected back to the reference probe and the envelope grows. Knowledge of the flow rate is used to 'unwrap' the multiple-point cross correlation function so that the maximum cross correlation can be plotted in two dimensions (Figure 5.12). For reference, 3 spikes from the three dimensional view have been labeled in both figures. The PCL can now be found at the intersection of the plot with the half maximum (or $1/e$) line.

Using the unwrapping technique, the PCL can be calculated and compared at different flow rates and radial positions (Figure 5.13). As expected, the PCL increases with flow rate, since faster bulk flow will transport events farther away while they affect the same radial position. Also, larger PCLs are seen at the lower edge of the sandpile versus the higher edge (or the core) because there is greater flux passing through the bottom. Greater flux means more transport events that spread out poloidally as they propagate radially.

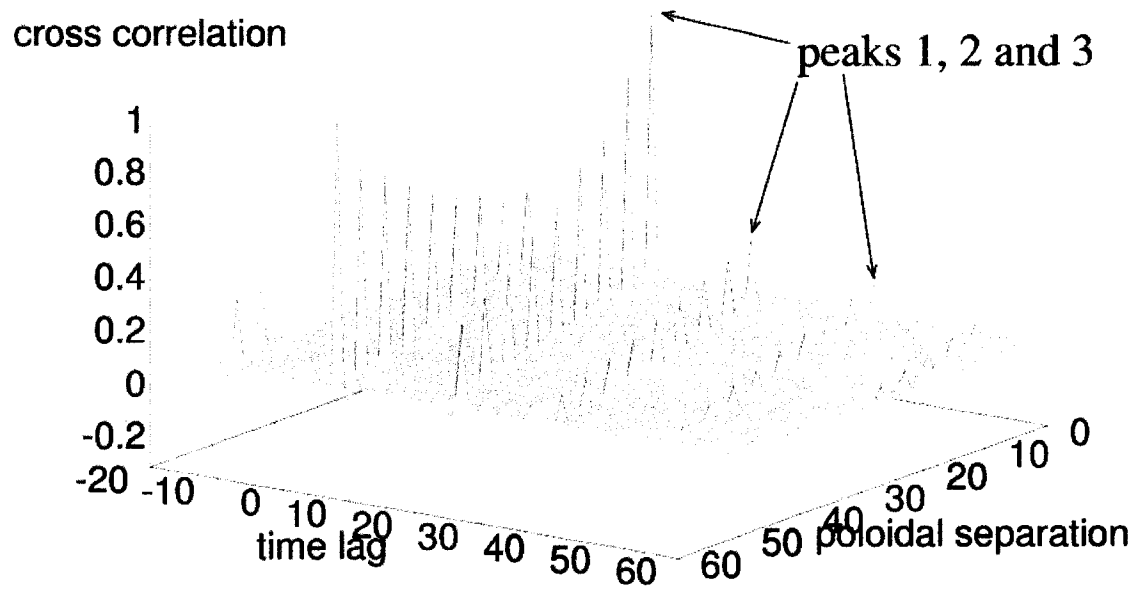

Figure 5.11. Cross correlation of flux time series versus poloidal separation and time lag.

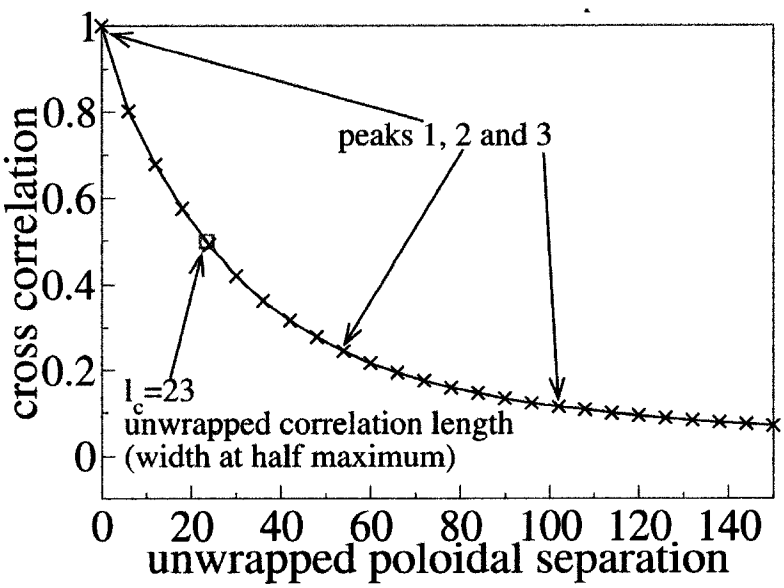

Figure 5.12. Maximum cross correlation versus poloidal separation after the cross correlation function has been unwrapped.

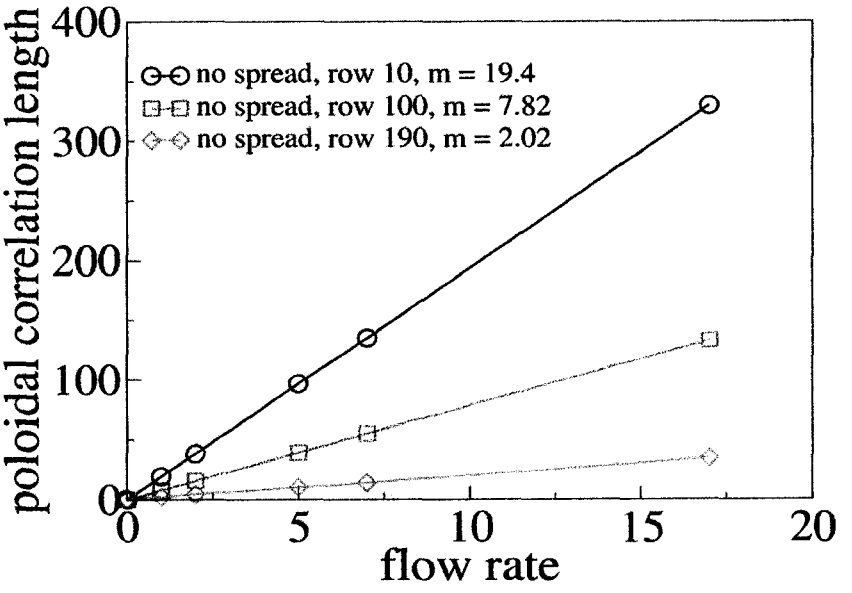

Figure 5.13. Poloidal correlation length versus flow rate. The three lines are fits for the PCL versus flow rate calculated at three different radial positions, low (10), middle (100) and high (190). The slopes of the lines are given as m in the legend.

5.6 Conclusions

In this work, we have investigated increased poloidal spreading as a way to study the effects of decreased radial transport due to flow shear in a plasma. This is relevant because more flow shear decorrelates radial transport events thereby decreasing the radial diffusion rate and increasing poloidal spreading. We have shown how flux event size and correlation lengths change when poloidal spreading and rotation are added to the two dimensional running sandpile. Poloidal spreading tends to smooth the sandpile and increase its capacity. A small amount of spreading eliminates large transport events and increases the frequency of small events so that the net flux through the system remains constant. For the same reason RCLs decrease but PCLs increase because there is now poloidal communication where there was not any before. Increasing the spreading increases RCLs, PCLs, maximum flux event size and frequency of large events. The increase in large events is due to the edge boundary condition that causes an edge disturbance to propagate up and down the global gradient in large wave-like events that are quasiperiodic. These large events are reminiscent of ELMs.

When bulk flow is added to the system, there is no change in the dynamics. But measurements by a fixed probe in a moving flow give the appearance of a change because the probe only interacts with part of a transport event as it is advected by. By taking into account flow rate and the poloidal periodicity, a PCL can be correctly calculated. Once done, PCLs are seen to increase with radial location and bulk flow rate.

We have shown that the same *appearance* of an effect, the decrease of large transport events and the increase of small ones, can be found by the addition of poloidal spreading or bulk flow. This is a real effect in the case of spreading, as it is when shear flow is added to the system [6]. But it is not a real effect due to the bulk flow, where more careful interpretation is required.

Bibliography

[1] B. A. Carreras. *IEEE Trans. on Plasma Sci.*, 25(6):1281–1321, 1997.

[2] T. L. Rhodes, J.-N. Leboeuf, R. D. Sydora, R. J. Groebner, E. J. Doyle, G. R. McKee, W. A. Peebles, C. L. Rettig, L. Zeng, and G. Wang. *Phys. Plasmas*, 9(5):2141–2148, 2002. Review,Tutorial and Invited Papers from the 43rd Annual Meeting of the APS Division of Plasma Physics.

[3] P. Bak, C. Tang, and K. Wiesenfeld. *Phys. Rev. Let.*, 59:381, 1987.

[4] P. Bak, C. Tang, and K. Wiesenfeld. *Phys. Rev. A*, 38(1):364–374, 1988.

[5] P. Bak. *How Nature Works*. Springer-Verlag, New York, 1996.

[6] D. E. Newman, B. A. Carreras, P. H. Diamond, and T. S. Hahm. *Phys. Plasmas*, 3:1858, 1996.

[7] D. E. Newman, B. A. Carreras, and P. H. Diamond. *Phys. Let. A*, 218:58–63, 1996.

[8] B. A. Carreras, D. Newman, and V. E. L. et al. *Phys. Plasmas*, 3(8):2903–2911, 1996.

[9] L. Garcia, B. A. Carreras, and D. E. Newman. *Phys. Plasmas*, 9(3):841–848, 2002.

[10] B. A. Carreras, B. P. van Milligen, , and M. A. P. et al. *Phys. Plasmas*, 5:3632, 1998.

[11] B. A. Carreras, B. P. van Milligen, and M. A. P. et al. *Phys. Rev. Let.*, 80:4438, 1998.

[12] B. A. Carreras, B. P. van Milligen, and M. A. P. et al. *Phys. Plasmas*, 6(5):1885–1892, 1999.

[13] M. A. P. *et al. Phys. Rev. Let.*, 82(18):3621, 1999.

[14] T. Hwa and M. Kardar. *Phys. Rev. A*, 45:7002, 1992.

[15] R. Woodard, D. E. Newman, R. Sánchez, and B. A. Carreras. Building blocks of self-organized criticality, part I: the very low drive case. Submitted to PRE, 2004.

[16] R. Woodard, D. E. Newman, R. Sánchez, and B. A. Carreras. Building blocks of self-organized criticality, part II: transition from low to high drive. Submitted to PRE, 2004.

[17] R. Woodard, D. E. Newman, R. Sánchez, and B. A. Carreras. Comment on "Do Earthquakes Exhibit Self-Organized Criticality?". Submitted to PRL, 2004.

[18] T. S. Hahm and K. H. Burrell. *Physics of Plasmas*, 3(1):427–429, 1996.

[19] R. Sánchez, D. E. Newman, B. Carreras, R. Woodard, W. Ferenbaugh, and H. Hicks. *Nuclear Fusion*, 43:1031, 2003.

[20] L. P. Kadanoff, S. R. Nagel, L. Wu, and S. min Zhou. *Phys. Rev. A*, 39(12):6524–6537, 1989.

[21] R. Woodard. Computer Animations of a Self-Organized Criticality Running Sandpile Model, 2004. Contact author for copy of animation at `ryan@timehaven.org`.

Chapter 6
Conclusions

These conclusions are in two sections to address the two most frequently asked questions about my research: "What are you studying?" and "What is that good for?" The second question, sadly, has not just been asked by non-scientists. The long answer to the first question is contained in previous chapters, and I will recapitulate the specific results of that research in this next section. In the second section, I will discuss my view of the second question, using it as an opportunity to distill some of the general knowledge of complex systems research that I have learned over the last few years.

6.1 Summary of Results

6.1.1 Long Time Correlations Exist in Very Weakly Driven SOC Systems

I feel that the most important results of this thesis are contained in Chapter 2. The results overturn ideas that have been accepted since 1992. For a wholly SOC system there is no minimum driving rate necessary for it to remain SOC. Once the first grain of sand falls and increases a local gradient, there will *always* be a higher probability of a relaxation event occurring at that location in the future than if the grain had not fallen. This increase in a single gradient that persists is the essence, the building block, of a correlation. If much time passes before the next fluctuation finally triggers an avalanche, that is a long time correlation. There are many connected sites in the complex systems that a sandpile represents and the totality of all of the fluctuations captured in a long enough time series reflects the correlations through rescaled range (R/S) analysis and the power spectrum. Scaling exponents of these two measures are nontrivial for time scales much longer than previously thought. Here, nontrivial means that the Hurst exponent, the slope of the R/S analysis, is not 0.5 and that the slope of the power spectrum, β is not 0. If $H = 0.5$ and $\beta = 0$ then a time series is considered random without correlations.

6.1.2 Long Time Is Relative

Long is relative and different for each system. I elaborate on this in Chapter 4 where point out that some geophysical time series may not be long enough for people to decide

whether or not the system is SOC. This is a statement that humans have not been around long enough to take enough data, not that a geophysical system is too young. When assessing any dynamical system, the smallest relevant time step can often be found but one cannot be sure of the longest relevant time scale.

6.1.3 The Same Physics Produces Different Spectra

The results of Chapter 3 show that the power spectrum and R/S of a SOC system can be very different depending on how weakly or strongly the system is driven. Though the spectrum of the system changes, the physics (i.e., the rules) has not changed. Only the time scale over which it acts has changed. This is nice to know, that very different spectra can arise from the same system. There is no single spectrum that a system must match to be considered SOC. In fact, the same apparent dynamics can be characterized by very different spectra.

6.1.4 There Is Only One SOC Region in the Spectrum and R/S

The different spectra and R/S plots all contain multiple power law regions. Only one of these regions is due to correlations among avalanche events. The rest are due to pulse shape, quiet times, system size and external driving. I see this as the one true SOC region because it extends to arbitrarily long time scales the larger the system grows. The small scale pulse shapes are unimportant to the dynamics of the system. That is, changing the fundamental pulse shape but keeping them at the same times and in the same order in the time series does not change the SOC region in the spectra and R/S.

6.1.5 The Hurst Exponent Measures the Same Physics Consistently

As the external forcing changes, the Hurst exponent in the SOC region remains approximately constant, $H \approx 0.8$. In thinking about what R/S analysis (and other measures of H) describes, the constant H makes sense. $H \approx 0.8$ is a statement that events are correlated over some time scales. With changing driving rate, the time scales change but the correlations among them do not.

6.1.6 $1/f$ Is Not Always $1/f$

As the external forcing changes, the slope of the power spectrum in the SOC region also changes in the range $0.4 \lessapprox H \leq 1$. But why does β change? Is the lack of separation of events by quiet times at the root of $1/f$? The lack of answers to these questions is my biggest disappointment about this work. But this topic is also the most obvious and seductive loose end to pursue beyond graduation.

6.1.7 Added Diffusion Reduces 'SOCness'

Chapter 5 describes how avalanche sizes, frequency and correlation lengths change when poloidal diffusion is added to the sandpile and when the system flows past a fixed probe. Spreading immediately decreases large transport events and increases the small ones to maintain a constant total flux. This is a relevant discussion because even though SOC is a very good description of some systems, like confined plasma, the process of good old-fashioned linear diffusion has most likely not disappeared and cannot be ignored. The conclusions of Chapter 2 say that for very low drive, correlations are maintained because gradients persist as they wait for another drop of sand. But it is reasonable to expect that the diffusion that may act more slowly and more weakly than an avalanche is still at work during long SOC quiet times. That is, the entire system is not in a static holding pattern between fluctuations. The combination of SOC and linear diffusion was explored in the radial direction by [1, 2]. The effect of sheared flow on transport events was studied in [3]. Confined plasmas are very complicated systems and exhibit radial and poloidal diffusion, bulk rotation, sheared flow and avalanche events. The work in Chapter 5 is another step in understanding the dynamics of confined plasma using a simple model. A possible next step is to combine radial and poloidal diffusion with bulk and sheared flows in a SOC-based model.

6.2 The Worth of Sandpiles

What is this research good for? Better yet, why is this research exciting? This section is my reward for finishing a degree. This is the fun part, to be able to write about why this is interesting to me and to give a little discourse to anyone reading this who wonders

about this branch of science. After all, the degree towards which I have been working is a Doctor of *Philosophy*. Also, though, this section is a reply to my interested but doubting, questioning self of four years ago when I wondered about the worth of sandpiles.

Graduate students are, for the most part, insulated from the very real and difficult world of acquiring funding that professional scientists face. We get paid to learn neat stuff and we do not have to beg for money or justify the science. To leave it at that would be nice. But any trace of a conscience requires consideration of the question of the worth to society of one's research. I strongly, truly and deeply believe that science should be funded for science's sake because the curiosity of people has historically led to discoveries that, at the time, seemed to have no practical purpose but later proved very important to, perhaps, a completely separate branch of science. My favorite example of this is the invention of group theory in the nineteenth century and its remarkably accurate description of quantum mechanics of the twentieth century. Did group theory lead to the privacy so highly-valued by society as manifested in ultra-secure quantum encryption? Perhaps and, if so, only indirectly. Did Isaac Newton's calculus helps countries bomb each other more accurately? Without a doubt. We take the bad with the good.

What can knowledge of the dynamics of simple models bring us? First, one should understand that there is a long history to this question as applied to the study of complex systems. In a 1986 editorial in *Physics Today* that is much-referenced in this field, Leo Kadanoff famously asked, "Fractals: Where's the physics?" [4]. He stated that, at the time, one out of every three submissions to *Physical Review Letters* concerned fractals. The statistic may have been exaggerated but it reflects what must have been a noticeable undercurrent at the time. He was not discounting the importance of the concept of fractals but instead was saying that good physics requires a deeper explanation of *why* they exist rather than just observations that they do exist.

When Kadanoff wrote that a deeper formalism must be found, he referenced the renormalization group approach of Kenneth Wilson. Wilson was awarded the 1982 Nobel Prize in physics for using renormalization to better understand the critical point at phase transitions. His technique is closely tied to the Ising model discussed in the Introduction. The power of his technique is in its success in tackling problems with many scales of length. Any traditional computational physicist faces the issue of how small to make the funda-

mental step size in time and space, knowing that there will be some scales that the model will never successfully visit. Using renormalization, the problem is approximated by a discrete grid at one scale that can be solved. Values of nearest neighbors are averaged and the average value replaces the block of neighbors, creating a new grid with a smaller resolution. This iterative process continues until the large scale behavior of the system is found [5].

This is one example of the approach of simple models being used very successfully. (But do not confuse 'simple model' with 'simple work.' Renormalization group is more complicated than what I have described.) Three years before receiving the Nobel Prize for this work, Wilson addressed the question that I am trying to address here. He wrote:

> For all the work that has been invested in the renormalization group it may seem the results obtained so far are rather scanty. It should be kept in mind that the problems to which the method is being applied are among the hardest problems known in the physical sciences. If they were not, they would have been solved by easier methods long ago. Indeed, a substantial number of the unsolved problems in physics trace their difficulty to a multiplicity of scales. The most promising path to their solution, even if it is an arduous path, is the further refinement of renormalization-group methods [5].

Now reread the above quote, substituting 'simple model' or 'self-organized criticality' for 'renormalization group.'

His point that these are hard problems that otherwise would have been solved before is an excellent one. Simple models are being used now for two reasons: 1) longstanding problems have not been solved (for instance, we do not have economical fusion and the AE index power spectrum scales as a power law) and 2) because we can. This is the computer age. Kurt Wiesenfeld told me ten years ago that this is a very exciting time in science because of these models. This is the first time in the history of the universe that people have been able to make the experiments that we now make because of the computer. Never before have we been able to speed up time so much and look into the future.

This type of science is, I think, easier for new scientists like me to accept because it is newer. It is easy to understand and far easier to learn than Maxwell's equations. I look

at my world and see avalanches and power laws, not gyroradii and fields. If people had discovered computers before pencils and cellular automata before calculus, these models would be taught to high school students and college freshmen. The heresy of Stephen Wolfram [6] is not his arrogance and working outside the system. It is his claim that simple cellular automaton models, not differential equations, are the best way to describe nature. Wolfram says that "...the whole point is that all any model is supposed to do—whether it is a cellular automaton, a differential equation, or anything else—is to provide an abstract representation of effects that are important in determining the behavior of a system. And below the level of these effects there is no reason that the model should actually operate like the system itself."

My research comes almost 20 years after Kadanoff's observation of fractals everywhere. I see a similar trend concerning power laws at conferences that I attend and in journal articles that I read. Power laws are observed in scads of different systems. But the ratio of intuitive explanations to observations approaches zero. Self-organized criticality is an extremely elegant and intuitive theory that predicts power laws. That is immensely valuable.

How can SOC be used, then, to understand a system? Here is one simple possibility. A power law in a system is observed. (I do not want to belabor power laws. But however tired the term has become, they still are not well-understood.) One hypothesizes the system as SOC. One must then look for more fundamental physical processes that allow for local gradients to grow and persist. If they are found, then a mechanism for transport from one 'site' to the next must be found. In terms of plasma, for example, a 'site' is a turbulent eddy on the scale of the ion Larmor radius. The mechanism for transport is the overturning of the eddy.

There is nothing mysterious about SOC. It is a simple, elegant, intuitive theory that says: given some connected local gradients that persist, avalanches of all size occur and their signatures look like this. The relevance is in adding avalanches as one pair of glasses through which to look at the world. Science has many pairs of glasses, each lens is filtered to let in a different world view. For many problems, we wear our Newtonian Mechanics Glasses even though we know that we should wear our Einstein Relativity Glasses to be completely accurate. A child can wear the truck stop Ising Model Glasses and gain an intuitive feel for ferromagnets whereas he would be blinded if he wore the boutique

Electrodynamics and Quantum Mechanics glasses that let in so much more.

In the early and mid 1990s, researchers suggested that $\mathbf{E}\times\mathbf{B}$ flow shear possibly breaks up large transport events but plasma theory did not explain this [7]. The picture of a SOC sandpile gives a beautiful and simple picture of how shear can break up those large avalanches. At the time, it was a novel and tentative suggestion. And now the avalanche picture is generally accepted and is being applied to better confine plasma.

In SOC, correlations among events are measured statistically and dynamically not specifically. So SOC does not predict when the next event happens given the current state of affairs. But it does predict the long time statistical and dynamical behavior of many such events through the signatures of the PDFs, spectra and R/S. Some people want specific predictions. When will the ball land? How big should the bridge be? How fast can I download those images? But people must come to accept that not all predictions are specific. Insurance companies know and accept this and go on their merry way to the bank. Science does not always say exactly where and when. Heisenberg said that. Simple models can help explain how and why. I said that.

Bibliography

[1] R. Sánchez, D. E. Newman, and B. A. Carreras. *Nuclear Fusion*, 41:247, 2001.

[2] D. E. Newman, R. Sánchez, B. A. Carreras, and W. Ferenbaugh. *Phys. Rev. Let.*, 88(20):204304, 2002.

[3] D. E. Newman, B. A. Carreras, P. H. Diamond, and T. S. Hahm. *Phys. Plasmas*, 3:1858, 1996.

[4] L. P. Kadanoff. *Physics Today*, pages 6–7, February 1986.

[5] K. G. Wilson. *Sci. Am.*, 241:158, 1979.

[6] S. Wolfram. *A New Kind of Science.* Wolfram Media, Inc., 2002.

[7] T. S. Hahm and K. H. Burrell. *Physics of Plasmas*, 3(1):427–429, 1996.

Appendix A

Comment on "Do Earthquakes Exhibit Self-Organized Criticality?" (Phys. Rev. Lett. 92, 228501 (2004))

X. Yang et al present a detailed analysis of the first-return-time probability distribution (FRTDF) for earthquakes with magnitude equal to or larger than some prescribed threshold M [1]. The data were extracted from the Southern California Seismographic Network (SCSN) catalog. Their conclusion is that the observed behavior fundamentally opposes what would be expected if the dynamics was governed by self-organized criticality (SOC). In this comment, we will however argue that the results reported in Ref. [1], far from discarding SOC for modelling earthquake dynamics, provide further evidence in favor of such a description when interpreted properly.

The opposite conclusion drawn by *Yang et al* is due to a common misconception about the nature of SOC temporal features. It is contained in the sentence: "One implication of earthquakes being SOC is that an earthquake does not know how large it will become or, in other words, the magnitude of an earthquake is completely random for a given quake ...." (second page, first paragraph). Would this statement hold, the test for SOC behavior they propose would be adequate, since any measure of the temporal evolution of the system activity should be invariant under shuffling or reordering of the quakes in the sequence. *Yang et al* perform this test on the FRTDFs, finding them not invariant after the reordering. They interpret this result correctly as a signature of strong temporal correlations for quakes with magnitude larger than some minimum threshold but then they claim that this is in contradiction with the idea of SOC.

However, the notion that the hallmark of SOC is the succession of events with power law distributed but otherwise random sizes is false. The existence of dynamical temporal correlations among events of sufficiently large size is inherent in SOC. This was already reported in Ref. [2], which used the randomly driven running sandpile introduced by *Hwa et al* [3] to study the statistics of the quiet times between events selected according to a similar threshold. As the threshold increases, the quiet times cease to be distributed according to a Poisson (random) law. Instead, a power law region replaces the original exponential law (see Fig. 2 in Ref. [2]) and becomes larger as the threshold value is increased, up to a system size dependent limit. Notice that this behavior, which reveals the existence of a

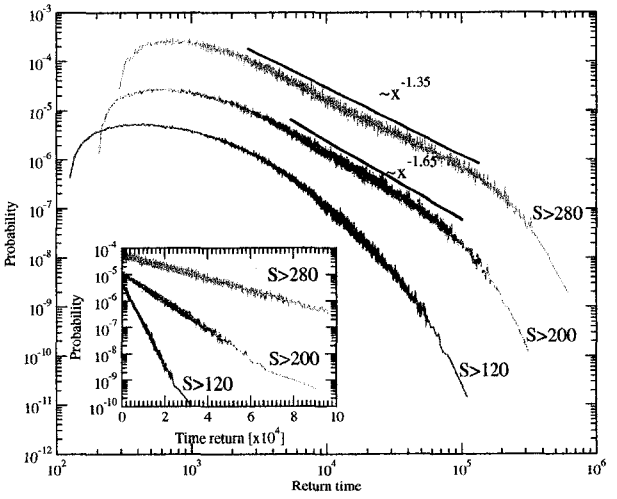

Figure A.1. FRTDFs of the instantaneous avalanching activity in a $L = 2000$ sandpile for avalanches with sizes above different thresholds (pdfs shifted for clarity). Inset: FRTDFs (in lin-log scale) for same data after shuffling avalanches.

correlated triggering of large avalanches, is very similar to that found for the earthquake FRTDF by *Yang et al* (see Fig. 1 of Ref. [1]). In fact, when the FTRDFs of the instantaneous avalanching activity are constructed for the running sandpile, they are found to behave in an identical manner to the quake FTRDFs. They are also not invariant after reordering, but become instead distributed according to an exponential law (see Fig. A.1, and compare with Figs. 1, 2 and 3 of Ref. [1]). The lack of invariance after reordering of events is true for any chosen temporal measure of a system governed by SOC dynamics. Take, for instance, the power spectrum of the instantaneous avalanching activity in the sandpile. It is also found that the signatures associated with temporal correlations observed at the lowest frequencies disappear in the reshuffled sequence. The power spectrum becomes instead flat (random) for all time scales longer than the duration of a single avalanche [4, 5].

Bibliography

[1] X. Yang, S. Du, and J. Ma. *Phys. Rev. Let.*, 92:228501, 2004.

[2] R. Sánchez, D. E. Newman, and B. A. Carreras. *Phys. Rev. Let.*, 88(6):068302, 2002.

[3] T. Hwa and M. Kardar. *Phys. Rev. A*, 45:7002, 1992.

[4] R. Woodard, D. E. Newman, R. Sánchez, and B. A. Carreras. Building blocks of self-organized criticality, part I: the very low drive case. Submitted to PRE, 2004.

[5] R. Woodard, D. E. Newman, R. Sánchez, and B. A. Carreras. Building blocks of self-organized criticality, part II: transition from low to high drive. Submitted to PRE, 2004.

Appendix B

Slides from Oral Defense

Building Blocks of Self-Organized Criticality

Ryan Woodard
Physics Department
University of Alaska Fairbanks
Friday the 13th of August 2004

I will discuss my research of complex systems described by self-organized criticality, a theory that describes how long time correlations can emerge from simple small-scale interactions.

- An explanation of the origin of $1/f$ in a power spectrum
- Different spectra produced by same dynamics
- A constant dynamical measure as external forcing changes
- Power spectrum and R/S related differently than previously thought
- A SOC-based explanation of large transport events due to diffusion in confined plasmas

Muchas, muchas gracias amigos

- David Newman (*****)
- Hilary (******)
- Raúl Sánchez and Ben Carreras (el comité españa)
- Nick Watkins and Brad Werner
- John Olson (for many years)
- Brenton Watkins, Renate Wackerbauer, Martin Truffer
- Dave Covey and Chris Swingley (GNU/Linux gnurus)
- Mary Parsons and Barbara Day (especially the past two weeks)
- Bob and Ann (The Race)

This thesis was made possible by Free Software and:
Richard Stallman, Linus Torvolds, Leslie Lamport LaTeX,
Guido van Rossum, Evgeny Stambulchik Gnuc

Difficult Math and Simple Model

10 years + 6 homes + 6 offices + 5 advisors + 4 research projects = 1 Ph.D.

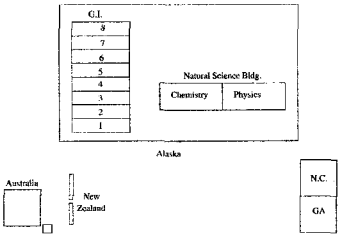

Difficult Math and Simple Model

10 years + 6 homes + 6 offices + 5 advisors + 4 research projects = 1 Ph.D.

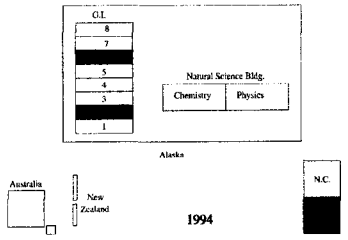

1994

Difficult Math and Simple Model

10 years + 6 homes + 6 offices + 5 advisors + 4 research projects = 1 Ph.D.

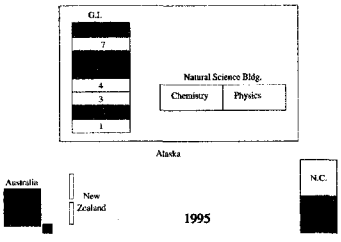

1995

Difficult Math and Simple Model

10 years + 6 homes + 6 offices + 5 advisors + 4 research projects = 1 Ph.D.

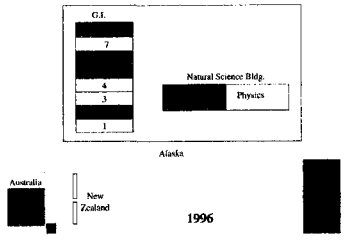

1996

Difficult Math and Simple Model

10 years + 6 homes + 6 offices + 5 advisors + 4 research projects = 1 Ph.D.

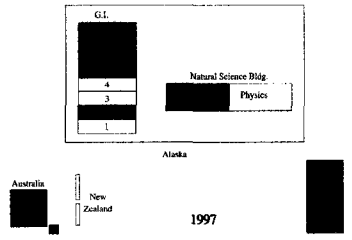

Difficult Math and Simple Model

10 years + 6 homes + 6 offices + 5 advisors + 4 research projects = 1 Ph.D.

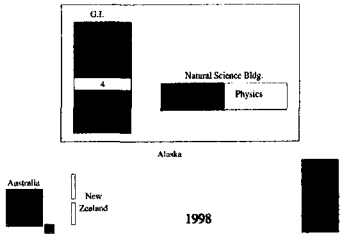

Difficult Math and Simple Model

10 years + 6 homes + 6 offices + 5 advisors + 4 research projects = 1 Ph.D.

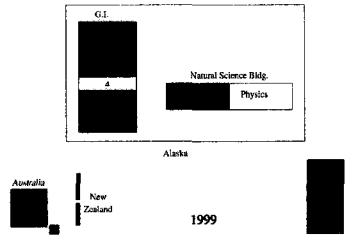

Difficult Math and Simple Model

10 years + 6 homes + 6 offices + 5 advisors + 4 research projects = 1 Ph.D.

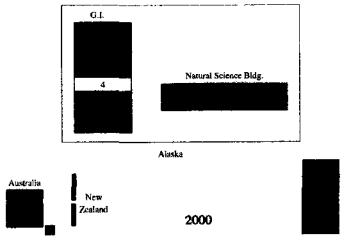

Difficult Math and Simple Model

10 years + 6 homes + 6 offices + 5 advisors + 4 research projects = 1 Ph.D.

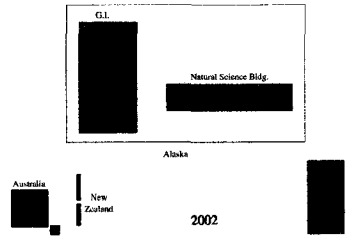

Outline

- Introduction
  - Lingo: complex system, time series, events, dynamics
  - How and why we measure randomness/correlations in time series
  - Three measures that I used: Probability distribution functions (PDFs), power spectrum, rescaled range (R/S) analysis
  - Development of SOC
- Research results: general theory
  - Different power spectra from same system
  - Spectra and R/S related differently than previously thought
  - Memory in system $\longrightarrow$ particular SOC dynamics
- Research results: applied SOC (no space)
  - Confinement problem in plasmas for fusion research
  - A two dimensional SOC approach to understand plasma transport

Introduction to Complex Systems

- Complex systems: whole is more than sum of parts, responses are not intuitive.
  - Many interacting, connected parts, local physics
  - Multiple time and length scales
- Observe some system (Denali fault, Black Rapids Glacier, magnetosphere, NYSE)
- Dynamics: how system changes with time (noun, singular)
- Measure some part of system as function of time, $X(t)$ (slip, surge, density, Dow Jones Industrial Index)
- 2 simple questions to write your story:
  - **Is $X(t)$ random? = Are there correlations?**
  - **Why or why not?** (The real physics)

Events Can Be Defined In Time Series

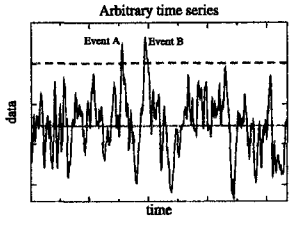

Threshold can be arbitrary

Intuition Test I: Time Series

'Random time series': What pictures come to mind?

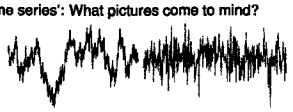

We have intuitive feel for random but how is it quantified?

- Probability distribution/density function (PDF), histogram, frequency–magnitude plot

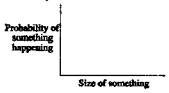

Intuition Test II: PDFs

What pictures and *explanations (physical processes)* of PDFs enter your mind when you hear 'random'?

- Gaussian (bell curve)  Rolling 2 dice, test scores
- Uniform (flat)  Pick a number between 1 and 100
- Poisson  Photon counts, radioactive decay
- Power law  $(y = cx^{-\beta})$? (One answer: SOC)
  (Alaska earthquake data)

Use Multiple Measures to Characterize Time Series

PDFs are silent about *dynamics*—how system evolves with time.

Time series can have PDFs shown but not be 'as random'.

How else can one quantify randomness (correlations)?

- Power spectrum = |Fourier transform|^2
  = Fourier transform (autocorrelation)
- The Hurst exponent H
  - Estimated with rescaled range (R/S) analysis

PDF + spectrum + R/S = nice toolbox

Intuition Test III: Power Spectrum

What *explanations (physical processes)* enter your mind when you see the following spectra?

- Spikes in spectrum (periodicities) 
- Flat spectrum (random: Gaussian, uniform, Poisson) 

- Power law 

? ("Hint: SOC")

A scientist's job: explain why spectrum is not flat (i.e., why series is not completely random).

What is meaning of β? Special case: $1/f$?

Estimate Hurst Exponent With R/S Analysis

$$\text{Rescaled range} = \frac{R(\tau)}{S(\tau)} = \frac{\text{range}}{\text{std. dev.}}$$

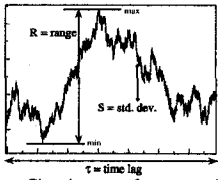

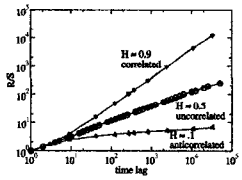

- Plot R' versus τ for same series.
- Slope on log-log axes is estimate of Hurst exponent, $H \in (0, 1)$.

H Is Measure of Correlations

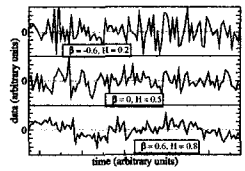

- $H < 0.5$: anticorrelated (rough, trends do not persist)
- $H = 0.5$: uncorrelated (random)
- $H > 0.5$: correlated (smooth, trends persist)

Correlated and anticorrelated: current state depends on past history.

For some Gaussian PDFs, $\beta = 2H - 1$.

Until recently, accepted as always true.

Common Characteristics of Many Systems With Long Time Correlations

Power law PDFs observed in earthquakes, rainfall, auroral events, power grid blackouts, avalanches, forest fires.

What do all of these systems have in common?

- Well-defined size
- External forcing, fluctuations
- Local gradients grow and persist (diffusion not strong)
- Threshold gradient
- Response to exceeding threshold
- Other similarities

Self-organized criticality (SOC) proposed to describe such systems.

Development of SOC

- *Bak, Tang, Wiesenfeld* PRL 59 (1987) (BTW):
  "...show that certain extended dissipative dynamical systems naturally evolve [self-organized] into a critical state, with no characteristic time or length scales [criticality]."
- Introduce simple cellular automaton model: the sandpile.

SOC presents a **simple model** with a **physical mechanism** for **memory** in a system that produces **correlations** among separate events over **long time scales**.

Prototypical SOC model: the sandpile

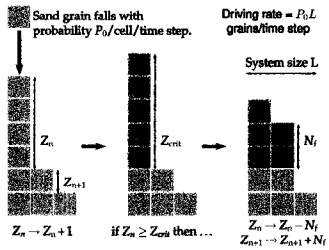

This is the model of *Hwa & Kardar* PRA 45 (1992).

4 parameters completely characterize SOC system

parameter	sandpile	tectonics	space plasma
L	size	fault	magnetospheric scales
P_0	external drive (sand)	slip rate	solar wind fluctuations
Z_{crit}	threshold	critical stress	plasma pressure, current gradients
N_f	response	local reduc. of stress	plasma/MHD instabilities
event	avalanche	earthquake	burst of plasma

Average SOC Global Gradient Less Than Critical Slope

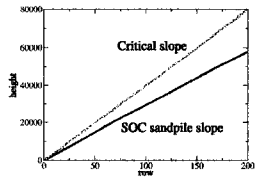

Yet still there is steady state, constant transport (flux).

Important point for plasma instabilities, later.

Define Event Duration and Quiet Times in Sandpile Flip Time Series

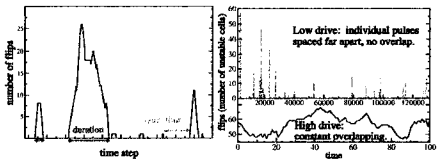

Have arrived full circle: Is this time series random?

Now we analyze the SOC time series.

PDFs of SOC Scale With System Size

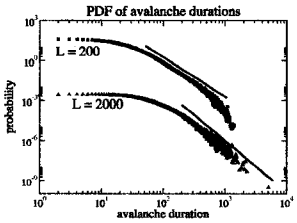

Same small-scale physics produces larger events in larger system

How does system "know"? Remember this question for later.

Power Spectra Change With Driving Rate

All new results begin here.

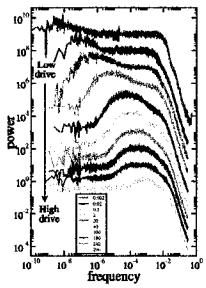

- Physics of system same, rate of forcing faster or slower.
- Mountain is indicator, dynamics move to shorter time scales.
- $1/f$ at high drive.
- At low drive (nonoverlapping), system is *not* simply random superposition of events.
- Not expected.
- Thought overlap was needed Such as simultaneous earthquakes
- Flat region at very low drive fooled everyone

New Regions Found in Power Spectra

All new results begin here.

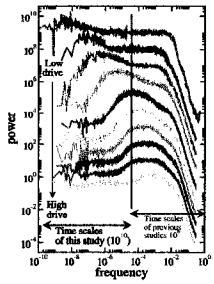

- Physics of system same, rate of forcing faster or slower.
- Mountain is indicator, dynamics move to shorter time scales.
- $1/f$ at high drive.
- At low drive (nonoverlapping), system is *not* simply random superposition of events.
- Not expected.
- Thought overlap was needed Such as simultaneous earthquakes
- Flat region at very low drive fooled everyone

Each Power Law Region Has Different Cause

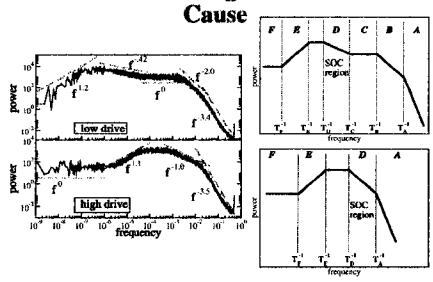

SOC Region: Correlations Among Events

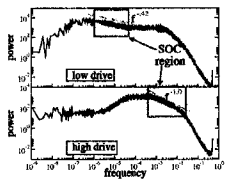

Already interesting because β changes with driving rate.

Same system, same rules, same dynamics ⟶ different spectra.
Before: People thought dynamics was different. People were wrong.

Pause.

Hurst Exponent Constant With Driving Rate

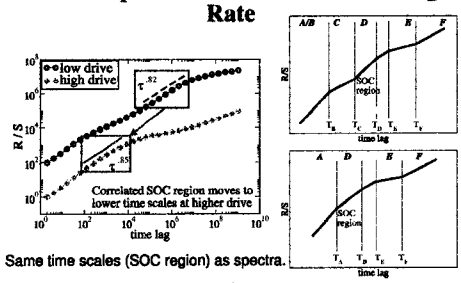

Same time scales (SOC region) as spectra.

Stronger drive ⟶ shorter time scales.

H Constant, β Changes With Driving Rate

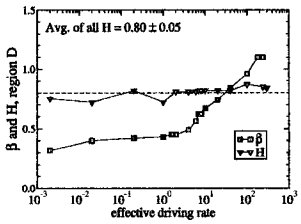

Over 5 orders of magnitude of driving rate, $\beta \neq 2H - 1$.*

Why is H constant?

Memory mechanism produces correlations, constant H

Dynamics, hence, H constant at all driving rates.
Memory stored in local gradients of other systems.

Decreasing Quiet Times Change β?

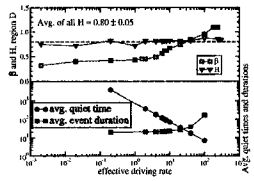

Same effect: artificially remove quiet times ⟶ $1/f$ *not* due to overlap

Summary of general results: $1/f$, β (?) vs. H (consistent), memory

Next: Application to confined plasma

SOC Application: Confined Plasmas

For fusion, need large triple product, $nT\tau$.

- dense enough n, hot enough T, long enough time τ
- Confinement time an issue.
- Figure courtesy of http://www.ph.utexas.edu/dept/research/tajima/gtt.html.

Confinement time reduced because of gradient-driven turbulent diffusion

- High nT in core, low in edge (think sandpile gradient)

ELMs observed: large transport events, quasi-periodic

Plasma Transport Scales With System Size

- Low confinement time due to anomalous (turbulent) transport
  Turbulence is gradient driven
  Early idea: larger device → longer confinement time
  (did not work)

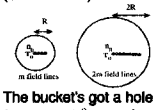

If random walk, $\tau \sim N^2$
(N = number of steps)

- The bucket's got a hole in it; hole scales with size of bucket (as N not N^2, so τ does not increase enough).
- As with sandpile, larger events in larger system.
- How does plasma 'know' bucket got bigger?
- Coherent transport events. Fundamental new picture.

Model Poloidal Spreading In Sandpile to Make More Realistic

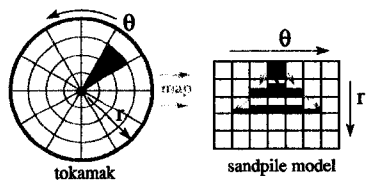

Spreading added because diffusion expected in two dimensions, not just radial.

PDFs Change With Added Spreading

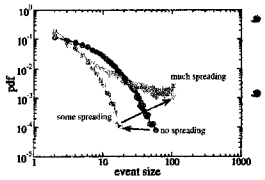

- Some spreading: lowers response, events do not propagate, fewer large events
- Much spreading: smooths system, all gradients closer to critical, more large events, triggered from edge (ELMs)

Observations of plasma:

- More 'some-spreading-like' in core (fast radial transport)
- More 'much-spreading-like' at edge (slow down radial transport, ELMs)

Animation

Cool.

Conclusions: General Theory

- Simple models for complex systems have physical insight
- SOC: your new picture for long time correlations, power laws
- Use spectra and R/S to quantify randomness/correlations
- Same system with same physics and dynamics can have very different spectra
  - Quiet times decrease, durations increase with stronger forcing
  - Possible path to understanding $1/f$ (NZ project)
- $H \approx 0.8$ regardless of strength of external forcing
  - SOC region moves to shorter time scales with stronger forcing
  - Physics is constant, memory stored in gradients
  - Hurst, 1951, found $H \approx 0.75$ for many geophysical systems

Conclusions: Applied

- Poloidal diffusion changes dynamics in 2D sandpile
  - Small amount reduces response so avalanches do not grow large
  - Large amount smooths system, increases large events, become quasi-periodic like ELMs (observed in edge of plasma device)

This very simple model gives a very intuitive picture of plasma dynamics. Actual plasma physics is a guide to make model reasonable.

Breakpoints Agree

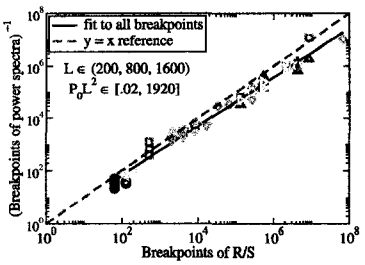

Calculating slopes/breakpoints

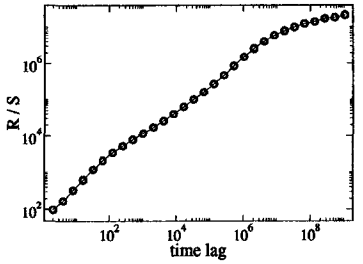

Calculating slopes/breakpoints

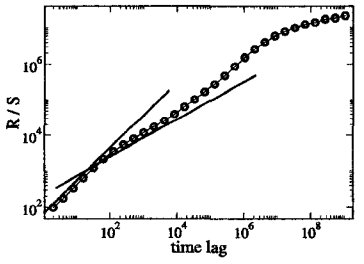

Calculating slopes/breakpoints